

ULTRASTRUCTURE OF THE PULMONARY ADENOMA  
OF THE STRAIN A (HESTON) MOUSE

by

Robert E. Brooks, B. S., M. S.

A THESIS  
Presented to the Department of Pathology  
and the Graduate Division of the University of Oregon Medical School  
in partial fulfillment of  
the requirements for the degree of  
Doctor of Philosophy

June 1967

APPROVED:

.....  
[REDACTED]  
.....  
(Professor in Charge of Thesis)

.....  
[REDACTED]  
.....  
(Chairman, Graduate Council)

## ACKNOWLEDGEMENT

It is with sincere appreciation that I wish to acknowledge the advice, support, and encouragement given to me in this work by Dr. Sefton R. Wellings.

I am extremely grateful to Dr. Robert A. Cooper for his critical review of this manuscript, and for offering many useful suggestions to improve the thesis.

It is a pleasure to acknowledge the expert technical assistance of Mrs. Mary Bens Rau in part of this study.

Finally, I wish to thank my wife, Frances, and my son, Allen, for aid in preparing the figures.

Part of the thesis work was conducted while I was a recipient of United States Public Health Service special research fellowship No. 1-F3-CA-28, 512-01 from the National Cancer Institute. Support for the remainder of the research for this thesis was obtained from United States Public Health Service grants No. HD-00104 from the National Institute for Child Health and Human Development, and No. CA-08158 from the National Cancer Institute awarded to Dr. Sefton R. Wellings.

## TABLE OF CONTENTS

Introduction.....	Pg. 1
Material and Methods.....	Pg. 20
Results.....	Pg. 24
Discussion.....	Pg. 42
Summary.....	Pg. 64
References.....	Pg. 66
Abbreviations for Figures.....	Pg. 79
Figures.....	Pg. 81

## LIST OF ILLUSTRATIONS

- Figure 1. Gross photograph of mouse lung with multiple subpleural tumors.....Pg. 81
- Figure 2. Low magnification light micrograph of a lung showing multiple tumor loci.....Pg. 81
- Figure 3. Medium magnification light micrograph of a typical mouse lung adenoma.....Pg. 82
- Figure 4. Higher magnification light micrograph of a pulmonary adenoma.....Pg. 82
- Figure 5. Type B cell of a normal, eleven week old, Group III mouse -- effect of fixation.....Pg. 83
- Figure 6. Type B cell of a normal, eleven week old, Group II mouse --- effect of fixation.....Pg. 84
- Figure 7. Type B cell of a normal, eleven week old, Group III mouse -- effect of fixation.....Pg. 85
- Figure 8. Type B cell of a urethane treated, eleven week old, Group III mouse -- effect of fixation.....Pg. 86
- Figure 9. Type B cell of a normal, twenty-one day old, Group IV mouse -- effect of fixation.....Pg. 87
- Figure 10. Type B cell of a five month old, normal, Group I mouse -- effect of fixation.....Pg. 88
- Figure 11. Tumor cells of a forty-three day old, Group IV mouse --- effect of fixation.....Pg. 89
- Figure 12. Tumor cells of a fifteen month old, untreated, Group I mouse --- effect of fixation.....Pg. 90

- Figure 13. Tumor cells of a fifteen month old,  
untreated, Group I mouse -- effect of fixation....Pg. 91
- Figure 14. Tumor cell and macrophage of a ten month  
old, urethane treated, Group V mouse --  
effect of fixation.....Pg. 92
- Figure 15. Tumor cells of a ten month old, urethane  
treated, Group V mouse -- effect of fixation.....Pg. 93
- Figure 16. Tumor cells of a fifteen month old, urethane  
treated, Group V mouse -- effect of fixation.....Pg. 94
- Figure 17. Tumor cells of a fifteen month old, urethane  
treated, Group V mouse -- effect of fixation.....Pg. 95
- Figure 18. Tumor cells of a fifteen month old, urethane  
treated Group V mouse -- effect of fixation.....Pg. 96
- Figure 19. Type B cell of an eleven week old, Group III  
mouse -- effect of urethane.....Pg. 97
- Figure 20. Type B cell of an eleven week old, Group III  
mouse -- effect of urethane.....Pg. 98
- Figure 21. Type A cell of an eleven week old, Group III  
mouse -- effect of urethane.....Pg. 99
- Figure 22. Type B cell of an eleven week old, Group III  
mouse -- effect of urethane.....Pg. 100
- Figure 23. Type B cell of a twelve week old, Group III  
mouse -- effect of urethane.....Pg. 101
- Figure 24. Tumor cells of an eighteen week old, Group III  
mouse -- effect of urethane.....Pg. 102

- Figure 25. Tumor cells of a twelve month old, Group V mouse..Pg. 103
- Figure 26. Tumor cells of a sixteen month old, Group V  
mouse.....Pg. 104
- Figure 27. Alveoli of a seven day old, Group IV mouse--  
effect of urethane.....Pg. 105
- Figure 28. Type B cell of a seven day old, Group IV  
mouse -- effect of urethane.....Pg. 106
- Figure 29. Type B cell of a nine day old, Group IV mouse --  
effect of urethane.....Pg. 107
- Figure 30. Type B cell of a seven day old, Group IV mouse --  
effect of urethane.....Pg. 108
- Figure 31. Alveolar macrophage of a nine day old, Group IV  
mouse -- effect of urethane.....Pg. 109
- Figure 32. Tumor cells of a forty-three day old, Group IV  
mouse -- effect of urethane.....Pg. 110
- Figure 33. Tumor cells of a fifty-six day old, Group IV  
mouse -- effect of urethane.....Pg. 111
- Figure 34. Tumor cells of a forty-three day old, Group IV  
mouse -- effect of urethane.....Pg. 112
- Figure 35. Tumor cells of a fifty-six day old, Group IV  
mouse -- effect of urethane.....Pg. 113
- Figure 36. Tumor cells of a fifty-six day old, Group IV  
mouse -- effect of urethane.....Pg. 114
- Figure 37. Tumor cells of a forty-three day old,  
Group IV mouse -- effect of urethane.....Pg. 115
- Figure 38. Tumor cells of a forty-three day old,  
Group IV mouse -- effect of urethane.....Pg. 116

- Figure 39. Tumor cells of a fifty-six day old, Group IV  
mouse -- effect of urethane.....Pg. 117
- Figure 40. Tumor cells of a fifty-six day old, Group IV  
mouse -- effect of urethane.....Pg. 118
- Figure 41. Tumor cell and macrophage of a fifty-six  
day old, Group IV mouse.....Pg. 119
- Figure 42. Tumor cells of a fifty-six day old, Group IV  
mouse -- effect of urethane.....Pg. 120
- Figure 43. Tumor cells of a twelve month old,  
untreated Group I mouse.....Pg. 121
- Figure 44. Tumor cell of a sixteen month old, untreated,  
Group I mouse.....Pg. 122
- Figure 45. Tumor cell of a twenty-one month old,  
untreated Group I mouse.....Pg. 123
- Figure 46. Tumor cell of a twelve month old, untreated,  
Group I mouse.....Pg. 124
- Figure 47. Type B cell of a seven day old, Group IV  
mouse.....Pg. 124
- Figure 48. Tumor cell of a sixteen month old, untreated,  
Group I mouse.....Pg. 125
- Figure 49. Type B cell of a nine day old, Group IV mouse.....Pg. 125
- Figure 50. Tumor cell of a fifty-six day old, Group IV  
mouse.....Pg. 126
- Figure 51. Tumor cell of a fifty-six day old, Group IV  
mouse.....Pg. 126
- Figure 52. Tumor cell of a fifteen month old, Group V  
mouse.....Pg. 127



- Figure 53. Tumor cell of a fifteen month old, Group V  
mouse.....Pg. 127
- Figure 54. Tumor cells of a fifty-six day old, Group IV  
mouse.....Pg. 128
- Figure 55. Tumor cell of a forty-three day old, Group IV  
mouse.....Pg. 129
- Figure 56. Tumor cell of a fifteen month old, Group V  
mouse.....Pg. 129
- Figure 57. Tumor cell of a fifteen month old, Group V  
mouse.....Pg. 130
- Figure 58. Tumor cell of a fifteen month old, Group V  
mouse.....Pg. 130
- Figure 59. Tumor cell of a fifteen month old, Group V  
mouse.....Pg. 131
- Figure 60. Tumor cell of a fifty-six day old, Group IV  
mouse.....Pg. 131
- Figure 61. Tumor cell of a fifty-six day old, Group IV  
mouse.....Pg. 132
- Figure 62. Tumor cells of a sixteen month old, Group V  
mouse.....Pg. 132
- Figure 63. Tumor cell of a twenty-one month old, Group I  
mouse.....Pg. 133
- Figure 64. Tumor cell of a fifteen month old, Group V  
mouse.....Pg. 133
- Figure 65. Tumor cell of a twenty-one month old, Group I  
mouse.....Pg. 134

- Figure 66. Type B cell of a twelve month old, Group I  
tumor-bearing mouse.....Pg. 135
- Figure 67. Type B cell of a twelve month old, Group V,  
tumor-bearing mouse.....Pg. 136
- Figure 68. Tumor cells of a twenty-one month old, Group I  
mouse.....Pg. 137
- Figure 69. Macrophage of a forty-three day old, Group IV  
mouse.....Pg. 138
- Figure 70. Macrophage of a forty-three day old, Group IV  
mouse.....Pg. 138
- Figure 71. Macrophage and tumor cells of a fifteen month  
old, Group V mouse.....Pg. 139
- Figure 72. Tumor cells of a fifteen month old, Group V  
mouse.....Pg. 139
- Figure 73. Macrophage and tumor cells of a fifty-six  
day old, Group IV mouse.....Pg. 140
- Figure 74. Macrophage of a fifty-six day old, Group IV  
mouse.....Pg. 141

"The microscopic study of cells and tissues is a fascinating, aesthetically satisfying science fundamental to an understanding of normal histophysiology and the interpretation of disease processes."

Don W. Fawcett, 1966

"Let us grasp the opportunity to integrate our methods and our knowledge into an experimental biological science where structure and function will at last be considered as indissoluble and strictly complementary."

W. Bernhard and R. Lepus, 1964

"... our aim is not the confirmation of an idea but the solution of a problem."

Charles Oberling, 1952

"One man's artifact is another man's assumption."

Jere Mead, 1962

## INTRODUCTION

## I. Statement of the Problem

Cancer researchers have relatively few experimental materials with which to work. Spontaneous and inducible tumors of highly inbred (homozygous) strains of mice represent one of the most studied of these materials. Of the mouse tumors, the pulmonary adenoma, occurring in high incidence in certain strains, has several advantages as an experimental system. The tumor occurs spontaneously, and can be induced by a variety of chemical carcinogens as well as by x-irradiation. This tumor is generally considered to be uninfluenced by hormones, and to have no viruses associated with it. Moreover, the tumor, growing subpleurally as a raised, white nodule, provides an easily assayable object for the testing of possible carcinogenic agents. For these several reasons, a large amount of data has been gathered concerning this tumor system. The resulting body of information serves as an excellent base for further studies.

Morphologically, the mouse lung adenoma is of simple construction. The tumor grows initially in a papillary form consisting of sheets of cuboidal to low columnar, epithelial-like cells with a thin, sparsely vascularized stroma. Later, the tumor usually becomes solid. The adenoma cells are recognized, with the electron microscope, to be similar to the type B alveolar epithelial cell, one of two alveolar cell types found in normal lung. A characteristic cytoplasmic inclusion, found in both the type B alveolar cell and adenoma cell, permits distinguishing these cells from other cells in the lung. This morphological marker simplifies the microscopic study of the lung tumor.

Microscopy is, perhaps, the most commonly used method for the study of tumors. However, microscopic studies of tumor cells have revealed few characteristics which substantially contribute to the basic understanding of the cancer process. This conclusion applies equally well to light microscopic studies and to the more recent electron microscopic studies. The examination of tumor cells at the greater resolving power of the electron microscope has failed to uncover significant, new information. It is possible, nevertheless, that ultrastructural studies of tumor systems may yet reveal useful data. This view is based, in part, on the observation that almost all published electron microscopic studies have dealt with mature tumors, single cases of human tumors, or have been confined to a search for viruses in tumor cells. Electron microscopic studies of well-defined, relatively simple tumor systems may yet prove fruitful.

The purpose of the study reported in this thesis is to determine if ultrastructural examination of mouse lung tumor cells can contribute useful knowledge for the cancer problem.

## II. A Survey of the Literature Relating to the Mouse Lung Tumor

### A. Gross and Light Microscopic Aspects

The first report of a spontaneous lung tumor in the mouse was made by Livingood (1) in 1896. The tumor, considered to be an adenocarcinoma of bronchial origin, was found in an albino mouse subjected to an experimental bacterial infection. Livingood described the tumor as projecting "... from the upper surface of the middle lobe as a small white boss about 5 mm. in diameter, slightly friable and

apparently softer in the center.... The greater part of the tumor is made up of infiltrating fingers of epithelial cells. The cells are of irregular columnar or polygonal type with oval vesicular nuclei.... The connective tissue stroma is very scanty, the infiltrating fingers alone seeming to restrain one another and causing, by mutual pressure, irregular growth."

During the decade following this paper, only a few investigators reported finding lung tumors in mice. A description of these early findings can be found in a review article by Haaland (2) written in 1905. It is not possible to determine from the photographs and descriptions given in these early reports whether the tumors described were all typical pulmonary adenomas.

In 1907, Tyzzer (3) reported on twenty spontaneous tumors found in old mice originally kept for breeding purposes. The micrographs presented clearly portray the typical mouse pulmonary adenoma. Because of some variability in growth pattern of the tumor, Tyzzer preferred to call it a "papillary cystadenoma."

Murray (4), in 1908, reviewed the literature on spontaneous cancer in the mouse and offered material from his own studies of lung adenoma. He pointed out that tumor cells with two nuclei are frequently seen and attributed this to direct nuclear division without cytoplasmic division. He also noted that lung tumors have been found, almost entirely, in animals that also had spontaneous mammary tumors, but this association was thought to be accidental.

The literature on spontaneous tumors of the mouse was reviewed again in 1910 by Jobling (5). From his own observations, he reported nine primary lung tumors in eight animals, of which probably only about

one half were typical adenomas.

In 1914, Slye, Holmes, and Wells (6) reviewed results from their own studies and entered into what was the first extensive discussion of the nature of the mouse lung tumor. Included in this report was a tabulation of the findings from six thousand autopsied mice of the Slye stock at the University of Chicago. This stock was bred to study the influence of heredity upon the incidence of tumors, and all mice were allowed to live out their lives. About four thousand of the autopsied mice had reached an age when lung tumors occur spontaneously (about one year). These investigators found a total of 160 mice with tumors (23 of the animals with lung tumors had tumors elsewhere in the body). Thus, about 2 - 3% of the Slye stock mice had spontaneous lung tumors. These authors considered that the tumors could originate either from bronchial or alveolar epithelium. Or, to put this in another way, the origin of the tumor could not be morphologically determined by comparing tumor cells with either normal bronchial or alveolar epithelium. Nevertheless, they noted that in the early stages of tumor growth, a thickening of the alveolar epithelium took place; a finding common, also, in lung inflammations. In fact, these investigators thought that the tumor originated at sites in which inflammatory hyperplasia had occurred, and believed they had observed all stages from hyperplasia to papillary adenocarcinoma. It was pointed out that the tumors usually arose beneath the pleura and extended towards the bronchi and larger blood vessels, and occasionally invaded the bronchial tree. On the other hand, tumors were found that were thought to have arisen from

the bronchi. Cystic tumors were not observed, and for this reason these authors regarded Tyzzer's term "papillary cystadenoma" to be inappropriate. Slye et al (6) were among the first to note definite metastases from the primary lung tumor. Secondary growths were found in mediastinal lymph nodes, the chest wall, diaphragm, and kidney. They also pointed out that mitotic figures were infrequently found, but that cells in apparent amitotic division were frequently noted.

It is interesting to record that 17 years after the above report by Slye et al (6), the same group, Wells, Slye, and Holmes (7), published further findings based on a very much larger group of animals. Thus, "Of 147,132 mice coming to autopsy in the Slye laboratory, where every mouse is allowed to live out its span of life, 2865 mice had lung tumors, or about 2%."

Murphy and Sturm (8), in 1925, attempted to produce epidermal cancer by painting mice with a coal tar derived from coke oven residues. An incidental finding in this study was the presence of lung tumors in as many as 21 mice of a group of 23 animals treated with the coal tar. The authors described the tumors as being identical in appearance to those reported previously by Livingood (1), Haaland (2), Tyzzer (3), and Murray (4).

Magnus (9), in 1939, administered dibenzanthracene to mice by stomach tube in an effort to produce stomach cancer. He found that 95% of the mice developed lung tumors, as compared with 4% of a control group.

Bittner (10), also in 1939, reported that 75% of the Strong "A" stock mice, later to be called strain A, showed lung tumors at 18 months of age.



Shimkin (11), in the same year, administered methylcholanthrene or dibenzanthracene intratracheally in strain A mice and produced, thereby, a 90% incidence of typical lung adenomas, as compared with a 20% incidence at the same age in controls.

These early reports of mouse lung tumors provided a basis for two different lines of investigation: 1) the testing of various chemicals to determine if they were carcinogens for mouse lung, and 2) the examination of the genetic basis of the lung tumor.

Andervont, in a long series of studies (12 - 19) determined the incidence of lung tumors in several strains of mice following the subcutaneous administration of 1,2,5,6-dibenzanthracene. It was found that mice of strains having the highest incidence of spontaneous lung tumors also had the greatest susceptibility to carcinogens, i.e., induced pulmonary tumors occurred at earlier ages than did spontaneous tumors, and wherever only one or two tumors formed spontaneously, multiple tumors developed under the action of carcinogenic chemicals. In a study wherein the carcinogenic action of several polycyclic hydrocarbons were tested, Andervont and Shimkin (20) showed that although 1,2,5,6-dibenzanthracene was highly carcinogenic, 1,2-benzanthracene was seemingly not at all carcinogenic. Also, these workers showed that a chemical which was highly active in producing pulmonary adenomas was not necessarily effective in producing other typical mouse tumors, for instance, sarcomas.

In 1943, Nettleship, Henshaw, and Meyer (21) reported that the anesthetic, ethyl carbamate (urethane), used to anesthetize  $C_3H$  mice undergoing experimental radiation treatment, promoted pulmonary tumors in this strain of mouse. At the same time, these investigators

tested the effect of urethane on the A strain mouse. A small group of mice were given 14 weekly injections of a 10% aqueous solution of urethane at the rate of 100 milligrams per 100 grams body weight, and sacrificed  $4\frac{1}{2}$  months later. At this time, 8 out of 8 treated mice had lung tumors, whereas only 1 out of 10 untreated control mice showed tumors. Moreover, the urethane treated mice invariably had multiple lung tumors. These findings were pursued by Henshaw and Meyer (22) who sought to determine the minimal number of urethane injections that would cause an increase in tumor incidence. It was found that one injection of urethane, in the amount given above, was sufficient to produce a 100% incidence in a small group of strain A mice  $4\frac{1}{2}$  months after injection. Control mice showed only a 5% incidence at this time. The urethane treated mice averaged  $9\frac{1}{2}$  tumors per animal.

The nature of the specific effect of urethane in causing pulmonary adenomas in mice has been sought by many investigators. Larsen (23) attempted to produce lung tumors in mice using anesthetic agents other than urethane. The negative results from this attempt was considered to indicate that the anesthetic action, as such, was unlikely to be the basis of the carcinogenic action of urethane. In later experiments, Larsen (24) tested several other esters of carbamic acid and found little or no carcinogenic activity with isopropyl, n-propyl, and trichloroethyl esters. Alkylated derivatives of urethane were found to have some, but less activity than ethyl carbamate (Larsen (25)). Degradation products of urethane were found to be without effect (26). However, Berenblum, Ben-Ishai, Haran-Ghera, Lapidot, Simon, and Trainin (27) reported that N-hydroxy urethane had the same carcinogenic

activity as urethane. This compound has been examined in a separate study by Boyland and Nery (28) who found that administered urethane is metabolically converted, in low yield, to N-hydroxy urethane and also to the N- and O-acetyl derivatives in rat, rabbit and man. These authors suggested that the process of N-hydroxylation is an essential step in producing what may be the actual carcinogen: an aromatic, amino or acetamido derivative of urethane. Other suggestions concerning the mode of action of urethane will be presented following a consideration of the histogenetic aspects of the tumor. However, it should be noted that a recent report by Kaye and Trainin (29) indicated that although N-hydroxy urethane was indeed carcinogenic, urethane produced up to five times the number of lung adenomas, depending upon the level of carcinogen administered.

#### B. Histogenesis

The histogenesis of the mouse lung adenoma has been studied by several workers. Grady and Stewart (30), in 1940, induced tumors in strain A mice by either 1,2,5,6-dibenzanthracene or methyl cholanthrene. During the first two weeks following administration of these carcinogens, a cellular increase involving the alveolar wall in the subpleural areas was noted, although no active proliferation, as judged by mitotic activity or binucleate cells, could be seen. During the second two weeks, cellular accumulation became more numerous. During the fifth and sixth weeks, about 20% of the mice showed small tumor nodules in their lungs. Histologically, the tumors consisted of alveoli lined with cuboidal cells. Immediately surrounding the early tumor nodules

were small collections of cells attached to the alveolar walls. In some cases, mitotic figures were observed in these cells. During the seventh and eighth weeks, about 35% of the mice had lung tumors, occurring multiply in most cases. As the tumors grew in size, the central portion became organized as loosely packed columns of cuboidal cells resting on a thin core of capillaries and connective tissue. The peripheral portion of the tumor retained the more typical alveolar structure. From these studies, Grady and Stewart (30) concluded that the tumor arose from alveolar cells, not bronchiolar cells. However, because at that time the nature of the cells lining the alveoli had not been established, these authors could not determine the exact cell of origin.

In 1947, Orr (31) reexamined the question of the histogenesis of mouse pulmonary adenomas. In this case, urethane was used as the inducing agent. He described a papillary and solid type of tumor similar to that found by Grady and Stewart (30). However, Orr thought that he noted an antecedent inflammatory process and suggested that the tumor cells progressively replaced the leucocytes and lymphocytes in the area -- an area he described as "chronic collapse inflammation." Moreover, Orr considered the tumors to be of bronchial origin.

In 1951, Mostofi and Larsen (32) repeated the work of Orr, except that urethane was administered orally in the drinking water, instead of by injection as Orr had done. These investigators could find no evidence indicating that the tumor arose in sites of inflammation. In addition, in support of the view of Grady and Stewart (30), the adenomas were considered to arise from alveolar cells.

Shimkin and Pollisar (33), in 1955, made a careful microscopic

examination of the urethane-induced mouse lung tumor to determine if an exact dose-response relation could be found. In the course of this study, it was learned that following a single intraperitoneal dose of urethane, administered as 1.0 milligram per gram body weight, a relatively consistent response was obtained. An increased alveolar cellularity was seen starting from the first day after injection. This increased cellularity reached a peak 4 weeks later and then gradually subsided, so that by 15 weeks normal levels were reached. Hyperplastic foci of cells were seen by 3 weeks and by 5 weeks about 600 such foci were found per animal. Microscopically recognizable tumors were noted as early as 3 weeks following the single injection of urethane. The tumors consisted of large cells in adenomatous arrangement. The number of tumors increased up to about 7 weeks and then remained steady, eventually reaching about 36 per mouse.

### C. Action of Urethane

The ease with which urethane induces lung tumors in susceptible strains of mice has attracted much interest regarding the mechanism of action of urethane as a carcinogen. This interest has remained to the present time, because it is now known that urethane causes, in addition to lung tumors, leukemia, lymphomas, and other tumors in mice as well as in other species (34).

Skipper, Bennett, Bryan, White, Newton, and Simpson (35), by labelling the carbonyl carbon or the ethoxy carbon of urethane with  $C^{14}$ , were able to show that urethane was almost entirely broken down in the body to  $CO_2$ , ethyl alcohol, and ammonia by simple hydrolysis. Within

24 hours, at least 97% of the administered label was lost in the expired air.

The experiments of Shimkin and Polissar (33), previously noted, also provided information on dose response. Repeated administration of urethane did not increase the size of any one tumor. Division of the urethane dose over a period of several days gave the same number of tumors as that produced when the total dose was administered at one time. This finding has been interpreted by Shimkin (36) to indicate that the action of urethane is an acute one and prolonged exposure to the carcinogen is not necessary. Moreover, it was concluded that urethane controls the induction of the tumors, but does not control their growth.

In 1958, Berenblum, Haran-Ghera, Winnick, and Winnick (37) repeated and extended the earlier analysis of Skipper *et al* (35) on the metabolism of urethane. The later investigation showed that the carbonyl moiety of the urethane molecule was almost completely lost to the body within 24 hours after administration. However, somewhat more of the ethyl moiety was retained after 24 hours. Incorporation of both labels was noted in proteins after 24 hours. Homogenates of lung and liver were examined for C<sup>14</sup> label. It was learned that lung mitochondria had six times the retention of C<sup>14</sup> per milligram of protein than lung nuclei. In a subsequent experiment, it was learned that isolated lung mitochondria, *in vitro*, were able to take up (bind) urethane to a definite extent whereas liver mitochondria did not bind urethane under the same conditions.

Haddow and Sexton (38), in 1946, had suggested that urethane may

produce a deviation in purine synthesis, but it was not until 1957 that a possible biochemical mode of action for urethane was proposed by Rogers (39). Rogers had noted that urethane had been reported to be a mitotic poison (40). He therefore focussed attention on the possibility that urethane, in some manner, may influence normal nucleic acid synthesis. Rogers gave mice various nucleic acid-related substances immediately prior to a single dose of urethane, and noted the effect of each substance on tumor production. He found that a DNA hydrolysate, given just prior to urethane administration, markedly reduced the number of mice bearing tumors. Of the various DNA precursors tested, following the above procedure, cytidylic acid, thymine, and orotic acid showed variable but definite tumor-reducing properties. The analysis of these and other related, small as well as large, molecules enabled Rogers to formulate a hypothesis to account for the carcinogenic action of urethane. He suggested that urethane interferes with nucleic acid synthesis, possibly at the level of the conversion of ureidosuccinic acid (carbamyl aspartic acid) to orotic acid, and, in some manner, produces a carcinogenic intermediate: an atypical pyrimidine which may become incorporated into DNA and thenceforth passed from parent to daughter cell.

Recently, Kaye and Trainin (29) repeated some of the above work of Rogers (39) to verify the relationship between pyrimidine administration and lung tumor induction by urethane in the strain SWR mouse. These workers found that thymine, orotic acid, and thymidine were ineffective in reducing the number of lung adenomas in mice when injected together with a single dose of urethane. However, it was

determined that when thymine was administered in the drinking water of control mice, there was a reduction in the number of spontaneous adenomas.

The anesthetic properties of urethane serve as a possible clue to the biochemical action of urethane.

Keilin and Hartree (41), working with a crude heart muscle homogenate active in the rapid oxidation and reduction of cytochromes, showed that the addition of one-tenth volume of a 30% solution of urethane caused an irreversible oxidation of cytochromes a, a<sub>3</sub>, and c, and an irreversible reduction of cytochrome b. These findings were interpreted as indicating that urethane acted to prevent the cytochrome system from reacting with oxygen.

Haddow and Sexton (38) pointed out that the concentration of urethane used by Keilin and Hartree (41) was very large and could hardly be related to the dosage causing narcosis: about 1 - 10 milligrams per gram body weight. It was for this reason that Haddow and Sexton, as previously noted, suggested that it was more likely that urethane interfered with purine synthesis.

Some investigators, nevertheless, continued to believe that the principal action of urethane was on respiration. The most notable of these was Warburg, who in 1956 (42), referring to experiments performed in 1921 (43), stated that "Urethane is a nonspecific respiratory poison. It inhibits respiration as a chemically indifferent narcotic, since it displaces metabolites from cell structure."

Cornman (40), in a review article concerning the effects of urethane, cited reports showing that urethane in some cases decreases,



but in most cases increases the uptake of oxygen by various organisms.

Lee (44) recently undertook experiments designed to test the concept that urethane may uncouple oxidative phosphorylation. Using a rat liver mitochondrial preparation, he was unable to show an uncoupling effect by urethane.

The effect of urethane on mitosis may also provide clues as to the action of urethane.

Boylard and Rhoden (45) attempted to relate the metabolic and mitotic effects of urethane. They found that when urethane was given to tumor-bearing rats in doses sufficient to inhibit mitoses in jejunal mucosa and Walker carcinoma, and to mice in doses sufficient to produce lung tumors, no reduction of respiration or glycolysis was detected either in mouse lung or jejunum, or in rat Walker carcinoma, jejunal mucosa, kidney medulla, or brain homogenates.

Ahlstrom (46) expressed the view that urethane is one of several interphasic mitotic poisons acting on the "resting" nucleus. The action of such poisons is to cause chromosomal fragmentation, chromosomal bridging, translocation, and other defects in the first and possibly succeeding mitotic divisions after administration of the poison. Ahlstrom suggested that urethane, in particular, may act as both a cytoplasmic and nuclear poison.

It would appear, then, that the action of urethane is, as yet, not definitely known. In relation to cancer, as previously noted, there has accumulated a large amount of evidence that urethane is a multipotential carcinogen (34, 47). Hepatomas, melanomas, carcinomas, and leukemias have been caused by urethane. Tannenbaum and Mattoni (47)

noted that urethane influences tumor production by lowering the age of tumor appearance and by increasing the number of tumors per animal, but only in those cases where the tumor would occur "spontaneously" in small numbers at a later age. Based on this observation, these authors suggested that urethane action is one of "... augmentation, enhancement, or potentiation rather than induction de novo."

#### D. Genetic Aspects

The genetic factors involved in the mouse lung adenoma have been carefully studied in a long series of investigations by Heston (48-51), and Heston and Deringer (52, 53). The known variable incidence of adenomas, from almost zero to 100%, in the several available inbred strains of mice was used as a basis for these studies. Heston found that at least seven genes were associated with pulmonary adenomas of the mouse, of which only one, "lethal yellow", was related to an increase in tumor incidence; the other six were related to decreases in incidence. Moreover, the "lethal yellow" gene was found to be associated with pulmonary tumors either when they arose "spontaneously" or were induced with nitrogen mustard, methyl cholanthrene, or urethane, but not when tumors were induced with dibenzanthracene (54).

From experiments in which lung transplants from high incidence strain A and low incidence strain C57L were made to the F<sub>1</sub> hybrids, it was determined that the genes controlling the occurrence of pulmonary tumors were expressed specifically in the end organ -- the lung (54). Previous studies (50) had indicated that the high incidence strain A and the low incidence strain C57L mice differed by at least four pairs

of genes effecting the occurrence of lung adenoma.

#### E. Electron Microscopic Studies

Five electron microscopic studies of urethane induced mouse lung adenoma have been reported.

Klärner and Giesecking (55) examined 36 adenomas from strain A mice injected intraperitoneally with 1 milligram per gram body weight of urethane in 0.9% NaCl solution twice daily for 3 days. These investigators were able to substantiate the light microscopic conclusions of Grady and Stewart (30), and Mostofi and Larsen (32) that the adenoma arose from alveolar cells. This was based on the observation that typical osmiophilic, lamellar bodies, found in certain alveolar lining cells, were also present in the tumor cells. Klärner and Giesecking considered that the tumor cells divided amitotically, as normal mitotic divisions were not observed. In addition, cytoplasmic inclusions, suggesting the presence of virus, were described. This latter observation was emphasized in the report, for, prior to this investigation, there had been no evidence for virus involvement in the mouse lung tumor. Virus-like particles, about 200 Å in diameter, were found in localized regions of tumor cell cytoplasm.

In 1962, Okada, Daido, and Ishiko (56) reported on their electron microscopic studies of the mouse lung tumor. Tumors were induced in strain dd, an inbred albino strain, by four consecutive, weekly, intraperitoneal injections of urethane, at the rate of 1 milligram per gram body weight. These workers also considered the tumor to arise from alveolar cells. However, they also mentioned the presence of

non-alveolar, ciliated, and non-ciliated cells in the tumor.

"Hyperplastic foci", similar to those described by Shimkin and Polissar (33) were also noted. It was concluded that the tumors originated from alveolar cells and that the presence of ciliated cells indicated the metaplastic potentialities of the alveolar cells. No remarkable cytoplasmic or nuclear findings were reported, rather, the authors commented on the extreme benignity of the tumor cells.

Svoboda (57), in 1962, published an electron microscopic study of lung tumors induced in Swiss mice by urethane administered in the drinking water. Mice received 0.1% urethane in drinking water for 13 weeks and were sacrificed from 5 to 50 weeks after administration of urethane was begun. This study was technically superior to the others described above. Good pictures of the cytoplasmic regions thought by Klärner and Giesecking (55) to be related to virus production, revealed little or no such resemblance, and Svoboda concluded that virus was not present in the tumor cells. The emphasis of Svoboda's report was placed on the ultrastructure of the mature tumor cells, particularly on bizarre and atypical cytoplasmic, lamellar, and other inclusions. No conclusions were drawn by Svoboda from these various observations.

Drieessens, Dupont, and Demaille (58), in 1963, reported on the same tumor induced, in this case, in Swiss mice by urethane added to the drinking water and consumed at the rate of about 5 milligrams per day per mouse. The findings of this group differed in certain ways from the previous reports in the literature. Sequential sacrificing of groups of mice revealed that during the first 10 weeks of urethane

treatment a common inflammatory reaction of an interstitial pneumonic type occurred and that during the second 10 weeks a benign tumor developed. The tumor is described as solid or papillary in form and to consist of dark and clear cells. A description of the cells emphasized the presence of lamellar, myelin-like intracytoplasmic bodies. No mention was made of the presence of virus-like particles. Other findings were not remarkable.

In 1964, Kitamura (59) induced pulmonary adenomas in strains A and dd mice by intraperitoneal injection of urethane (amounts not reported). This author described, but did not illustrate, hyperplastic foci of alveolar epithelium in the early stages of tumor growth.

In addition to the above reports of tumors induced with urethane, electron microscope studies of lung adenomas induced by other carcinogens have also been reported.

Svoboda (57) induced mouse lung tumors by brushing a 0.6% solution of methylcholanthrene in benzene over the backs of unshaved mice, 3 times a week for 5 weeks. Mice were sacrificed from 21 - 50 weeks after the first painting. No differences could be found between the lung adenomas induced with methylcholanthrene and those produced by urethane.

Kitamura (59) induced mouse lung tumors by intraperitoneal injection of 20-methylcholanthrene, and also with isonicotinic acid hydrazid in newborn strain A and dd mice. The author noted that diffuse proliferating areas of alveolar epithelium developed before the formation of adenomas; however, these areas were not illustrated. Tumor cells illustrated were not identified as to carcinogen employed,

and revealed no new ultrastructural findings.

Hattori, Matsudo, and Wada (60), in 1965, reported an electron microscopic study of mouse lung adenomas induced in dd0 strain mice by: 1) intraperitoneal injection of 0.2 milliliters of a 1% solution of isonicotinic acid hydrazid -- a total of 60 milligrams given in 10 weeks, and 2) intraperitoneal injection of 0.2 milliliters of 5% urethane in saline -- a total dose of 100 milligrams in 10 weeks, followed by four consecutive, weekly, subcutaneous injections of 0.5 milligrams of 4-nitroquinoline 1-oxide in saline. These authors described the resultant tumor in much the same way as had the previous investigators. However, they pointed out that adenoma cells contained what was interpreted to be cholesterol crystals. These "crystals" corresponded in appearance to certain membrane bounded, needle or crescent shaped, empty clefts described and illustrated by Svoboda (57) in many tumor cells. Kitamura (59) had also noted these empty structures, and had also termed them cholesterol crystals.

## MATERIALS AND METHODS

Strain A (Heston) mice, obtained as A He/J strain mice from the Jackson Laboratory, Bar Harbor, Maine, were used throughout this study. Mice were housed in wire cages, with the exception that breeding mice and their offspring were housed in plastic cages with cedar shavings for bedding. All mice received Purina laboratory chow and tap water, except as noted.

Adult and young animals were killed by cervical dislocation. Very young animals were decapitated. Lung tissue was immediately removed from the mice for light and electron microscopic study. Tissue taken for light microscopy was fixed in 10% formalin, processed in a routine manner for paraffin embedding, and stained with haematoxylin and eosin. Tissues taken for electron microscopy were fixed in one of several fixatives: 1) 1% osmium tetroxide ( $\text{OsO}_4$ ), buffered with veronal-acetate, pH 7.4, with sucrose added (61), or 2) 1%  $\text{OsO}_4$ , buffered with phosphate, pH 7.4 (62), or 3) 1.33%  $\text{OsO}_4$ , buffered with s-collidine, pH 7.4 (63), or 4) 1.5% glutaraldehyde, buffered with 0.067 M cacodylate, pH 7.4, containing 1% sucrose, and 25 mg%  $\text{CaCl}_2$  (64 - 66), or 5) either a 1:1 or 3:2 mixture of 4) above with 1%  $\text{OsO}_4$ , buffered with 0.067 M cacodylate, pH 7.4, a variation on the method of Trump and Bulger (67). Fixation with any of the above solutions was carried out for 1 to 3 hours, either at melting ice or refrigerator temperature, except that tissues fixed by method 5) were always fixed for 1 hour at melting ice temperature. Tissues fixed by method 4) were washed in 0.2 M sucrose in 0.1 M cacodylate buffer for 24 hours or more, and postfixed in 1 or 2% osmium tetroxide either in cacodylate

or veronal-acetate buffers, for 2 hours. Some tissues fixed by method 5) were also rinsed in cacodylate-sucrose for 2 hours, and then post-fixed in 1%  $\text{OsO}_4$  for 2 more hours. Finally, a few tissues were fixed in a solution similar to that described in method 2), except that the pH of the solution was adjusted to 6.8. Half of these tissues were later postfixed in a mixture of 1% paraformaldehyde and 1% glutaraldehyde in phosphate buffer for 1 hour, a variation on a method suggested by Ross and Klebanoff (68).

Following fixation, the lung tissues were dehydrated in increasing concentrations of ethanol, starting at 50%, passed subsequently from 100% ethanol into propylene oxide, and embedded either in EPON 812 (Shell), or in Araldite (Durocupan-FLUKA) epoxy resins according to the methods of Luft (69).

Sections of plastic embedded tissue were produced with an LKB Ultratome or a Servall Porter-Blum II microtome using either glass or diamond knives. Thick sections, about 1 micron in thickness, were cut for light microscopic examination, and stained with an Azur II - methylene blue stain (70). Thinner sections, about 600 - 1000 Å in thickness, were mounted on coated or uncoated electron microscope specimen screens, and the sections treated for contrast enhancement with a saturated solution of uranyl acetate, and with Reynold's (71) basic lead citrate solution. Most sections, "stained" with the above solutions, were first treated with Reynold's solution, then with uranyl acetate, and finally once again with Reynold's solution. Sections were treated for various times with these contrasting agents. The resultant "stained" sections were examined either with an RCA EMU 3G electron microscope operated at 50 KV, with a 40 micron objective aperture, or



with a Philips EM 200 electron microscope operated at 60 KV, with a double condenser, anti-contamination cold-finger, and a 50 micron objective aperture.

Lung tissue was taken from the following groups of mice:

1) untreated mice of various ages, 2) young mice treated with urethane by injection, 3) young mice treated with urethane by administration in their drinking water, 4) neonatal and young mice born of mothers receiving urethane for various times either during or following pregnancy or during both periods, and 5) mothers of the previous group. In addition to tumor tissue, normal lung tissue was taken from all experimental groups of mice.

Group I. Older male mice used for breeding, older female breeders, and female mice that failed to conceive provided the source of lung tissue for "spontaneous" tumors. Mice in this group were sacrificed from 3 to 21 months of age and examined for lung tumors.

Group II. Four to eight week old mice, of both sexes, were given an intraperitoneal injection of a 10% solution of urethane in water at the rate of 1 milligram per gram body weight. All mice received only one injection. Pairs of mice, one male and one female, were sacrificed daily for the first week following injection, and thereafter weekly for a period of seven weeks. This experiment was repeated with a small group of 3 month old mice. Lung tissue was taken only during the first week following administration of urethane in this latter group.

Group III. Eleven week old mice, of both sexes, received a drinking water containing 0.1% urethane. Pairs of mice, one male and

one female, were sacrificed daily for the first seven days, and thereafter weekly for ten weeks. Untreated control mice were sacrificed, in pairs, at less frequent intervals.

Group IV. Pregnant females were given a solution of 0.1% urethane as their drinking water during various, defined periods during pregnancy, or following delivery, or during both times. Offspring from mothers treated in this manner were sacrificed, in pairs, at various ages up to eight weeks. Both normal and tumor tissue was taken from these young mice.

Group V. Mothers of Group IV animals were sacrificed from 6 to 9 months after receiving urethane in their drinking water. Duration of exposure to urethane in the drinking water varied from 3 to 28 days.

## RESULTS

## I. Gross and Light Microscopic Observations

## A. Untreated Mice (Group I)

More than 90% of the group had visible tumors by 12 months of age. Of this tumor group, about 10% had two to six tumors, about 20% had multiple tumors (more than six), and the remainder had single tumors. Single tumors varied in size from just barely visible to about 3 x 3 x 2 mm.

## B. Young Mice Injected with Urethane (Group II)

In this series of mice, small, but grossly visible, tumors were found in five mice in the sixth and seventh weeks following administration of urethane. Microscopically, with the exception of the tumors noted above, no effect of the urethane on the lungs could be detected.

## C. Young Mice Administered Urethane in Their Drinking Water (Group III)

In this series of mice, grossly visible tumors were found in four mice from the sixth to the tenth weeks. Microscopic tumors were detected from the fifth to the tenth weeks. Other than for the presence of these tumors, the experimental lungs did not appear to differ from the control lungs.

## D. Neonatal and Young Mice Born of Mothers Receiving Urethane in Their Drinking Water (Group IV)

Neonatal mice showed definite microscopic changes in their lungs. Week old, and older mice, receiving urethane in utero or from their mother's milk, or both, showed a mononuclear cell infiltration of the interalveolar septa. The nature of the infiltrating cell could not be

determined. The effect of the cell infiltration was to greatly increase the thickness of the interalveolar septa. In some cases, only part of the lungs were involved, in other cases, virtually all lobes were effected. Although this involvement appeared as an interstitial pneumonia, polymorphonuclear neutrophils were absent, and a positive identification of the infiltrating cells as lymphocytes could not be made.

Of 28 mice allowed to live longer than 4 weeks, grossly visible tumors occurred in 6 mice, 43 to 56 days old. Possible microscopic tumors were noted in 16 and 28 day old mice. Identification could not be certain in the latter cases, because there existed the likelihood that the "tumors" could also be very large foci of atypical infiltrating cells of the type noted above.

#### E. Mature Mice Receiving Urethane in Their Drinking Water (Group V)

All mice, mothers of those in Group IV, showed multiple tumors 6 to 9 months after receiving urethane in their drinking water.

#### F. Summary of General Observations Relating to All Groups

The gross appearance of a mouse lung having multiple tumors is shown in Figure 1. Single tumors appear as raised, pale colored, generally spherical bodies, ranging in size from barely visible to over 3 millimeters in diameter. Large, irregularly shaped tumors are frequently found and are thought to arise from the growing together of two or more adjacent tumors.

Tumors are found in any location in all lobes of the lung (Fig. 2). Only the very smallest tumors clearly show the basic papillary form

of growth. A tumor as small as that shown in Figure 3 already appears solid, and the pattern of growth is difficult to determine. At higher magnifications (Fig. 4), it can be seen that the tumor grows as double sheets or columns of cuboidal to low columnar cells. Only an occasional rounded end of such cell columns gives a hint of the original papillary pattern of growth. Sheets of tumor cells growing into normal alveolar spaces could be seen at the edge of the tumors. Older tumors were identifiable by the pleomorphic features of the tumor cells, and especially by vacuolization of the nuclei. Mitoses were very infrequent in all tumors. The stroma underlying the columns of adenoma cells was thin and inconspicuous. No capsule surrounded the tumors, but some alveoli adjacent to the growing edge of the tumors were compressed or distorted. There was no obvious reaction by the normal lung tissue to the tumors.

## II. Electron Microscopic Observations

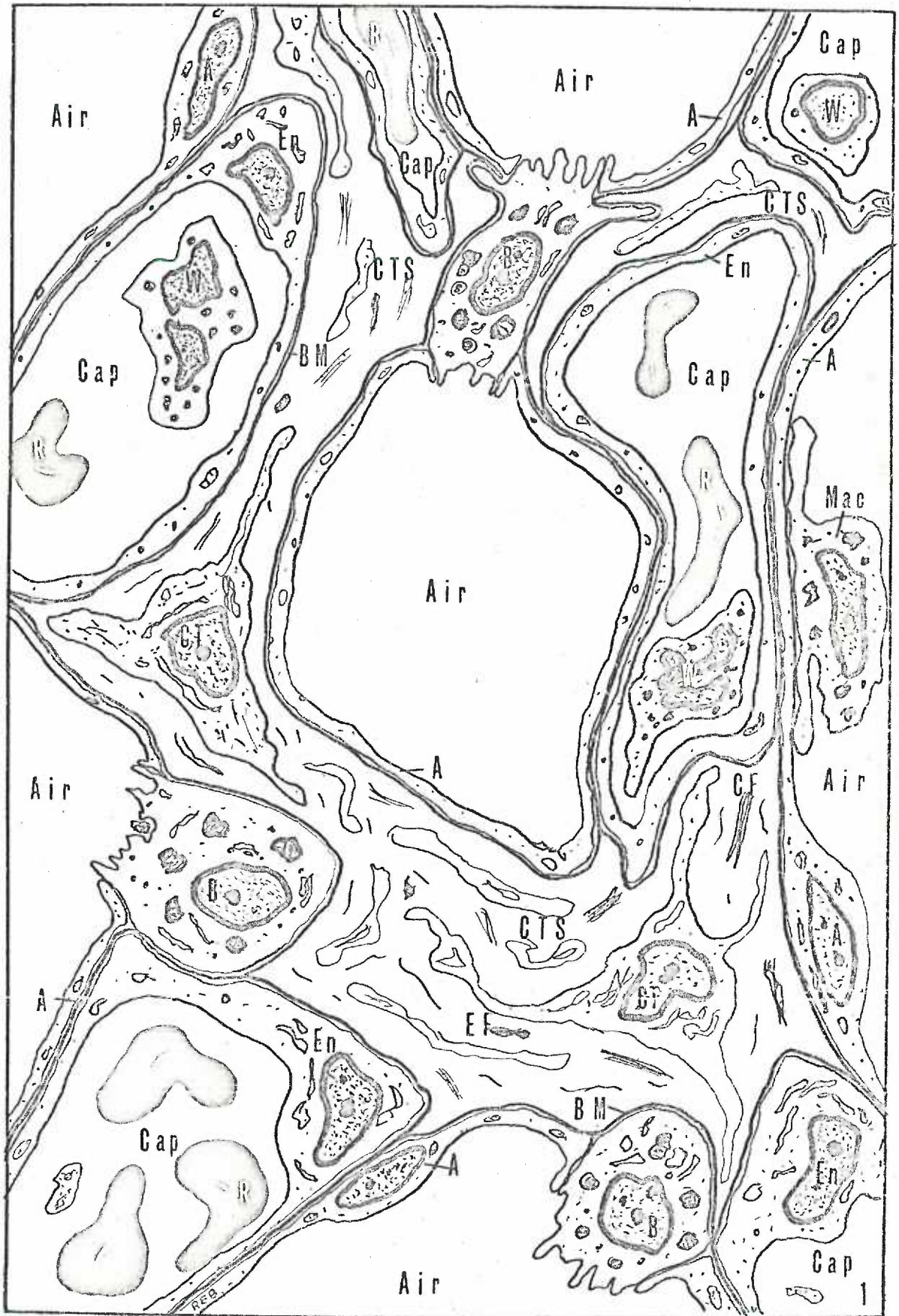
### A. Normal and Tumor Tissue -- Effect of Fixation

While the effect of fixation on many components of the cell is not known, certain classes of substances are poorly preserved by most commonly used fixatives. Since variation in the structure of certain cell components in the material in this study was found, Figures 5 - 18 illustrate examples of both normal and tumor tissue preserved with several different fixative solutions. These preliminary figures are intended to show structural variation incident to fixation and to introduce the reader to the comparative ultrastructure of normal mouse lung and the alveolar cell adenoma.

The alveoli of the lung consist of epithelial-lined air spaces (see Text-Fig. 1 on page 28). The walls or septa of these spaces are populated by connective tissue cells and contain extracellular connective elements (collagen and elastic fibers) as well as endothelial-lined blood capillaries. The lumen of the capillary is separated from alveolar air by a thin layer of endothelium, a narrow basement membrane, and an attenuated layer of epithelium. In the mouse, this triple layer may be one micron or less thick. The epithelium consists, for the most part, of plate-like cells -- the type A alveolar cells. A second epithelial cell, the type B cell, is cuboidal to low columnar in shape and is found scattered singly between the type A cells, often at points of alveolar angulation or deep in niches within the alveolar wall. In some cases, the type B cell appears to extend completely across the alveolar wall to border on two different alveolar air spaces. Examples are found where the type B cell appears to have been caught while moving by extension and penetration through an alveolar septum from one air space to an adjacent one.

Both the type A and B cells rest on a continuous basement membrane which separates the epithelium from the mesenchymal tissue. The junction between type A cells is one of simple overlapping, with a "tight junction seal" at the lumen. The junction between type A and type B cells is usually in the form of a "cuff" consisting of type A cytoplasm extending up along the sides of the type B cell for a distance of about one micron. A "tight junction seal" occurs between these two cell types at the end of the junction.







Alveolar macrophages are relatively numerous in normal mouse lung. These cells have never been observed to be in contact with the basement membrane, but rather are separated from it by an intervening layer of either type A or type B alveolar cell cytoplasm. No septal macrophages have been observed in normal mouse lung, and alveolar macrophages are not apparently derived from either the two alveolar cell types, or from blood cells. Therefore, the origin of the alveolar macrophage is, at present, uncertain. For further information on normal lung ultrastructure, articles by Brooks (72, 73), and Sorokin (74) should be consulted.

Because the cytosome, a cytoplasmic organelle found in the tissues under study, serves as a marker, consideration of this structure, as it is effected by fixation, will be made first.

It is evident that the cytosomes present in both the type B alveolar cells (Figs. 5-10), and the pulmonary adenoma cells (Figs. 11-13) appear remarkably similar in sections from tissues preserved with the same fixative. The cytosome is an irregular, oval, or rounded, membrane-enclosed body having a maximum diameter of about 1.5 microns. It may be composed of myelin-like, osmiophilic, approximately parallel lamelli arranged concentrically in one plane (Fig. 5). When a collidine buffered osmium fixative is used (Fig. 6), the osmiophilic lamelli are virtually absent from the cytosome, indicating an extraction of certain substances by this fixative. Nevertheless, it can be observed that some dense material remains at the periphery of the cytosome and has not been extracted (Fig. 7).

A rather pronounced vacuolization and disruption of the cytosomes can occur with the same fixative in cells that demonstrate good fixation of other cell organelles (Fig. 8).

The aldehyde-based fixatives employed in this study generally fail to preserve cytosomal structure in normal, type B cells (Figs. 9, 10). This is usually less true for tumor cell cytosomes (Figs. 11 - 13), suggesting an apparent difference in composition of the type B and tumor cell cytosomes. An example is seen in Figure 11 where a dense, membrane-enclosed body, interpreted as a cytosome, appears markedly different from the adjacent lamelli-containing cytosomes. The interpretation above is further supported by findings in other aldehyde fixed tumor cells (Figs. 14, 16, 17). With the use of aldehyde-based fixatives, the cytosomes of tumor cells are frequently non-lamellar. In fact, they commonly have a solid composition and appear to be made up of two or more components. In addition, a dense crystalloid (Fig. 16) may appear in some cytosomes.

In addition to the ubiquitous cytosomes, both the type B alveolar and tumor cells are characterized by numerous mitochondria, multi-vesicular bodies, a widespread Golgi apparatus (or multiple Golgi regions), and a moderate amount of granular endoplasmic reticulum. Agranular reticulum does not occur in these cell types, with the exception possibly of some membranous material near the Golgi regions which could be considered to be agranular reticulum. Numerous small vesicles, some coated (fuzzy vesicles, alveolate vesicles, etc.), occur throughout the cytoplasm, but are mainly found near the Golgi membranes and plasma membrane (outer cell membrane). The plasma membrane of the apical portion of both cell types almost always takes the form of

irregularly shaped, short microvilli. An unusual form of what is considered to be granular endoplasmic reticulum -- but may be agranular reticulum -- is found in many of these cells (Figs. 5, 19). In one plane of section, it may take the form of a long U, the body of the U being the dilated cisternae of the reticulum; while in cross section, this structure appears ring- or cup-shaped. Various clefts, or open spaces, can be noted in the type B cells (Fig. 19). Such clefts may be related to the structure noted above, and both clefting and dilatation of the cisternae may be artifacts produced by the fixatives used.

Alveolar macrophages, whether in normal lung (Fig. 7) or in tumor (Fig. 14) show identical features. The macrophages are very active cells which may have almost the same types and number of cytoplasmic organelles as do the type B alveolar cells or tumor cells. Because of this, in some sections, macrophages may be confused with type B or tumor cells. The main points of difference between these cells are the presence of pleomorphic cytoplasmic inclusions consistent with mycoplasma within the macrophage cytoplasm, and the usually greater numbers of cytosomes in the epithelial cells. However, cytosomes, having the same appearance as in type B alveolar or tumor cells, are also observed in macrophages. A further distinguishing feature is the blunt cytoplasmic projections, and pseudopods of the macrophage. As already noted, both the type B alveolar and tumor cells are characterized by short, narrow surface microvilli.

#### B. Effect of Injected Urethane

Mice receiving urethane by intraperitoneal injection did not

show recognizable cellular alterations. The alveolar cells were not detectably different from those seen in Group III mice. Moreover, tumors forming in mice 6 to 7 weeks after urethane administration were similar in ultrastructure to both spontaneous and induced tumors found in the other groups of mice. Accordingly, lung cells from Group II mice have not been illustrated in this report.

C. Effect, on Young Mice, of Urethane Administered in  
Drinking Water

Type B cells from mice receiving urethane for 2, 4, and 6 days (Figs. 19, 22, 23), and a type A cell from a mouse receiving urethane for 4 days (Fig. 21) are illustrated. No ultrastructural effect of the urethane treatment can be detected. Tumor cells (Fig. 24), from a tumor occurring in a mouse of this series treated with urethane for 8 weeks, show the same characteristics as cells of induced and "spontaneous" tumors to be described in later sections. The tumor cells in Figure 24 are located at the edge of normal lung. It is noted that the junction formed by type A cell and tumor cell is the same as that between type A and normal type B cells, namely, a long, cuff-type junction.

D. Effect, on Mature Mice, of Urethane Administered in  
Drinking Water

Tumor cells from these Group V mice are illustrated in Figs. 25 and 26. Large tumors in older animals are made up, for the most part, of active cells similar to those illustrated. However, some degenerating cells can always be found in these tumors. Such cells, although retaining many cytosomes, mitochondria, and other organelles, are

recognized by vacuolization of the nuclei, and reduction in the number of ribosomes and cell organelles. Inclusions within the nuclei are common findings in tumor cells (Fig. 25). Such inclusions may give rise to the vacuolization found in degenerating cell nuclei.

Some cytosomes are clearly made up of several components. Two cytosomes indicated in a tumor cell in Figure 26 have at least three components: a dense lamellar or crystalloid portion, a membrane-enclosed vesicular portion, and a finely granular matrix.

The Golgi and endoplasmic reticulum cisternae tend to be dilated in some tumor cells (Fig. 26). Numerous small vesicles are consistently observed near the Golgi regions.

In addition to typical organelles, structures that can not be readily identified are occasionally encountered. One such structure occurs in a tumor cell illustrated in Figure 25. This is a large, membrane-delimited mass presenting a "moth-eaten" appearance.

Tumor cells are joined by short, interdigitating cytoplasmic processes alternating with parallel stretches of closely apposed membranes, and are joined at their apical margins by a tight junction. This mode of attachment can not be compared to the normal case, as no instance of two adjacent type B alveolar cells has been observed in normal mouse lung. It is reasonable to believe that type B cells divide from time to time; however, such divisions have not been observed in normal lung examined with the electron microscope.

#### E. Effect, on Young Mice, of Urethane Administered in Maternal Drinking Water

Because the effect of carcinogens is thought to be more acute

for young animals, the major emphasis in this study has been placed on neonatal mice which indirectly received urethane in utero and on suckling mice receiving urethane from their mother's milk.

As noted by light microscopy, treatment of the mothers with urethane tended to produce a thickened alveolar septum in the lungs of their offspring. The nature of the cells causing this thickening could not definitely be determined by light microscopy. However, on electron microscopic examination, the cells involved are recognized to be normal connective tissue cells -- fibroblasts (Fig. 27). An examination of a number of normal and urethane treated neonatal mouse lungs suggests that urethane tends to slow down the normal thinning of the alveolar wall. At birth, the alveolar septa are considerably thicker than they are in adult lung. Normally, almost all of the reduction in wall thickness takes place in the first few days of life; while, in urethane treated mice, this reduction extends over several weeks, but eventually reaches that seen in normal lung.

The cells shown in Figure 27, from a seven day old mouse treated with urethane for six days in utero, do not have characteristics that would distinguish them from similar cells in untreated mice.

The type B cells of urethane treated young mice have the usual cytosomes, multivesicular bodies, and other cell organelles typical of this cell type (Figs. 28-30). There is no evidence of either diminution or increase in cellular activity, as would be reflected by cytoplasmic alteration.

Similarly, the alveolar macrophages from these Group IV mice do not show evidence of being effected by urethane (Fig. 31). The macrophages are particularly active during the neonatal period when

there is usually an increased discharge or sloughing off of materials into the air spaces. Cytoplasmic bodies thought to be mycoplasma appear in the macrophages within the first week of life.

Gross tumors occur in the young urethane-treated mice in the sixth week of life, and microscopic tumors are present earlier. Tumor cells from six and eight week old mice are shown in Figures 32 through 42.

As previously noted, the tumor cells grow in sheets (Figs. 32, 33) around a thin stromal core containing connective tissue cells and capillaries. The cells are joined together in the manner previously described.

At low magnification, where many cells can be observed (Figs. 33, 34), it is evident that tumor cell cytosomes are pleomorphic. This structural complexity is even more clearly seen at moderate magnifications (Fig. 35,36). The exact form taken by the tumor cell cytosomes is not entirely dependent on the fixative used, because the same fixative may produce different results. It is probable that other factors, such as depth of cell in the tissue block, location of the cell with respect to air spaces, and alteration of fixative by certain cell products, might cause the structural variation noted in different cells.

The angular, crystalloid nature of the dense portion of the cytosome is illustrated in Figures 37-39, and 41. The differences in crystalloid structure are well seen in Figure 38 where small, large, and multiple crystalloids are found within the several cytosomes of one cell. The relatively large number of multivesicular

bodies, Golgi regions, and granular endoplasmic reticulum profiles in tumor cells indicate the very close structural similarity between these cells and the type B alveolar cells. However, the presence of fine cytoplasmic fibrils (Fig. 39) in some osmium-fixed tumor cells represents one possible difference between these two cell types. Fibrils of this size appear to be confined to the apical border (terminal web) in the normal type B cells.

A side-by-side comparison of tumor cells and macrophages (Fig. 41) reveals that, in addition to the several differences already described, the cytoplasm of the tumor cells is more dense than that of the macrophages; probably as a result of a lesser concentration of cytoplasmic constituents per unit volume of macrophage cytoplasm. A source of possible confusion in the identification of these cells relates to the similarity between certain forms of mycoplasma in macrophages, and peculiar sections of cytosomes in type B and tumor cells (Fig. 42). When the cytosome is sectioned through its dense portion, the resulting membrane-bounded, often curved, dark body could be mistaken for an elementary or dense-body form of mycoplasma.

#### F. "Spontaneous" tumors of Older Mice

The ultrastructural characteristics of cells from "spontaneously" occurring tumors of 12, 16, and 21 month old mice are illustrated in Figures 43-46, and 48. At the electron microscopic level, it may be seen that the tumor cells from this group of mice are similar to those in the urethane induced tumors previously illustrated.

#### G. Relation of the Multivesicular Body to the Cytosome

Evidence relating the multivesicular body to the cytosome of



normal type B alveolar cells has been reported by Sorokin (74). The findings of the present study are corroborative in this respect. The same relation would be expected in tumor cells. Micrographs pertaining to these two cytoplasmic organelles are presented as Figures 47 through 54.

The origin of the vesicles found in the multivesicular bodies is suggested both by invagination of the plasma membrane (Fig. 47), and by vesicular "budding off" from the Golgi membranes (Figs. 46 and 51). However, the mechanism for assembling the vesicles into a membrane enclosed body is not apparent. One possibility, suggested by the irregular outline of a multivesicular body shown in Fig. 51 (hollow arrow), is that vesicles may accumulate in a loose grouping, with the outermost ones rupturing and their membranes joining to become an envelope for the innermost vesicles (see also Fig. 64).

The appearance of a multivesicular-like component in the cytosome is shown in Figures 47 through 49, 51, and 54. Based on this type of observation, Sorokin (74) has suggested the derivation of the cytosome from the multivesicular body. Possibly an intermediate stage is revealed by the different densities noted in multivesicular bodies (for example, see Fig. 50). However, if this is true, it is not clear how the pleomorphic cytosomes (Fig. 51, solid arrows) fit into the postulated sequence of changes. The nature of this sequence is further confused by the difference in cytosome structure following aldehyde-osmium combination fixation (Fig. 52). Here, the internal vesicles contain a very dense substance, while the surrounding matrix material is less dense.

At higher magnification (Fig. 54), osmium fixed cytosomes contain

vesicles loosely filled with fine granular or filamentous material, a zone of parallel, osmiophilic lamelli in loose array, and a dense matrix substance in which may be found an even denser crystalloid mass.

#### H. Crystalline Structure of a Component of the Tumor Cell Cytosome

A crystalloid component of the tumor cell cytosome can be visualized following either osmium or glutaraldehyde fixation (Figs. 55-60); however, the fine structure of the crystalloid is best revealed when the latter fixative is used (Figs. 56-60). At high magnification, the crystalloid is seen to be made up of dark and light bands, each approximately  $33 \text{ \AA}$  wide. This crystalloid is either not preserved, or is not present in normal type B alveolar cells, and therefore provides a basis for differentiating normal type B cells from tumor cells. However, it has been noted that tumor cells that face what appear to be functional air spaces usually do not have cytosomes containing crystalloids.

#### I. Special Cytoplasmic Structures of Tumor Cells

Because the purpose of this study is to find differences between the normal type B alveolar cells and the relatively well differentiated adenoma cells, any structural feature found in one and not the other should be recorded.

The presence of what are interpreted to be masses of glycogen particles can be found in some tumor cells (Figs. 60-62). Such masses are not present in all sections of tumor cells. The glycogen may be in the form of discrete particles (Figs. 60, 61), or in clumps of particles surrounded by a relatively homogeneous electron-lucent

matrix material (Fig. 62). As is seen in Figure 60, the glycogen may occur in relation to membranes. The origin of these membranes cannot be readily determined, but there is little resemblance to the granular endoplasmic reticulum. The empty spaces adjacent to these membranes in Figure 60 are probably artifactual.

The apparent discharge of cytosomal material into an alveolar air space (Fig. 63) is not an unusual feature in either tumor cells or type B cells, but is pointed out here because the cytosome is being "discharged" into a non-functional air space as judged by the cytoplasmic debris observed in the space.

As already shown, glutaraldehyde fixation causes the various cytoplasmic components to have different appearances. The multivesicular body is evidently very sensitive to fixation and may present markedly different structures. The glutaraldehyde fixed cell illustrated in Figure 64 contains several organelles considered to be multivesicular bodies. The bodies in question have very irregular borders and contain homogeneous material in addition to the vesicles. One multivesicular body (hollow arrow) appears to be forming in the manner previously suggested, that is, from fusing vesicles. However, an alternate interpretation, based on the example in this illustration, is that uncoated vesicles fuse around coated vesicles to give the final multivesicular body.

Vacuolization of the tumor cell nuclei, previously referred to, is illustrated in Figure 65. The cell shown appears to be bi-nucleated. This is not an uncommon finding in the mouse lung tumor and has been observed by many light microscopists and is ascribed by some to amitotic division. The nuclei of the cell illustrated in Figure 65

has several types of "inclusions"; some are probably true inclusions, while others may be portions of cytoplasm surrounded by projections of the convoluted nucleus. It must be noted, however, that certain oval inclusions have a regularity of form and type of structure suggestive of bacterial spores. The cell depicted provides an example of possible degeneration; however, the mitochondria, cytosomes, and multivesicular bodies appear to be normal.

#### J. Type B Alveolar Cells in Tumorous Lungs

It is desirable to illustrate type B cells from lungs of tumor-bearing mice (Figs. 66, 67). Cells of this type might have been expected to show evidence of some alteration caused either by urethane, or possibly by substances given off by tumor cells. However, the type B cells from mice with "spontaneously" occurring tumors (Fig. 66), or from urethane induced tumors (Fig. 67) appear to be normal. An opportunity to compare what is thought to be a normal type B cell with an adjacent tumor cell is afforded by Figure 67. The major difference seen relates to the greater cytoplasmic density of the tumor cell, in part due to larger numbers of ribosomes.

One of the more unusual findings seen in the tumors is that of semi-attenuation by a cell, either a type B or a tumor cell, adjacent to blood capillaries -- in possible imitation of the functional capability of the type A alveolar cell (Fig. 68). This picture is encountered so rarely that further comment must await further data.

#### K. Macrophages in Tumors

This final section, on macrophages in tumors, is included because of the close spatial relationship that exists between tumor

cell and macrophage (Figs. 69-71, 73, and 74). The variety of intracytoplasmic membrane forms (Figs. 69-71) reflects the role of the macrophage as a scavenger.

Means for distinguishing tumor cell from macrophage have already been described, and features that may confuse the distinction have been noted. A further feature in this latter category is illustrated in Figures 71 and 72. Here, an unknown structure, made up of highly convoluted membranes, or tubules, shows a similarity in structure, if allowance is made for the difference in fixation of the cells and magnifications of the pictures.

The presence of mycoplasma in such great abundance in alveolar macrophages (Figs. 73, 74) cannot help but raise the question as to whether these infectious organisms may play a role in tumorigenesis. If such a relation exists, however, no ultrastructural evidence can be found in its support.

## DISCUSSION

## I. The Mouse Lung Tumor Cell -- Morphological Considerations

Tumor cells grow as epithelial sheets with "tight junction seals" at the apical border between cells and are elsewhere held together by interdigitating cellular projections and long stretches of closely apposed parallel membranes that resemble the adhering zonules of Farquhar and Palade (75). Desmosomes have not been seen between tumor cells. In general, the adenoma presents the appearance of what may be imagined to be a field of hyperplastic type B alveolar cells. However, one major characteristic of hyperplasia, an increase in the number of mitotic figures, is missing. In many hundreds of thin sections of lung tumor examined, no mitotic figures have been observed. This parallels the experience of light microscopists who have consistently noted the dearth of mitotic figures in the mouse lung tumor. These features, in addition to those to be discussed, combine to give the impression that the mouse lung adenoma is a slow-growing, well differentiated, essentially benign tumor.

Type B cells and tumor cells both contain numerous pleomorphic cytosomes, mitochondria, a very widespread Golgi apparatus, as well as small to moderate amounts of granular endoplasmic reticulum. Multi-vesicular bodies are present in relatively great numbers, as are various coated and uncoated cytoplasmic vesicles. In addition, the apical surface of both cell types is covered with many short, irregularly shaped microvilli.

The cytosome characterizes both cell types, and serves to

distinguish them from other cells in the lung. When tumor cells and normal type B cells are treated with the same fixative, the cytosomes usually appear identical in structure. The cytosome is most typically preserved as a membrane-bounded, oval or round body, about one-half micron in diameter, containing roughly parallel osmiophilic lamelli. Occasionally, the lamelli are concentrically arranged, but in some cases cytosomes are virtually devoid of lamelli or other materials. The lamellar material appears to be discharged into the alveolar air spaces, and remnants of such material can frequently be found in the air spaces, or phagocytized by alveolar macrophages.

Cytosomes are often more complex in structure than described above. Frequently, a thin rim of dense, non-lamellar material lines the inside of the cytosome membrane. Cytosomal structure preserved by osmium fixation is perhaps best seen in Figure 54. Here, it is evident that the cytosome has lamellar, vesicular, and matrix components. In addition, a crystalloid component occurs in many tumor cell cytosomes (see Figs. 54 and 55). Following glutaraldehyde-osmium combined fixation, however, the cytosome is observed to have a somewhat different structure, best seen in Figures 53, 56, and 57. Here, varying sized vesicles, some empty and some filled with a dark material, are found; but, osmiophilic lamelli are not present; and, crystalloids of different sizes are observed. Finally, a relatively homogeneous, dense matrix substance, somewhat pocked by empty spaces (possibly an artifact of fixation), surrounds the other elements of the cytosome.

Sorokin (74) has attempted to reconstruct, for the type B cell, a sequence of pictures purporting to show morphological changes leading from the multivesicular body to the cytosome. His presentation is convincing, and the postulated derivation of cytosome from multivesicular body is used as a basis for further discussion. In this regard, it should be recalled that several illustrations in this thesis tend to corroborate Sorokin's concept (see for example, Figs. 41, 42, 46, 48).

The multivesicular body in the type B cell is thought by Sorokin(74) to originate from Golgi vesicles. This origin has also been suggested by others for other cell types (see (66) and (76) for recent discussions of this question). However, the multivesicular body may also originate from vesicles (coated vesicles) pinched off at the cell surface and passed into the cytoplasm. Examples of both mechanisms can be found in illustrations presented in this thesis (see Fig. 51 for the former and Fig. 47 for the latter case.

Because the multivesicular body occurs in many different cell types, various opinions as to their origin and function have been expressed. Sotelo and Porter (77), who coined the name multivesicular body, noted and described this structure in the cytoplasm of the rat ovum. These investigators pointed out that a similar structure had already been described in seven previous articles and concluded from these several findings that multivesicular bodies "... occur normally as a constant component in animal cells." From their own study, the small vesicles within the body were thought to be discharged into the cytoplasm, inasmuch as the multivesicular bodies were often found



surrounded by many small vesicles of the same size as those within the body, and in addition, examples of partially opened bodies were noted. A dark, vesicle-containing, inner component, termed a nucleoid, was found in some multivesicular bodies. No function was ascribed to the multivesicular body by these authors, but the opinion was expressed that they were self-reproducing.

Palay (78) described multivesicular bodies in secretory neurons of the goldfish preoptic nucleus. In these neurons, the multivesicular body was tentatively postulated to give rise to the large, membrane-enclosed neurosecretory droplet synthesized by these cells.

Farquhar and Palade (79) found that when ferritin was administered intravenously to rats a phagocytic mesangial cell of the kidney glomerulus took up the ferritin, some of which became located in multivesicular bodies.

In an experiment designed to determine if the neurons of spinal ganglia could take up ferritin, Rosenbluth and Wissig (80) injected ferritin intraperitoneally into toad lumbar ganglia and also incubated excised toad lumbar ganglia in solutions containing ferritin. It was found that a small amount of ferritin crossed two barriers (sheath cells and basement membrane) to become incorporated into neurons, both under in vivo and in vitro conditions. Coated vesicles, derived from plasma membrane invaginations were found to contain ferritin particles. Other coated vesicles within the cytoplasm were observed to contain smaller vesicles of a size similar to that found in multivesicular bodies. In addition, ferritin particles were noted in fully formed multivesicular bodies. Other coated vesicles were seen to have a long cisternal extension or neck (pedunculated coated

vesicles), and intermediates between this structure and multivesicular bodies were illustrated. Some of these latter structures are not unlike those illustrated in Figure 64. It is probably of significance that ferritin was found only in coated vesicles and multivesicular bodies in the neurons examined by Rosenbluth and Wissig. These authors concluded that the function of the multivesicular body was "... the uptake and sequestration of macromolecular material from the environment of the neurons." If this interpretation is correct, it is somewhat puzzling that the neuron would have a mechanism to incorporate extraneous materials, inasmuch as such materials would act as a cytoplasmic burden which would be added to the burden already caused by autophagic processes within the cell. However, it may be that ferritin was taken up incidentally, and that other necessary substances are brought into the cytoplasm by the postulated mechanism. In any case, it remains unclear what necessary metabolites are brought into the cell in this manner, and how they are utilized once they are incorporated within multivesicular bodies.

Robbins, Marcus, and Gonatas (81) incubated HeLa tissue culture cells in a medium containing the fluorescent dye acridine orange in order to determine the nature of the acridine orange stained cytoplasmic particles found in these cells. It was learned that the acridine orange became incorporated into membrane-bound bodies, many of which resembled multivesicular bodies. It was thought that intermediate forms between the two structures could be recognized. Many of the dye-containing structures illustrated are remarkably similar in appearance to the cytosomes of the lung cells.

Gordon, Miller, and Bensch (82) treated strain L (Earle) tissue culture cells with a coacervate containing herring sperm DNA, gelatin, and colloidal gold by adding this mixture to the culture medium. The cells were found to take up this material and incorporate it into phagocytic vacuoles. The colloidal gold, being undigestible, served as a marker. The gold became localized in dense bodies and multivesicular bodies. These investigators suggested that the multivesicular body represents an intermediate structure related to intracellular digestion of both endogenous and exogenous substances, inasmuch as substances derived from degenerate cell organelles as well as those introduced by phagocytosis were thought to be seen in multivesicular bodies. The final stage in the digestive process was thought to be represented structurally by a dense body (residual body, lipofuscin-containing body, etc.) filled with unassimilable materials.

Merker (83) administered croton oil vaginally to rats and found that the vaginal epithelium responded by a very marked increase in multivesicular and dense bodies, as well as structures intermediate in appearance between the two. Merker concluded that the multivesicular bodies were specialized lysosomes related to the digestion of certain types of phagocytized substances.

These several studies suggest that the multivesicular bodies are almost certainly lysosomal in nature; perhaps, they are pre-lysosomes. De Duve, who originated the term lysosome, has recently reviewed the subject with Wattiaux (84). These authors list and discuss many functions attributed to lysosomes. As it is likely that the type B and tumor cell cytosome is lysosomal in derivation, it is of interest to note that De Duve and Wattiaux include the possibility

that some cells "... may possess a mechanism for unloading their lysosomes as a means, not of eliminating residues, but of discharging active enzymes into the extracellular spaces. Such a process would have the character of a secretion rather than of an excretion." Also, these authors state that, "In general, it may be said that all cells lining body cavities are engaged in pinocytotic processes followed by the lysosomal digestion of the engulfed products.... In some particular cases, the peculiarities of synthesis and breakdown lead to the formation of new products endowed with special biological properties...."

Balis and Conen (85) reported a cytochemical study on developing rat, and postmortem human newborn lung. These investigators described the localization of acid phosphatase to Golgi lamelli, some multi-vesicular bodies, and some cytosomes of type B alveolar cells. The acid phosphatase reaction product was not found in cytosomes being extruded from the cell, or in lamellar material in the air spaces. This study would appear to assure a lysosomal derivation for the alveolar cell cytosomes. Similar findings have been reported by Hatasa and Nakamura (86).

A crystalloid component of the type B cell cytosome has not as yet been reported in the literature, and none were found in the type B cell cytosomes in the material studied in this thesis. However, previously reported electron microscopic studies of the mouse lung tumor, although dealing with osmium fixed tissue, have similarly not described a cytosomal crystalloid. This failure most probably relates to tissue preservation rather than to basic cellular differences

between different groups of mice. The failure to find a crystalloid component in the normal type B alveolar cell in this study may be similarly caused. It is altogether conceivable that a cytosomal crystalloid is present in life in this cell type but is not successfully preserved by the fixatives so far employed.

The crystalloid may be suggested to be equivalent to the osmiophilic lamelli. This supposition is supported by the absence of lamelli in glutaraldehyde-osmium fixed tumor tissue, and their apparent replacement by the crystalloid. In addition, "fraying" at the edge of the crystalloid produces bands somewhat similar to the lamelli seen with other fixatives.

Whereas, cytosomal crystalloids have not been previously described, the U-shaped infolding of the endoplasmic reticulum noted in both type B alveolar and tumor cells has also been observed by Svoboda (52), who termed this structure a "cytoplasmic sequestration." Its conformation may result from an accumulation of a special secretory material within the endoplasmic reticulum, which is lost during tissue preparation. The identification of this membrane-bound, U-shaped structure as part of the granular endoplasmic reticulum is based on the finding of scattered ribosomes along the membranes. It is possible, however, that this ribosomal localization may be fortuitous, and the membranes may belong to the agranular reticulum system or may be an intermediate between the two systems.

The presence of empty spaces or clefts in the cytoplasm has also been noted by Svoboda (52), as well as by Kitamura (59), and by Hattori et al (60). They are considered by the last two groups of

authors to be "cholesterol clefts." Structures similar to these have also been described in foam cells in coronary artery plaques of rabbits fed cholesterol in their diets (87).

Glycogen occurs in many cell types, but the presence of masses of glycogen in a cell usually denotes a pathological process. The accumulation of large numbers of glycogen particles, either singly or in rosettes (Figs. 60, 61), or as membrane-bound "pools" (Fig. 62) may result from different biochemical lesions. Glycogen in membrane-enclosed masses has been described by Baudhuin, Hers, and Loeb (88), and Cardiff (89) in Pompe's disease. Excess glycogen produced by a cell is thought to be taken up by lysosomes and broken down by the enzyme alpha glucosidase which is found only in these bodies (88). In Pompe's disease (also known as type II glycogenosis), this enzyme is suspected to be absent.

Alveolar cells have not previously been described to contain glycogen. Moreover, most adenoma cells do not contain glycogen. It is possible that alpha glucosidase is not normally produced by the type B cells, or the derivative tumor cells. This would account for the accumulation of glycogen in membrane-bound bodies in the tumor cells but would not account for the presence of excess glycogen in the first place. The absence of an enzyme related to the normal catabolism of glycogen would result in abnormal accumulations of glycogen which would be taken up by lysosomes. Such an enzyme deficit in a small percentage of tumor cells might well be the result of the appearance of "spontaneous" mutants. Other possibilities, of course, exist and no conclusions can definitively be drawn without further investigation.

Before leaving this subject, it should be mentioned that glycogen masses were previously observed by other investigators in mouse lung tumor cells and variously identified. Klärner and Giesecking (55) thought the particle-filled pools, such as are illustrated in Figure 62, were cytoplasmic inclusions of viral origin. Svoboda (57), noting the same structures, denied the viral possibility, suggesting instead that the particles were "... ribonucleoprotein particles lying within dilated cisternae...." Such an interpretation seems improbable. Hattori et al (60) noted the same particles and pointed out that their affinity for lead resembled glycogen particles; however, these investigators rejected this identification by finding that glutaraldehyde fixed tissues, when incubated with saliva, retained the particles. Their histochemical findings were, however, not illustrated.

Inasmuch as a histochemical determination for glycogen was not carried out in this work, identification of the particulate material illustrated in Figures 60 to 62 as glycogen is morphological and depends on the similarity in appearance of these particles to glycogen illustrated by other investigators (88, 89).

Misidentification of alveolar macrophages with type B alveolar cells or tumor cells has not infrequently occurred in the literature. Svoboda (57), in his ultrastructural study of the mouse pulmonary adenoma, illustrates two cells containing many mycoplasma and identifies these cells as tumor cells. Recognizing that the particles may have been phagocytized, Svoboda suggested that the alveolar epithelial cells could function as fixed macrophages. Klärner and Giesecking (55) have also identified a portion of a cell containing mycoplasma as a

degenerating tumor cell having "microbodies".

The fact that the correct identification of alveolar macrophages in pulmonary adenomas of the mouse is not always easy has previously been discussed. The principal result of misidentification is that the description of the tumor cell becomes needlessly and misleadingly complicated. It should be pointed out, however, that the identification of mycoplasma in alveolar macrophages, one of the most distinguishing features of these cells, could not safely be made on a morphological basis alone prior to 1966. In that year, Organick, Siegesmund, and Lutsky (90) published an ultrastructural study of pulmonary pneumonia produced in germ free (gnotobiotic) mice by intranasal inoculation of Mycoplasma pulmonis. This report illustrated several mouse lung cells containing mature and elementary body forms of mycoplasma. Unfortunately, an alveolar macrophage, containing elementary bodies of the organism, was misidentified as a "granular pneumonocyte", another name for the type B alveolar cell. Moreover, other cells containing elementary bodies were not identified at all. Nevertheless, this report provides a satisfactory basis for recognition of mycoplasma.

### II. The Mouse Lung Tumor Cell -- General Considerations

The ultrastructure of the type B alveolar cell and the mouse lung tumor cell is very similar. This similarity strongly suggests that the latter is derived from the former, and from no other cell type.

The function of the type B cell is not yet definitely known. However, it is reasonable to assume that the cell's function is one of secretion. The evidence for secretion is based on ultrastructural evidence of discharge of cytosomal material and on the abundance of



Golgi membranes, endoplasmic reticulum, vesicles, and cytosomes in the cytoplasm. Since tumor cells generally show the same features as those of the type B cell, it seems reasonable that they have retained the capacity for secretion.

The question arises, however, as to the nature of the type B alveolar cell secretory product. In recent years, there has accumulated a substantial literature based on the concept that the alveoli are lined by a thin layer of some substance that acts to reduce the surface tension of an assumed layer of tissue fluid covering the alveolar cells (see (91) and (92) for references on this subject). Such a surface tension-reducing substance is termed a surfactant. The argument offered by the advocates of this concept is that when the effect of surface tension at the moist alveolar surface is taken into consideration, the balance of pressures that exist at the alveolar interface would allow plasma to seep out of the capillaries and into the air spaces. Because this leakage does not take place in normal lung, it is concluded that the surface tension at the alveolar surface must be reduced by the presence of a surfactant (93). Furthermore, a material showing excellent surface tension-reducing properties when spread on surfaces of aqueous solution has been extracted, in various ways, from whole or minced lung (94). This material has been identified as a dipalmitoyl lecithin (95), a somewhat unusual lecithin having saturated fatty acids. The suggestion has been made by several investigators (96,97) that this surfactant is the secretory product of the type B alveolar cell.

I believe that the necessity for a surfactant to be present to

reduce the surface tension at the alveolar surface is doubtful. The physiological reasoning for such a need assumes a spherical alveolus of small radius, and an alveolar septum having such slight intrinsic strength that it would be significantly effected by the surface tension in the assumed layer of tissue fluid covering the alveolar cells. There now exists reasonably good evidence that the alveoli are not spherical, but are instead polygonal in shape with relatively flat sides and sharply angular corners (98, 99). Also, there is no evidence that the alveolar cells are covered with a layer of tissue fluid. The alveolar air is highly humidified and may not be injurious to the alveolar cells. However, even if there were a thin layer of tissue fluid (plasma dialysate?), it would still remain to be shown how the tension within this layer could significantly effect the gross structures of an alveolar wall which has definite elastic and collagen fiber support.

In spite of the counterargument given above, it is possible that something akin to a surfactant does coat the alveolar surface. Indeed, any cellular debris having surfactant properties would tend to coat the alveolar surfaces if they were moist. The type B, or tumor cell, cytosome, when released into the alveolar air spaces, may well contain substances that would have surfactant properties. Although the osmiophilic lamellar or crystalline component of the cytosome would probably not be a dipalmitoyl lecithin -- osmium tetroxide is not thought to react with saturated fatty acids -- other components of the cytosome could have surfactant properties.

Another, perhaps more likely possibility is that lecithin, if

such is present in the cytosome, acts primarily as an emulsifying agent, bringing a relatively insoluble but active component of the cytosome into contact with the alveolar surface. This suggestion is currently being explored by the writer in a separate study based on the hypothesis that the relatively high normal concentration of oxygen in the alveoli might require the presence of an antioxidant which would serve to protect oxygen-sensitive biochemical entities -- lipoproteins, or certain components of oxidation-reduction systems in the more vulnerable alveolar cells. The active, but perhaps poorly soluble, cytosomal substance, speculatively referred to above, could be the antioxidant.

The hypothesis on oxygen toxicity and the need for an antioxidant in the lung may be related, even if only tenuously, to the lung tumor problem.

Because of interest in oxygen therapy in medicine, especially for the newborn infant with hyaline membrane disease, and in the use of oxygen at high concentration in aerospace research, a number of ultrastructural investigations have been carried out. For example, it has been learned that mice breathing 100% oxygen will die in about five days, apparently "drowning" from edema fluid leaking into the alveolar air spaces (100). Rat lung is seemingly less susceptible to oxygen toxicity than is mouse lung. Nevertheless, the reaction of rat lung to high oxygen concentrations is an increase in alveolar wall thickness, primarily due to widening of the connective tissue space and thickening of the endothelial cell cytoplasm. In addition, the number of type B alveolar cells is increased,

as is the amount of membranous material in the air spaces, presumably of type B cell origin (101). A second, recent study on the effect of oxygen on rat lung was reported by Kistler, Caldwell, and Weibel (102). This article should be consulted for references on this subject.

Kistler et al made a careful morphological comparison of oxygen-treated rat lung with normal lung and found that the widening of the alveolar septum was primarily caused by an accumulation of edema fluid in the connective tissue spaces. This fluid was later found to be replaced by fibroblasts and connective tissue fibers. There was also a concomitant destruction of about 50% of the capillaries. The primary site of damage was believed to be the endothelium. The alveolar epithelium was hardly effected, and when damage occurred it was produced mainly by pressure from the edematous underlying structures. In the most severely effected rats, about two-thirds of the alveoli were filled with an exudate. Of interest, in relation to the hypothesis being discussed, are illustrations of type B cells from oxygen-poisoned rats. These cells show a very marked dilatation of the cisternae of the granular endoplasmic reticulum. Also, large numbers of free ribosomes are seen in the cytoplasm. As these authors did not conceive of a relation between oxygen poisoning and the type B cell, this cell type is not sufficiently illustrated to permit further comment. However, future work on oxygen poisoning in mice, with special emphasis on the reaction of the type B cell, is planned by the writer. If the type B cell produces an antioxidant, it should react by showing signs of increased secretory activity. The results of such a study may answer the question posed by Kistler et al (102) who wrote, "The most puzzling observation relates to our finding that endothelial

cells are damaged first by an agent that has to traverse a similar tissue layer before reaching its target. The question why epithelial cells, which are directly exposed to the high oxygen pressure, are not damaged, whereas endothelial cells undergo such early and drastic changes, remains unanswered."

Heston and Pratt (103) compared mice treated with the carcinogen dibenzanthracene and subsequently exposed for 48 hours to atmospheres of 8% oxygen, normal air, or 100% oxygen. These investigators determined that animals exposed to 100% oxygen showed an increased number of lung tumors as compared to those breathing air, and the mice exposed to 8% oxygen showed a decreased number of tumors. They suggested that oxygen "... creates a physiologic state of relative susceptibility of the alveolar epithelial cells to the action of dibenz(a,h)anthracene." Similar results were obtained by Di Paolo (104). Falconer and Bloom (105) in discussing the genetic aspects of the mouse lung tumors stated that "... the site of action of the genes responsible for the genetically determined susceptibility to carcinogen is in the lung tissue itself.... The tissue specificity suggests that the operative environmental factors are likely to be those that effect the lung tissue directly, such as oxygen concentration...."

Before completing this section, the question of a relation between infection and tumors should be touched on. No evidence for such a relation has been obtained in this study. It is known that the mouse mammary tumor agent (Bittner virus) is present in the strain A mouse (10). However, few virus-like particles have been recognized in lung cells, and none are seen in the thesis figures. The presence

of mycoplasma, however, is another matter. This organism is present in normal and tumorous mouse lung. There is, as yet, no evidence suggesting a strong connection between mycoplasma and cancer. Although such organisms have been found in many cancers, they also occur in normal tissues. This, of course, does not rule out the possibility that mycoplasma may be tumorigenic. This could be indirectly tested by studying strain A mice under germ-free conditions to determine if lung adenomas form.

### III. Effect of Urethane on Cell Ultrastructure

No effect of urethane on cell ultrastructure could be detected in the present study. Furthermore, no obvious difference in morphology between tumor cells from "spontaneously" occurring tumors and those of urethane induced tumors could be demonstrated. Also, there were no differences noted between the tumors of young mice receiving urethane in utero or from their mother's milk and those arising "spontaneously" or by induction in older mice. Finally, no differences were found in the tumors of young mice subjected to urethane in utero only, in their mother's milk only, or through both pathways.

If these negative findings are correct, it must be concluded that the effect of urethane is on cell systems that do not show recognizable ultrastructural changes. Most of the nuclear systems would likely fall into such a category, as would many cytoplasmic systems. If urethane acts, for instance, as an alkylating agent (adding the ethyl group of ethyl carbamate), and if nucleic acids were effected, a mutation could be produced. However, the effect of the mutation may

not be structurally evident.

#### IV. Theoretical Considerations

Investigations of the various aspects of cancer have produced an immense quantity of data, much of which must, unfortunately, be considered as virtually lost. This conclusion is based on the observation that data tends to be retained when closely related to current theories, but lost when unrelated to any theory. Much of the morphologic data on cancer, particularly the ultrastructural findings, fall into the latter category. This unfruitful situation could be remedied if each investigator attempted to relate his findings to theory. This is especially true in the case of cancer where most modern theories are based on biochemical concepts. It can hardly be expected that the biochemically oriented theorist will want to dig deeply into the morphologic literature, or be able to appreciate what he finds even if he were to look there.

In spite of the foregoing argument, it must be admitted that the non-theorist is faced with too many theories on cancer, and too few that are satisfying. Rather than to attempt a review of the more prominent current theories, several ideas and portions of theories will be synthesized into a working hypothesis of cancer to which morphological data can be compared.

One of the simplest theories of cancer was suggested by Lederberg (106) in 1946. Lederberg pointed out that an analogy seemed to exist between a circumstance relating to Neurospora growth and cancer. A leucine deficient strain of Neurospora, growing in a medium containing leucine, is controlled, in terms of growth, by the

quantity of leucine in the medium. Occasionally, there will arise in such a mutant culture a back mutation to the wild type (leucine synthesizing) organism. This wild strain will, under the proper conditions, overgrow the leucine deficient strain. It was Lederberg's idea that the leucine deficient strain of Neurospora could be considered analagous to normal cells of multicellular organisms, and the wild strain of Neurospora analogous to cancer cells. The point of this theory is that, in multicellular organisms, normal cells of any particular type are incapable of uncontrolled synthesis of whatever substance regulates their growth, whereas cancer cells are capable of such synthesis.

It may be assumed that the growth of each cell type of a multicellular organism is carefully regulated. This regulation is, undoubtedly, mediated chemically. It is possible that in some cell types the definitive growth regulator is synthesized by the cell type in question, but synthesis is turned on and off from external sources. In other cell types, the growth regulator may be synthesized by cells of a different type. In either case, the "information" for the synthesis of the growth regulator exists in the genome of all cells of the organism, but is repressed in almost all of them. If, in any cell type capable of growth, this portion of the genome were to be derepressed (107), then such a cell could synthesize its own growth regulator. It would divide more rapidly than normal cells of the same type but not necessarily more rapidly than hyperplastic cells. A clone of altered cells would arise from the original cell. In spite of this alteration, the effected cell and its progeny would remain



specialized, inasmuch as that part of the genome related to specialization was not changed.

It is not known at this time what agents may cause this type of derepression. Any or all carcinogenic agents may be implicated.

If a daughter cell, arising from this clone of altered cells, should suffer a mutation effecting the specialization portion of the genome, a new clone would arise. In this case, the effect could be produced by any mutagenic agent, carcinogen or otherwise. The cells of the latter clone would tend to divide more rapidly than the cells of the former clone, because there would be less competition within these cells by metabolic systems related to the lost specialization. Further mutations effecting cell specialization would result in more rapidly dividing, less specialized clones of cells.

On the basis of this hypothesis, all cells that synthesized their own growth control substance would have to be regarded as cancer cells. Those that had become least specialized would be the most malignant in relation to the host organism.

Evidence to support this working hypothesis exists in the findings of Braun and Wood (108) on crown gall tumor in plants. Direct evidence from the animal kingdom is lacking, although many pieces of data are consistent with the hypothesis. In particular, the evidence gathered by many investigators (see Berenblum (109)) to show stages of tumor growth from initiation to promotion to progression tends to support certain aspects of the hypothesis. It is, however, not the purpose of this thesis to expand on the hypothesis offered here. Rather, this will be done in a separate publication at a later time.

The working hypothesis allows certain predictions to be made: 1) the earliest cancer cells should appear to be similar to hyperplastic cells of the same type, 2) if the growth control substance were diffusible, a zone of hyperplastic normal cells should surround tumors, and 3) if marked morphological differences, neglecting necrosis and degeneration, occur among the neoplastic cells making up a tumor, the cells showing the differences should be found in discrete groups. These groups would represent clones arising from a mutation or mutations in a parent cell. It is of interest to compare this hypothesis and the predictions arising from it with the findings on the mouse lung tumor presented in this thesis.

It is evident that the tumor cells appear very similar to the normal type B cells. The most obvious difference is the presence of a crystalloid in the tumor cell cytosome and its apparent absence, or difference in preservation, in the type B cell cytosome. As the cytosome is likely to be closely related to the type B cell function, it is possible to suggest that the initiation of the lung tumor is caused by urethane (the "complete" carcinogen) or some other agent which produces a metabolic alteration reflected by the cytosomal crystalloid. If such an alteration effected the function of the cell, and if a functional feedback system existed in this cell type, then it would be expected that cells altered in this manner would become hyperplastic.

There is a growing body of evidence that the neoplastic event, whatever that may be, occurs only at the time when DNA is replicated. Although this evidence is derived primarily from the viral carcinogenesis literature (see Temin (110), Dulbecco (111), and Sachs (112)),

it may also be applicable to all carcinogens. A hyperplastic group of cells could be regarded as a prime target for future carcinogenic action.

In the case of the mouse lung tumor, urethane, or some other agent, may effect the DNA of the cell (or other sensitive site) to bring about the definitive change -- the derepression suggested by the working hypothesis.

The second prediction of the hypothesis cannot be tested by the data obtained, inasmuch as a ring of hyperplastic type B cells could not be definitely identified near the adenoma. Also, if such cells were present, it could be argued that they had arisen first.

The third prediction of the hypothesis is difficult to examine by the electron microscopic method. However, it was noted that the glycogen-containing cells were grouped loosely together.

It must be admitted that other explanations of these findings exist, and that the working hypothesis must be strengthened in additional ways if it is to be useful.

## SUMMARY

Alveolar cells of the strain A (Heston) mouse, a strain having a high "spontaneous" lung tumor incidence, and lung tumor cells were examined with the electron microscope and their morphologies described and compared. The lung tumor cells contained cytosomes, cellular structures which in normal lung are unique to the type B alveolar cells. Thus, the derivation of the mouse pulmonary adenoma from this cell type would seem assured.

The principal difference between the normal type B cell and the tumor cell is that the tumor cell cytosome contains a crystalloid component that is either absent or, despite the use of similar fixation, not preserved in the type B cell cytosome.

No differences could be detected between cells of lung tumors arising "spontaneously" or those induced by urethane in young or old mice. Also, cells of lung tumors induced in young mice by giving the mothers urethane in their drinking water did not appear to differ from those above.

Findings are discussed in relation to a hypothesis suggesting that the function of the type B cell is the production of an anti-oxidant needed to protect the alveolar cells against the high oxygen concentration normally present in the alveoli. Additionally, the relationship of the findings in this study to a hypothesis suggesting that cancer occurs when cells become capable of synthesizing a substance that controls their own growth is considered.

Future experiments in the mouse lung tumor system are needed in order to definitively determine the function of the type B alveolar

cell. Once this function is determined, experiments can be designed, including induction of type B cell hyperplasia, by virtue of which the effects of superadded carcinogens, such as urethane, may be made more apparent.

## REFERENCES

1. Livingood, L. E. Tumors in the mouse. Bull. Johns Hopkins Hosp., 1896. 7, 177-178.
2. Haaland, M. Spontaneous tumors in mice. Imperial Cancer Research Fund (Great Britain), Fourth Scientific Report. London: Taylor & Francis, 1911. pp. 1-113.
3. Tyzzer, E. E. A series of twenty spontaneous tumors in mice, with the accompanying pathological changes and the results of the inoculation of certain of these tumors into normal mice. J. Med. Res., 1907-1908. 17, 155-197.
4. Murray, J. A. Spontaneous cancer in the mouse; histology, metastasis, transplantability, and the relation of malignant new growths to spontaneously affected animals. Imperial Cancer Research Fund (Great Britain), Third Scientific Report. London: Taylor & Francis, 1908. pp. 69-114.
5. Jobling, J. W. Spontaneous tumors of the mouse. Rockefeller Inst. Med. Res. Monographs, 1910. 1, 81-119.
6. Slye, M., Holmes, H. F., & Wells, H. G. The primary spontaneous tumors of the lungs in mice. Studies on the incidence and inheritability of spontaneous tumors in mice. J. Med. Res., 1914. 30, 417-442.
7. Wells, H. G., Slye, M., & Holmes, H. F. The occurrence and pathology of spontaneous carcinoma of the lung in mice. Canc. Res., 1941. 1, 259-261.
8. Murphy, J. B., & Sturm, E. Primary lung tumors in mice following the cutaneous application of coal tar. J. Exp. Med., 1925. 42, 693-700.

9. Magnus, H. A. The experimental production of malignant papillomata of the lung in mice with 1:2:5:6-dibenzanthracene. *J. Path. Bact.*, 1939. 49, 21-31.
10. Bittner, J. J. Breast and lung carcinoma in "A" stock mice. *Pub. Health Repts.*, 1939. 54, 380-392.
11. Shimkin, M. B. Production of lung tumors in mice by intratracheal administration of carcinogenic hydrocarbons. *Amer. J. Canc.*, 1939. 35, 538-542.
12. Andervont, H. B. Pulmonary tumors in mice: I. The susceptibility of the lungs of albino mice to the carcinogenic action of 1,2,5,6-dibenzanthracene. *Pub. Health Repts.*, 1937. 52, 212-221.
13. Andervont, H. B. Pulmonary tumors in mice: II. The influence of heredity upon lung tumors induced by subcutaneous injection of a lard-dibenzanthracene solution. *Pub. Health Repts.*, 1937. 52, 304-315.
14. Andervont, H. B. Pulmonary tumors in mice: III. The serial transmission of induced lung tumors. *Pub. Health Repts.*, 1937. 52, 347-355.
15. Andervont, H. B. Pulmonary tumors in mice: IV. Lung Tumors induced by subcutaneous injection of 1,2,5,6-dibenzanthracene in different media and by its direct contact with lung tissues. *Pub. Health Repts.*, 1937. 52, 1584-1589.
16. Andervont, H. B. Pulmonary tumors in mice: V. Further studies on the influence of heredity upon spontaneous and induced lung tumors. *Pub. Health Repts.*, 1938. 53, 323-337.

17. Andervont, H. B. Pulmonary tumors in mice: VI. Time of appearance of tumors induced in strain A mice following injection of 1:2:5:6-dibenzanthracene or 20-methylcholanthrene. Pub. Health Repts., 1939. 54, 1512-1519.
18. Andervont, H. B. Pulmonary tumors in mice: VII. Further studies on the serial transmission of lung tumors occurring in inbred mice. Pub. Health Repts., 1939. 54, 1519-1524.
19. Andervont, H. B. Pulmonary tumors in mice: VIII. The induction of pulmonary tumors in mice of strains D, M, C57 Brown, and C57 Black by 1:2:5:6-dibenzanthracene. Pub. Health Rpts., 1939. 54, 1524-1529.
20. Andervont, H. B., & Shimkin, M. B. Biologic testing of carcinogens. II. Pulmonary tumor induction technique. J. Natl. Canc. Inst., 1940. 1, 225-239.
21. Nettleship, A., Henshaw, P. S., & Meyer, H. L. The induction of pulmonary tumors in mice with ethyl carbamate (urethane). J. Natl. Canc. Inst., 1943. 4, 309-319.
22. Henshaw, P. S., & Meyer, H. L. Further studies on urethane induced pulmonary tumors. J. Natl. Canc. Inst., 1945. 5, 415-417.
23. Larsen, C. D. Survey of hypnotics in general with regard to pulmonary tumor induction in mice. J. Natl. Canc. Inst., 1947. 8, 99-101.
24. Larsen, C. D. Studies of pulmonary tumor induction in mice by derivatives of carbamic acid. Canc. Res., 1947. 7, 726.  
(Abstract)



25. Larsen, C. D. Pulmonary tumor induction with alkylated urethanes. *J. Natl. Canc. Inst.*, 1948. 9, 35-37.
26. Larsen, C. D. Studies on the mechanism of pulmonary tumor induction with urethan. *Canc. Res.*, 1950. 10, 230. (Abstract)
27. Berenblum, I., Ben-Ishai, D., Haran-Ghera, N., Lapidot, A., Simon, E., & Trainin, N. Skin initiating action and lung carcinogenesis by derivatives of urethane (ethyl carbamate) and related compounds. *Bioch. Pharmacol.*, 1959. 2, 168-176.
28. Boyland, E., & Nery, R. The metabolism of urethan and related compounds. *Bioch. J.*, 1965. 94, 198-208.
29. Kaye, A. M., & Trainin, N. Urethan carcinogenesis and nucleic acid metabolism: Factors influencing lung adenoma induction. *Canc. Res.*, 1966. 26, 2206-2212.
30. Grady, H. G., & Stewart, H. L. Histogenesis of induced pulmonary tumors in Strain A mice. *Amer. J. Pathol.*, 1940. 16, 417-432.
31. Orr, J. W. The histology and histogenesis of pulmonary adenomata of mice. *Brit. J. Canc.*, 1947. 1, 316-322.
32. Mostofi, F. K., & Larsen, C. D. The histopathogenesis of pulmonary tumors induced in Strain A mice by urethane. *J. Natl. Canc. Inst.*, 1951. 11, 1187-1221.
33. Shimkin, M. B., & Polissar, M. J. Some quantitative observations on the induction and growth of primary pulmonary tumors in strain A mice receiving urethane. *J. Natl. Canc. Inst.*, 1955. 16, 75-94.

34. Tannenbaum, A., & Silverstone, H. Urethan (ethyl carbamate) as a multipotential carcinogen. *Canc. Res.*, 1958. 18, 1225-1331.
35. Skipper, H. E., Bennett, L. L. Jr., Bryan, C. E., White, L. Jr., Newton, M. A., & Simpson, L. Carbamates in the chemotherapy of leukemia. VIII. Over-all tracer studies on carbonyl-labeled urethan, methylene-labeled urethan, and methylene-labeled ethyl alcohol. *Canc. Res.*, 1951. 11, 46-51.
36. Shimkin, M. B. Pulmonary tumors in experimental animals. *Adv. Canc. Res.*, 1955. 3, 223-269.
37. Berenblum, I., Haran-Ghera, N., Winnick, R., & Winnick, T. Distribution of C<sup>14</sup>-labeled urethans in tissues of the mouse and subcellular localization in lung and liver. *Canc. Res.*, 1958. 18, 181-185.
38. Haddow, A., & Sexton, W. A. Influence of carbamic esters (urethanes) on experimental animal tumors. *Nature*, 1946. 157, 500-503.
39. Rogers, S. Studies of the mechanism of action of urethane in initiating pulmonary adenomas in mice. II. Its relation to nucleic acid synthesis. *J. Exp. Med.*, 1957. 105, 279-306.
40. Cornman, I. The properties of urethane considered in relation to its action on mitosis. *Int. Rev. Cytol.*, 1954. 3, 113-130.
41. Keilin, D., & Hartree, E. F. Cytochromes and cytochrome oxidase. *Proc. Roy. Soc. B*, 1939. 127, 167-191.
42. Warburg, O. On the origin of the cancer cell. *Science*, 1956. 123, 309-314.
43. Warburg, O. Physikalische Chemie der Zellatmung. *Biochem. Z.*, 1921. 119, 134-166.

44. Lee, K. H. The action of ethyl carbamate on oxidative phosphorylation. *J. Amer. Pharm. Assoc.*, 1960. 49, 609-613.
45. Boyland, E., & Rhoden, E. The distribution of urethane in animal tissues, as determined by a micro-diffusion method, and the effect of urethane treatment on enzymes. *Bioch. J.*, 1949. 44, 528-531.
46. Ahlstrom, C. G. A short review of mitotic poisons. *Acta Path. Microbiol. Scand.*, 1951. Suppl. 91, 52-62.
47. Tannenbaum, A., & Maltoni, C. Neoplastic response of various tissues to the administration of urethan. *Canc. Res.*, 1962. 22, 1105-1112.
48. Heston, W. E. Lung tumors and heredity: I. The susceptibility of four inbred strains of mice and their hybrids to pulmonary tumors induced by subcutaneous injection. *J. Natl. Canc. Inst.*, 1940. 1, 105-111.
49. Heston, W. E. Relationship between susceptibility to induced pulmonary tumors and certain known genes in mice. *J. Natl. Canc. Inst.*, 1941. 2, 127-132.
50. Heston, W. E. Genetic analysis of susceptibility to induced pulmonary tumors in mice. *J. Natl. Canc. Inst.*, 1942. 3, 79-82.
51. Heston, W. E. Relationship between the lethal yellow ( $A^Y$ ) gene of the mouse and susceptibility to induced pulmonary tumors. *J. Natl. Canc. Inst.*, 1942. 3, 303-308.
52. Heston, W. E., & Deringer, M. K. Relationship between the lethal yellow ( $A^Y$ ) gene of the mouse and susceptibility to spontaneous pulmonary tumors. *J. Natl. Canc. Inst.*, 1947. 7, 463-465.

53. Heston, W. E., & Deringer, M. K. Relationship between the hairless gene and susceptibility to induced pulmonary tumors in mice. *J. Natl. Canc. Inst.*, 1949. 10, 119-124.
54. Heston, W. E. Genetics of neoplasia. In: W. J. Burdette (Ed.) *Methodology in mammalian Genetics*. San Francisco: Holden-Day, 1963. pp. 247-268.
55. Klärner, P., & Gieseck, R. Zur Ultrastruktur des Lungen Tumors der Maus. *Zeit. Krebsforsch.*, 1960. 64, 7-21.
56. Okada, Y., Daido, S., & Ishiko, S. Morphological studies of pulmonary tumors of the mice with special reference to their cytogenesis. *Acta Tuberc. Jap.*, 1962. 11, 73-82.
57. Svoboda, D. J. Ultrastructure of pulmonary adenomas in mice. *Canc. Res.*, 1962. 22, 1197-1201.
58. Driessens, J., Dupont, A., & Demaille, A. L'Adénome pulmonaire expérimental à l'uréthane chez la souris Swiss. II. Etude cytologique au microscope électronique. *C. R. Soc. Biol.*, 1963. 157, 560-563.
59. Kitamura, H. The fine structure of lung alveoli and its reactions. *Acta Path. Jap.*, 1964. 14, 147-167.
60. Hattori, S., Matsudo, M., & Wada, A. An electron microscopic study of pulmonary adenomas in mice. *Gann*, 1965. 56, 275-280.
61. Caulfield, J. B. Effects of varying the vehicle for OsO<sub>4</sub> in tissue fixation. *J. Biophys. Biochem. Cytol.*, 1957. 3, 827-830.
62. Millonig, G. Further observations on a phosphate buffer for osmium solutions. In: S. S. Breese, Jr. (Ed.) *Electron Microscopy*. Vol. 2. Biology. New York: Academic Press, 1962. pg. P-8.

63. Bennett, H. S., & Luft, J. H. *s*-Collidine as a basis for buffering fixatives. *J. Biophys. Biochem. Cytol.*, 1959. 6, 113-114.
64. Sabatini, D. D., Bensch, K., & Barrnett, R. J. Cytochemistry and electron microscopy. The preservation of cellular ultrastructure and enzymatic activity by aldehyde fixation. *J. Cell Biol.*, 1963. 17, 19-58.
65. Sabatini, D. D., Miller, F., & Barrnett, R. J. Aldehyde fixation for morphological and enzyme histochemical studies with the electron microscope. *J. Histochem. Cytochem.*, 1964. 12, 57-71.
66. Smith, R. E., & Farquhar, M. G. Lysosome function in the regulation of the secretory process in cells of the anterior pituitary gland. *J. Cell Biol.*, 1966. 31, 319-347.
67. Trump, B. F., & Bulger, R. E. New ultrastructural characteristics of cells fixed in a glutaraldehyde-osmium tetroxide mixture. *Lab. Invest.* 1966. 15, 368-379.
68. Ross, R., & Klebanoff, S. J. Fine structural changes in uterine smooth muscle and fibroblasts in response to estrogen. *J. Cell Biol.*, 1967. 32, 155-167.
69. Luft, J. Improvements in epoxy resin embedding methods. *J. Biophys. Biochem. Cytol.*, 1961. 9, 409-414.
70. Richardson, K. C., Jarett, L., & Finke, E. H. Embedding in epoxy resins for ultrathin sectioning in electron microscopy. *Stain Tech.*, 1960. 35, 313-323.
71. Reynolds, E. S. The use of lead citrate at high pH as an electron-opaque stain in electron microscopy. *J. Cell Biol.*, 1963. 17, 208-211.

72. Brooks, R. E. Ultrastructure of the pulmonary alveolar epithelial cells of the strain A (Heston) mouse. Unpublished master's thesis, Univ. Oregon Medical School, 1964.
73. Brooks, R. E. Concerning the nomenclature of the cellular elements in respiratory tissue. *Amer. Rev. Resp. Dis.*, 1966. 94, 112-113.
74. Sorokin, S. P. A morphologic and cytochemical study on the great alveolar cell. *J. Histochem. Cytochem.*, 1966. 14, 884-897.
75. Farquhar, M. G., & Palade, G. E. Junctional complexes in various epithelia. *J. Cell Biol.*, 1963. 17, 375-412.
76. Novikoff, A. G., Essner, E., & Quintana, N. Golgi apparatus and lysosomes. *Fed. Proc.*, 1964. 23, 1010-1022.
77. Sotelo, J., & Porter, K. R. An electron microscope study of the rat ovum. *J. Biophys. Biochem. Cytol.*, 1959. 5, 327-342.
78. Palay, S. L. The fine structure of secretory neurons in the preoptic nucleus of the goldfish (*Carassius auratus*). *Anat. Rec.*, 1960. 138, 417-443.
79. Farquhar, M. G., & Palade, G. E. Functional evidence for the existence of a third cell type in the renal glomerulus. Phagocytosis of filtration residues by a distinctive "third" cell. *J. Cell Biol.*, 1962. 13, 55-87.
80. Rosenbluth, J., & Wissig, S. L. The distribution of exogenous ferritin in toad spinal ganglia and the mechanism of its uptake by neurons. *J. Cell Biol.*, 1964. 23, 307-325.

81. Robbins, E., Marcus, P. I., & Gonatas, N. K. Dynamics of acridine orange-cell interaction. II. Dye-induced ultrastructural changes in multivesicular bodies (acridine orange particles). *J. Cell Biol.*, 1964. 21, 49-62.
82. Gordon, G. B., Miller, L. R., & Bensch, K. G. Studies on the intracellular digestive process in mammalian tissue culture cells. *J. Cell Biol.*, 1965. 25, No. 2, pt. 2, 41-55.
83. Merker, H. J. Über das vorkommen multivesiculären einschlusskörper ("multivesicular bodies") im vaginalepithel der ratte. *Zeit. Zellforsch.*, 1965. 68, 618-630.
84. De Duve, C., & Wattiaux, R. Functions of lysosomes. *Amer. Rev. Physiol.*, 1966. 28, 435-492.
85. Balis, J. U., & Conen, P. E. The role of alveolar inclusion bodies in the developing lung. *Lab. Invest.*, 1964. 13, 1215-1229.
86. Hatasa, K., & Nakamura, T. Electron microscopic observations of lung alveolar epithelial cells of normal young mice, with special reference to formation and secretion of osmiophilic lamellar bodies. *Zeit. Zellforsch.*, 1965. 68, 266-277.
87. Parker, F., & Odland, G. F. A light microscopic, histochemical and electron microscopic study of experimental atherosclerosis in rabbit coronary artery and a comparison with rabbit aorta atherosclerosis. *Amer. J. Path.*, 1966. 48, 451-481.
88. Baudhuin, P., Hers, H. G., & Loeb, H. An electron microscopic and biochemical study of type II glycogenosis. *Lab. Invest.*, 1964. 13, 1139-1152.

89. Cardiff, R. D. A histochemical and electron microscopic study of skeletal muscle in a case of Pompe's disease (glycogenosis II). *Pediatrics*, 1966. 37, 249-258.
90. Organick, A. B., Siegesmund, K. A., & Lutsky, I. I. Pneumonia due to mycoplasma in gnotobiotic mice. II. Localization of Mycoplasma pulmonis in the lungs of infected gnotobiotic mice by electron microscopy. *J. Bact.*, 1966. 92, 1164-1176.
91. Clements, J. A., & Tierney, D. F. Alveolar instability associated with altered surface tension. In: W. O. Fenn & H. Rahn (Eds.) *Handbook of Physiology*. Vol. II. Sect. 3. Respiration. Washington, D. C.: American Physiological Society, 1965. pp. 1565-1583.
92. Pattle, R. E. Surface tension and the lining of the lung alveoli. In: C. G. Caro (Ed) *Advances in Respiratory Physiology*. Baltimore: Williams & Wilkins, 1966. pp. 83-105.
93. Clements, J. A. Surface phenomena in relation to pulmonary function. *Physiologist*, 1962, 5, 11-28.
94. Klaus, M. H., Clements, J. A., & Havel, R. J. Composition of surface-active material isolated from beef lung. *Proc. Natl. Acad. Sci.*, 1961. 47, 1858-1859.
95. Clements, J. A. Surface tension in the lungs. *Sci. Amer.*, 1962. 207, 121-130.
96. Klaus, M., Reiss, O. K., Tooley, W. H., Piel, C., & Clements, J. A. Alveolar epithelial cell mitochondria as source of the surface-active lung lining. *Science*, 1962. 137, 750-751.
97. Buckingham, S., McNary, W. F., Jr., & Sommers, S. S. Pulmonary alveolar cell inclusions: Their development in the rat. *Science*, 1964. 145, 1192-1193.



98. Weibel, E. R., & Gomez, D. M. Architecture of the human lung. *Science*, 1962. 137, 577-585.
99. Staub, N. C. The interdependence of pulmonary structure and function. *Anesth.*, 1963. 24, 831-854.
100. Cedergren, B., Gyllensten, L., & Wersäll, J. Pulmonary damage caused by oxygen poisoning. An electron microscopic study in mice. *Acta. Paediat.*, 1959. 48, 477-494.
101. Schaffner, F., Felig, P., & Trachtenberg, E. Structure of rat lung after protracted oxygen poisoning. *Arch. Path.*, 1967. 83, 99-107.
102. Kistler, G. S., Caldwell, P. R. B., & Weibel, E. R. Development of fine structural damage to alveolar and capillary lining cells in oxygen-poisoned rat lung. *J. Cell Biol.*, 1967. 37, 605-628.
103. Heston, W. E., & Pratt, A. W. Effect of concentration of oxygen on occurrence of pulmonary tumors in strain A mice. *J. Natl. Canc. Inst.*, 1959. 22, 707-717.
104. Di Paolo, J. A. Effects of oxygen concentration on carcinogenesis induced by transplacental exposure to urethan. *Canc. Res.*, 1962. 22, 299-304.
105. Falconer, D. S., & Bloom, J. L. A genetic study of induced lung-tumors in mice. *Brit. J. Canc.*, 1963. 16, 665-685.
106. Lederberg, J. A nutritional concept of cancer. *Science*, 1946. 104, 428.
107. Monod, J., & Jacob, F. General conclusions: Teleonomic mechanisms in cellular metabolism, growth, and differentiation. *Cold Spring Harbor Symp. Quant. Biol.*, 1961. 26, 389-401.

108. Braun, A. C., & Wood, H. N. The plant tumor problem. *Adv. Canc. Res.*, 1961. 6, 81-109.
109. Berenblum, I. The study of tumours in animals. In: H. W. Florey (Ed.), *General Pathology*. Philadelphia: W. B. Saunders, 1962. pp. 622-658.
110. Temin, H. M. Genetic and possible biochemical mechanisms of viral carcinogenesis. *Canc. Res.*, 1966. 26, 212-216.
111. Sachs, L. An analysis of the mechanism of carcinogenesis by polyoma virus, hydrocarbons, and x-irradiation. In: H. Holzer and A. W. Holldorf (Eds.) *Molekulare biologie des malignen wachstums*. Berlin: Springer-Verlag, 1966. pp. 242-255.
112. Dulbecco, R. The induction of cancer by viruses. *Sci. Amer.*, 1967. 216, 28-37.

## ABBREVIATIONS USED IN FIGURE LEGENDS

A -- Type A alveolar cell  
Air -- Alveolar air space  
B -- Type B alveolar cell  
BM -- Basement membrane  
C -- Capillary  
CF -- Collagen fibers  
CM -- Chromatin masses  
Cn -- Centriole  
CT -- Connective tissue cell  
DB -- Dense body  
E -- Endoplasmic reticulum  
EF -- Elastic fibers  
EN -- Endothelial Cell  
Eos -- Eosinophil  
F -- fibrils  
G -- Golgi apparatus  
J -- Tight junction, or junctional complex  
L -- Lipid  
Lym -- Lymphocyte  
M -- Multivesicular body  
Mac -- Macrophage  
Mit -- Mitochondrion  
MV -- Microvilli  
N -- Nucleus  
NC -- Nucleolus

- NP -- Nuclear pore  
P -- Platelet  
Ps -- Pseudopod  
R -- Ribosomes  
RBC -- Red blood cell  
S -- Structural configuration of endoplasmic reticulum  
T -- Tumor cell  
V -- Vesicle, plain or coated  
X -- Cytosome of type B or tumor cell

#### EXPLANATION OF FIGURES

Photographs, unless otherwise designated, are electron micrographs made from thin sections of tissue embedded in Araldite, fixed in 1%  $\text{OsO}_4$  buffered with veronal-acetate, and examined with the Philips EM-200 electron microscope. Magnification values given refer to the final micrograph.

For exact details of tissue preparation, reference should be made to the Materials and Methods section.

In those cases of urethane administration in the drinking water, the concentration of the carcinogen was 0.1%.

Figure 1. Gross photograph of mouse lung with multiple subpleural tumors. Tumors (hollow arrows) occur in all lobes as raised, round or irregularly shaped masses having a lighter color than the surrounding normal lung tissue. X 3.5.

Figure 2. Low magnification light micrograph of a lung showing multiple tumor loci. In section, tumors (arrows) are seen to occur in several lobes. Most tumors have a subpleural location, but some appear to originate in the depths of the lung adjacent to large bronchi. X 8.5.

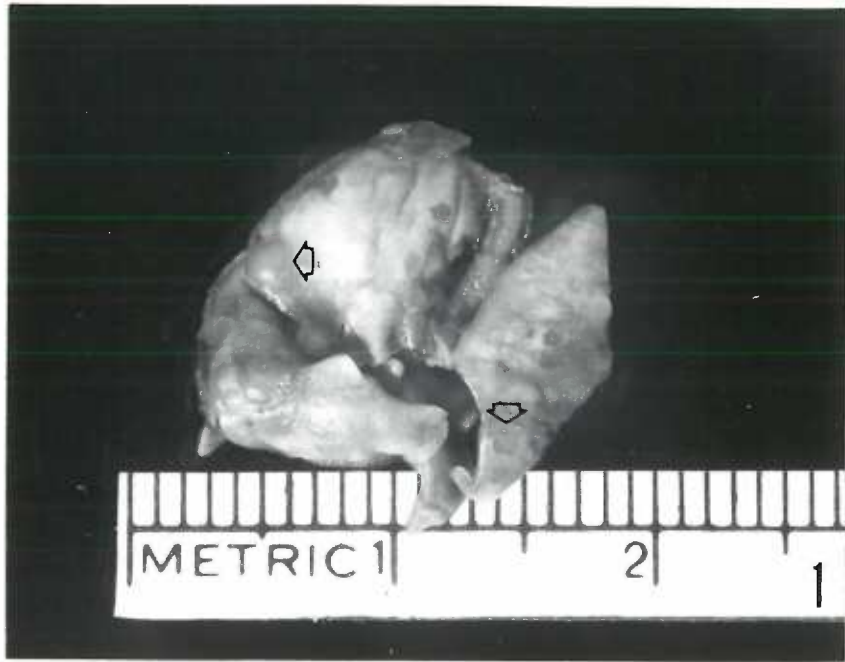


Figure 3. Medium magnification light micrograph of a typical mouse lung adenoma. The subpleural tumor illustrated (arrow) causes the pleural surface to be raised slightly and would probably be grossly visible. The largest part of the tumor mass has expanded into normal lung alveolar tissue. The unencapsulated tumor appears to blend into normal tissue at its borders. X 120.

Figure 4. Higher magnification light micrograph of a pulmonary adenoma. This micrograph, of the tumor illustrated in the figure above, reveals a pattern of curved sheets of cells. The tumor, although small, has become almost solid, with the virtual obliteration of air spaces. X 600.

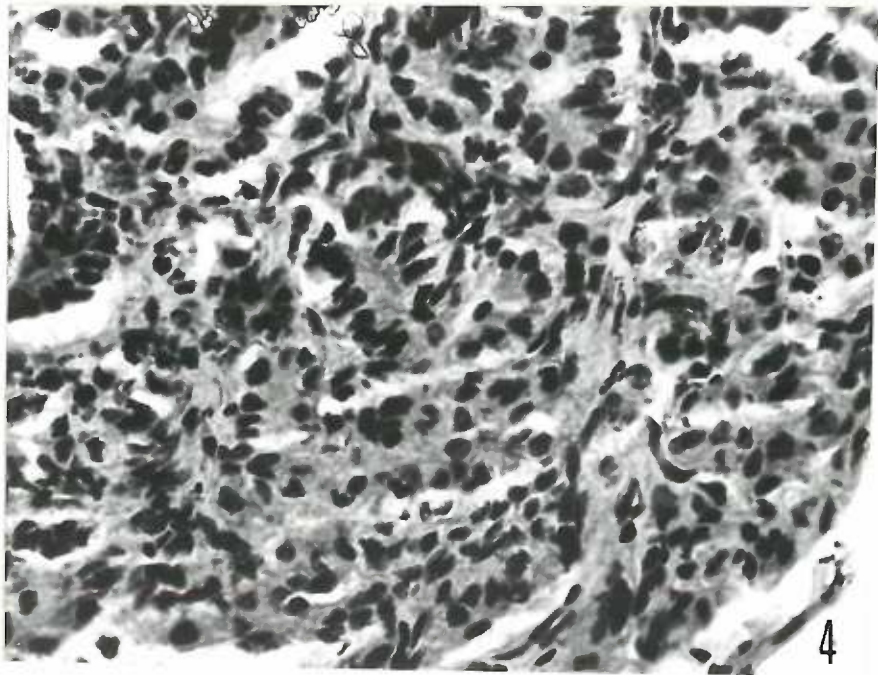
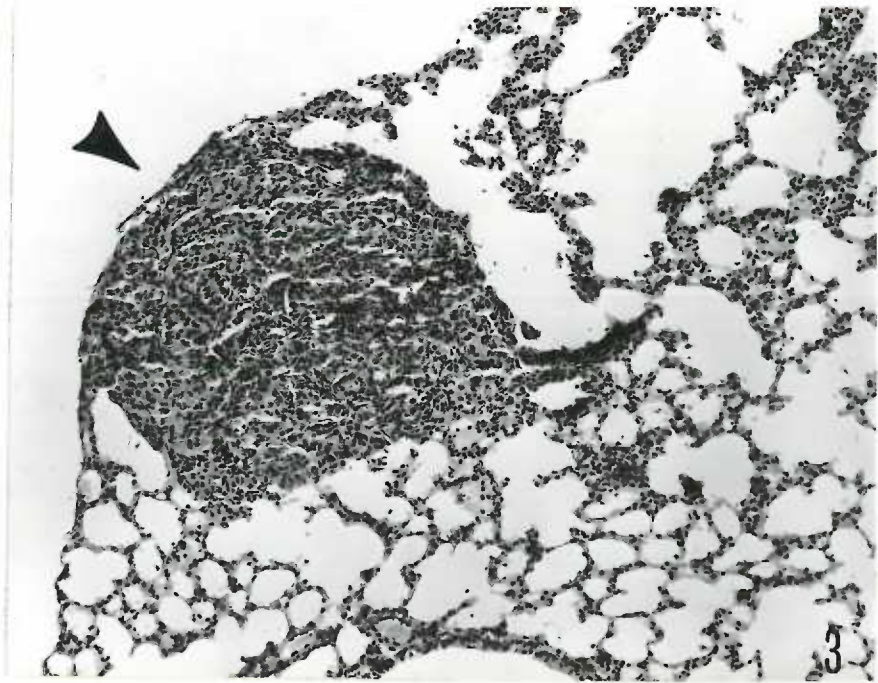




Figure 5. Type B cell of a normal, eleven week old, Group III mouse --- effect of fixation. The type B cell (B) appears to be passing through the alveolar septum (arrows) from one alveolar air space to an adjacent one. This cell type is recognized by the presence of cytosomes (X) that appear, with this fixative, as osmiophilic, lamellar masses, ranging in size from about one-fourth to one-half micron in diameter. Mitochondria (Mit) are numerous in this cell type. A peculiar intracytoplasmic membrane infolding (S) can be seen in some of these cells. The border of the cell typically shows irregular projections, or microvilli (MV). The alveolar air spaces (Air) are normally lined by attenuated cytoplasm of the type A (A) cell, a second alveolar epithelial cell type. The blood capillaries (C) are lined with the attenuated cytoplasm of endothelial cells (En). Epon embedded. RCA. X 15,000.

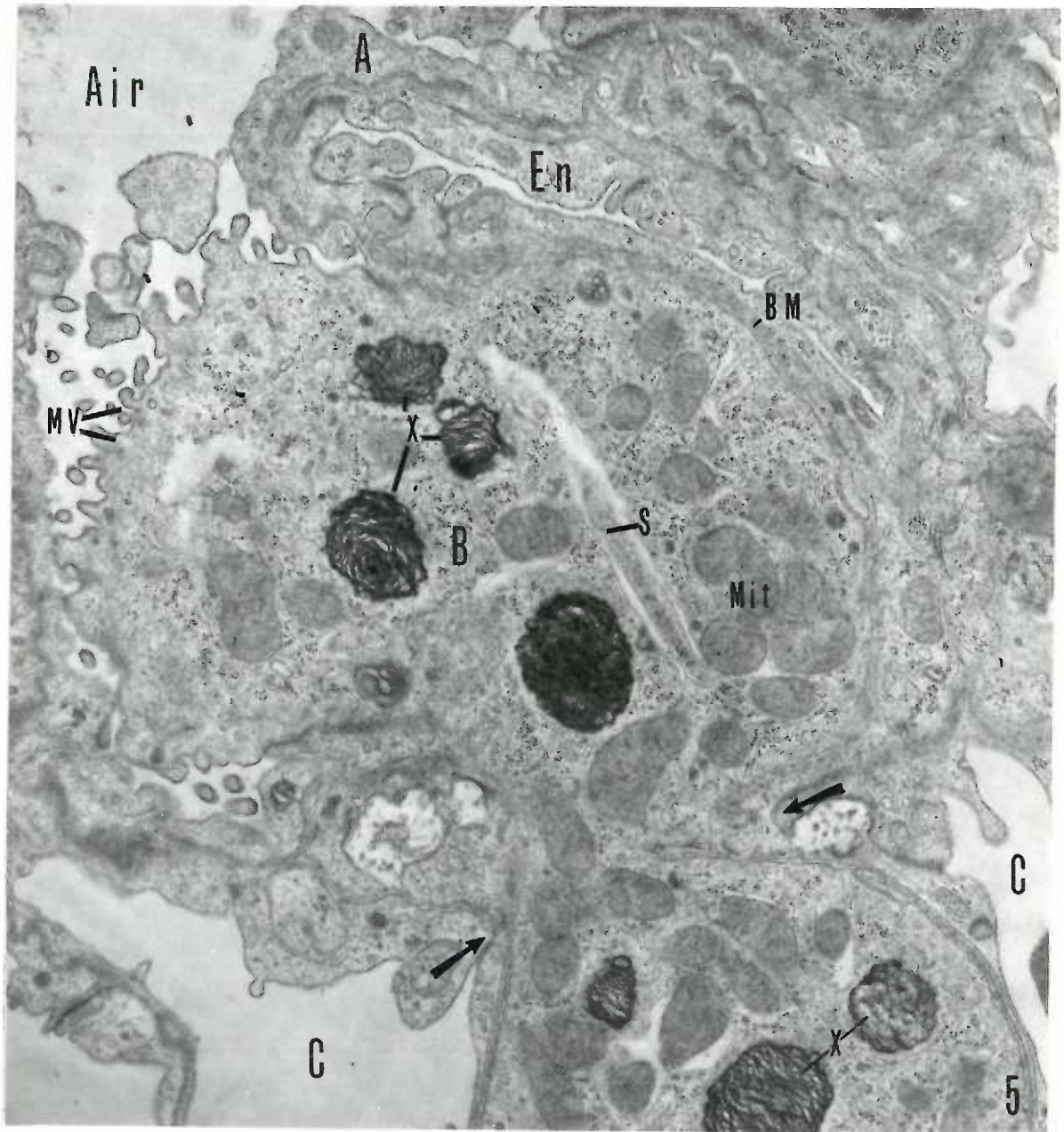


Figure 6. Type B cell of a normal, eleven week old, Group II mouse -- effect of fixation. The type B cell illustrated contains large, almost empty vacuoles (X) that correspond to the cytosomes seen in the previous figure. The remnants of some osmiophilic lamelli can be detected in the vacuoles. In addition, the mitochondria, cytoplasm, and nucleoplasm of this cell are markedly denser than in the same cell type previously illustrated. Epon embedded. Fixed in 1.33%  $\text{OsO}_4$  buffered with collidine. X 13,800.

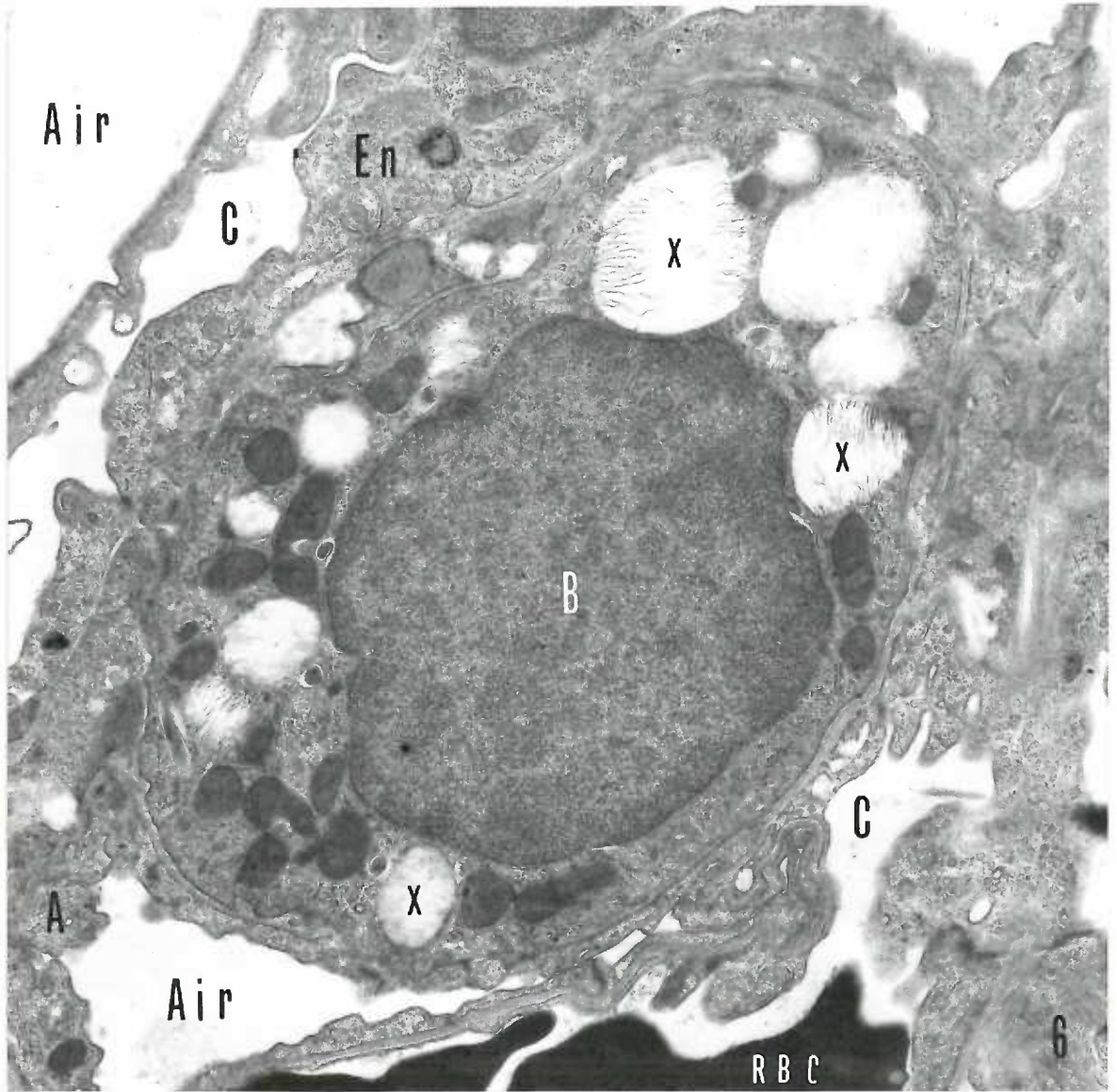


Figure 7. Type B cell of a normal, eleven week old, Group III mouse -- effect of fixation. The type B cell (B) is contrasted with the alveolar macrophage (Mac) in this illustration taken from tissue fixed in the same manner as the previous picture. The cytoplasm of the alveolar macrophage is voluminous. The cell borders are irregular. Broad, often long, pseudopods extend from the cell body. In all mouse lungs examined, the cytoplasm of the alveolar macrophages contain few to numerous, small, pleomorphic granules (single arrows) believed to be, in most instances, elementary bodies of mycoplasma (pleuropneumonia-like organisms -- PPLO). Such bodies are rarely, if ever, definitely identified in other normal lung cells. A large body in the macrophage (double arrows) is slightly similar in appearance to the cytosome (X) of the type B cell. Epon embedded. Fixed in 1.33% OsO<sub>4</sub> buffered with collidine. X 13,800.

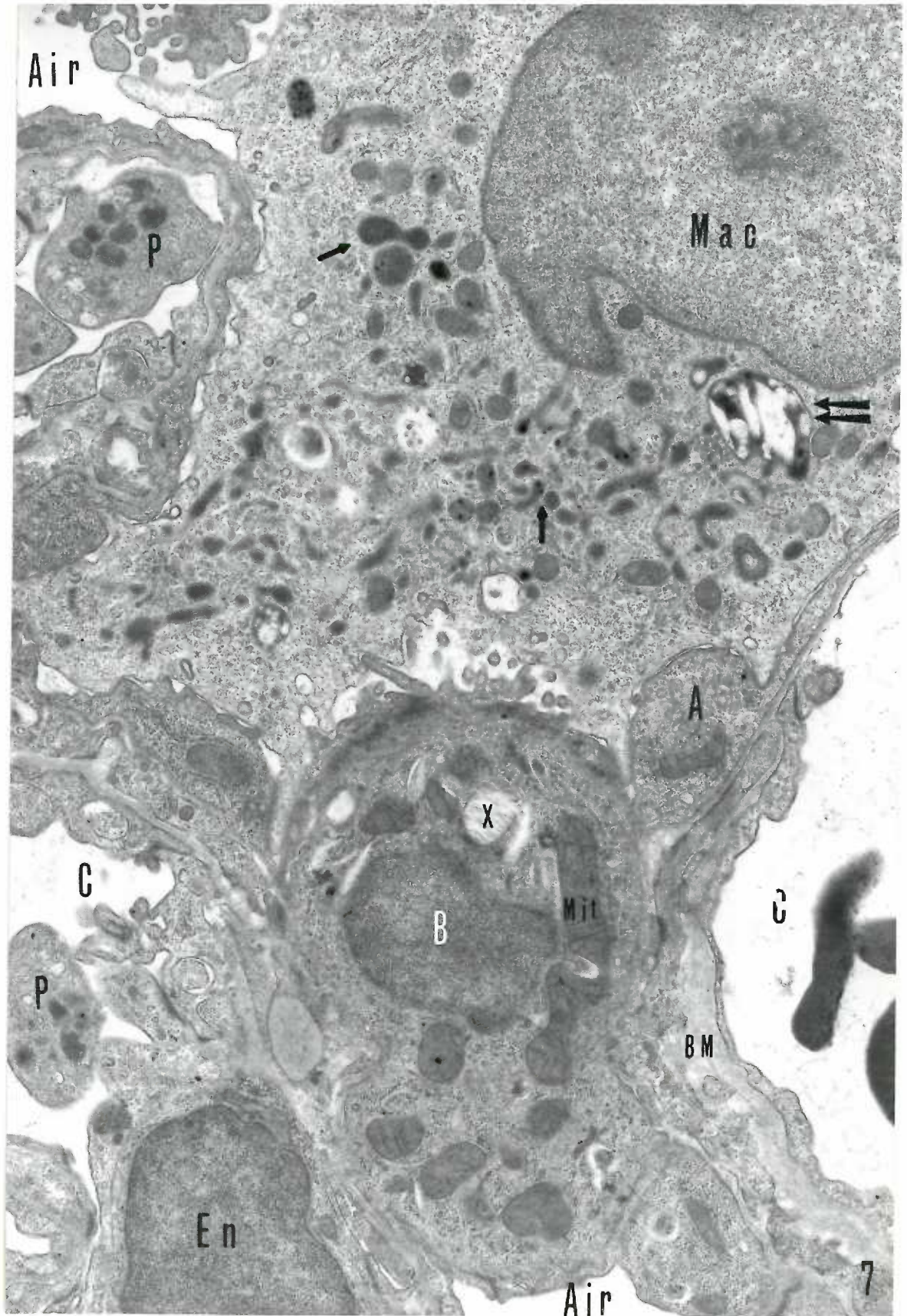


Figure 8. Type B cell of a urethane treated, eleven week old, Group III mouse -- effect of fixation. The type B cell (B) illustrated contains many poorly preserved cytosomes (X). This preservation of structure is not typical of the fixative used, but indicates one possible effect of fixation on this material. Epon embedded. RCA. X 15,500.

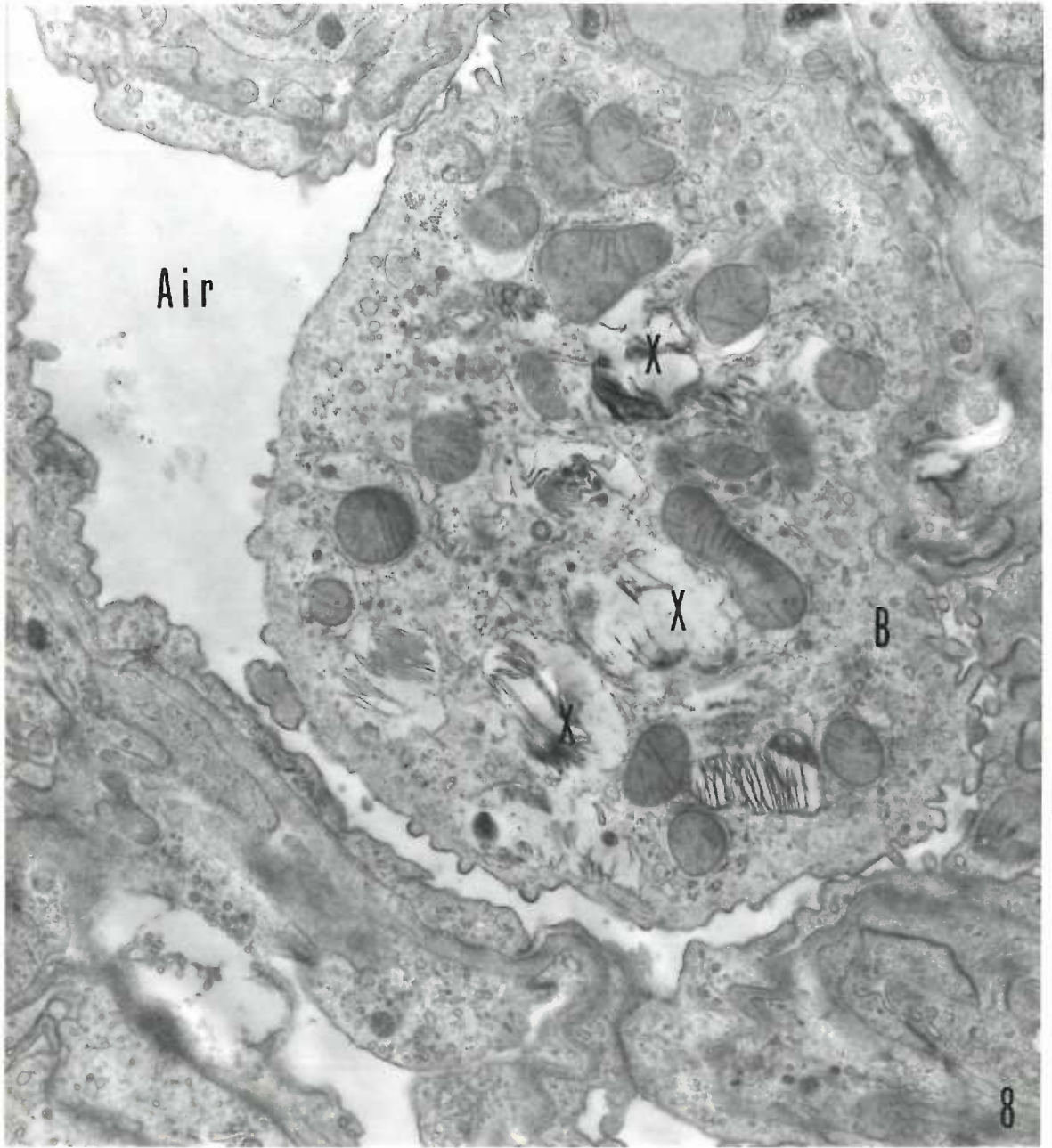




Figure 9. Type B cell of a normal, twenty-one day old, Group IV mouse -- effect of fixation. Aldehyde fixed cells are generally denser than their osmium-fixed counterparts. More of the substances making up the "ground cytoplasm" are apparently retained by these fixatives. The type B cell may be contrasted with the adjacent connective tissue cell (CT) in this micrograph. The cytosomes (X) of the type B cell are not well preserved in this normal cell. Fixed in glutaraldehyde and postfixed with  $\text{OsO}_4$ , both buffered with cacodylate. X 22,900.

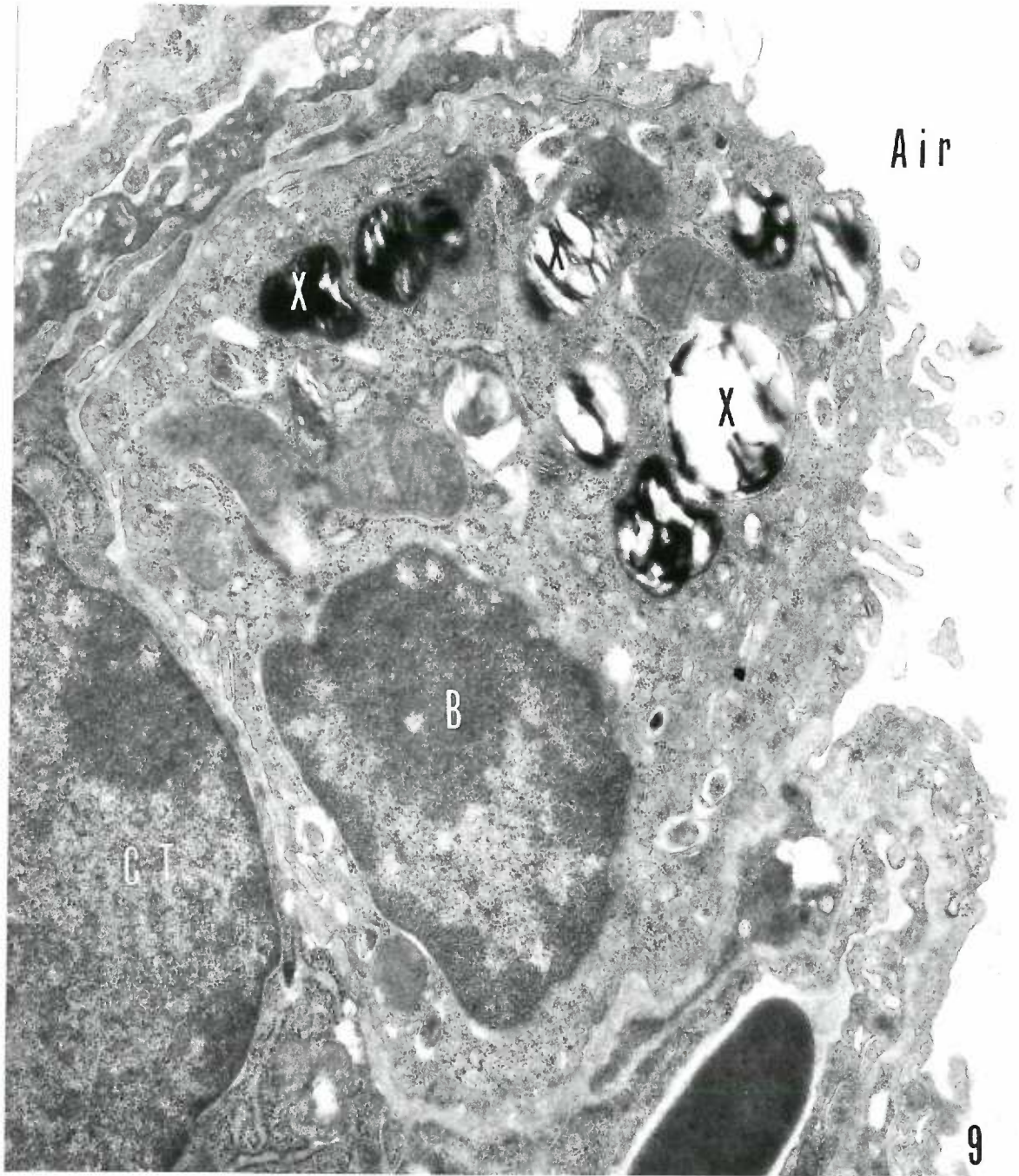


Figure 10. Type B cell of a five month old, normal, Group I mouse -- effect of fixation. The type B cell (B) of this normal animal shows fair preservation of the endoplasmic reticulum (E), but poor preservation of mitochondria (Mit), and cytosomes (X). However, the same fixative often gives good preservation of these elements, particularly in tumor cells (see Fig. 26). A group of small vesicles (V) in this cell appears well preserved. Fixed in glutaraldehyde - osmium (3:2) combination, buffered with cacodylate, and postfixed in  $\text{OsO}_4$  buffered with veronal-acetate. X 22,900.

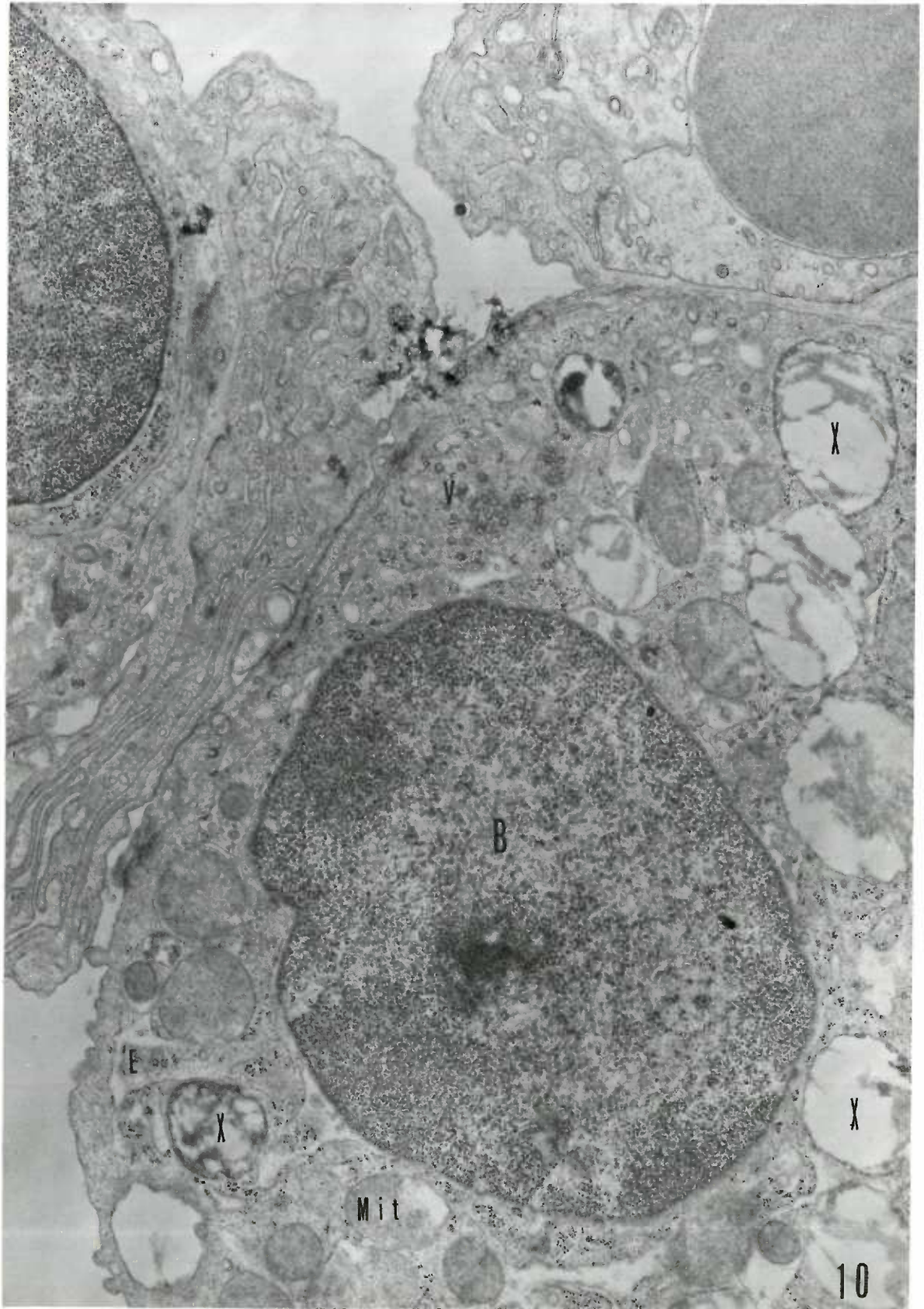


Figure 11. Tumor cells of a forty-three day old, Group IV mouse -- effect of fixation. The tumor was induced by administering urethane in the drinking water to the mother from the 12th through the 17th day of gestation. The tumor cells shown have a well developed endoplasmic reticulum (E), contain multivesicular bodies (M), and numerous cytosomes (X). This fixative, on this occasion, has produced probable artifacts of vacuolization in relation to the cytosomes (straight arrows). However, another form of what is considered to be the same body (curved arrows) presents an entirely different appearance. Here, a solid, or semi-solid, osmiophilic, membrane-enclosed, cytoplasmic body is seen. Microvilli (MV), and a prominent tight junction (J) are noted. X 22,900.



Figure 12. Tumor cells of a fifteen month old, untreated, Group I mouse -- effect of fixation. The tumor cells contain cytosomes (X) of the lamellar type. Mitochondria, endoplasmic reticulum, and other cell cell organelles are generally well preserved. One tumor cell (TT) appears to be caught in movement through a narrow opening in the connective tissue (arrows). Fixed in  $\text{OsO}_4$  buffered with phosphate. X 13,800.

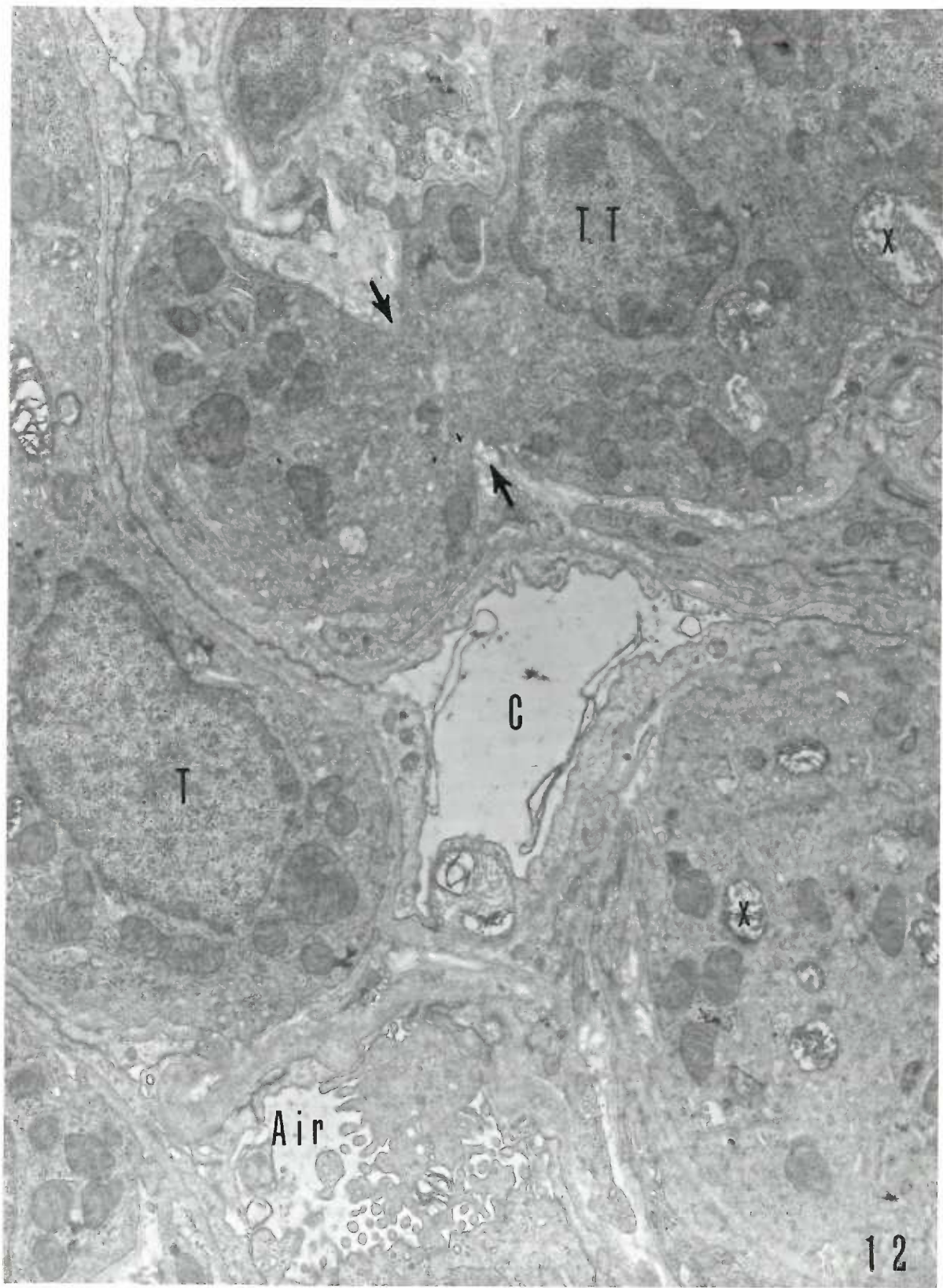




Figure 13. Tumor cells of a fifteen month old, untreated, Group I mouse -- effect of fixation. The cells of this "spontaneously" occurring tumor (T) appear similar to those in the previous figure. The cytoplasm and nucleoplasm is dense. Mitochondria, and Golgi apparatus (G) are well preserved. The cytosomes are somewhat more vacuolated than those preserved by some of the other fixatives. Fixed in  $\text{OsO}_4$  buffered with phosphate. Postfixed in a glutaraldehyde - formaldehyde mixture buffered with phosphate. X 13,800.

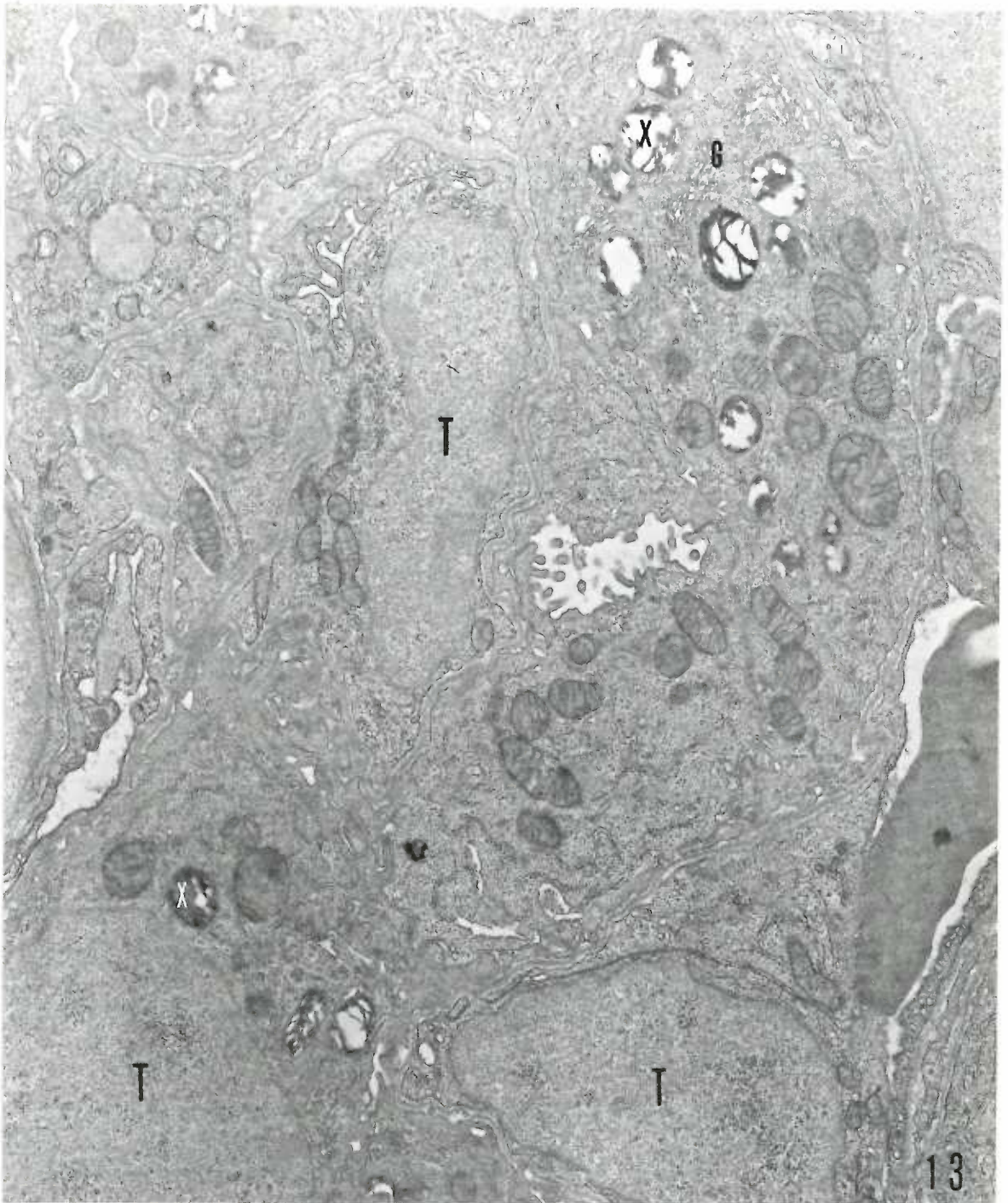


Figure 14. Tumor cell and macrophage of a ten month old, urethane treated, Group V mouse -- effect of fixation. One effect of glutaraldehyde fixation is the production of a mitochondrial vacuolization artifact (arrows). On the other hand, the cytosomes (X) show almost no vacuolization, and internal lamelli are less often seen. The cytoplasm of the macrophage is relatively well preserved, showing many forms of mycoplasma in the cytoplasm. One body in the macrophage (curved arrow) is somewhat similar in appearance to the cytosomes in the tumor cells. Fixed in glutaraldehyde and post-fixed with  $\text{OsO}_4$ , both buffered with cacodylate. X 22,900.

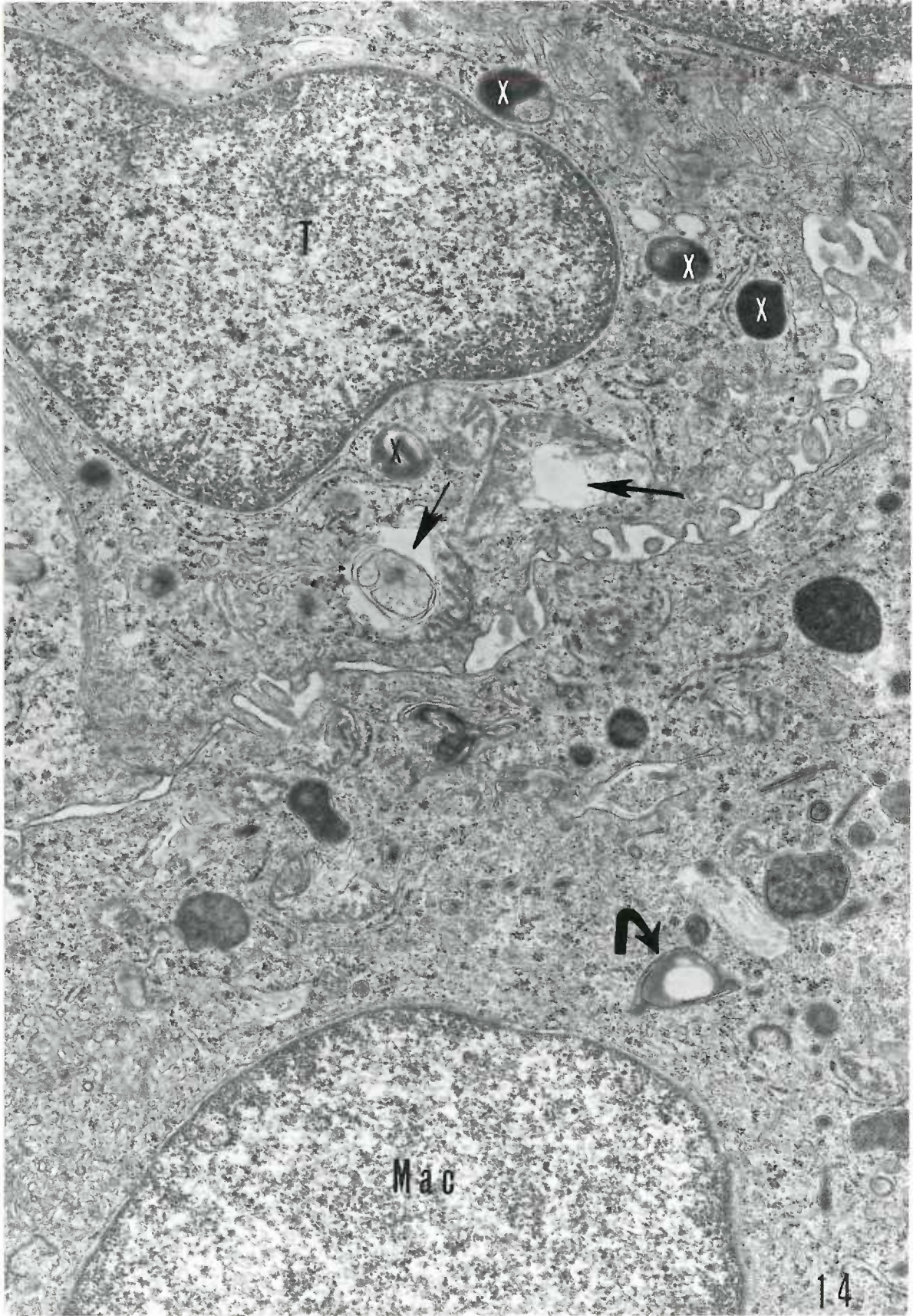


Figure 15. Tumor cells of a ten month old, urethane treated, Group V mouse -- effect of fixation. The fixative illustrated in this and in the preceding figure, although good, does not always produce uniform results. Also, several mitochondria (arrows) reveal poor preservation. Lipid droplets (L) have been retained, but are not as dark as usually seen with osmium-based fixatives. Fine cytoplasmic fibrils (F), and the internal structure of microvilli (MV) are well preserved. Fixed in glutaraldehyde and postfixed with  $\text{OsO}_4$ , both buffered with cacodylate. X 22,900.

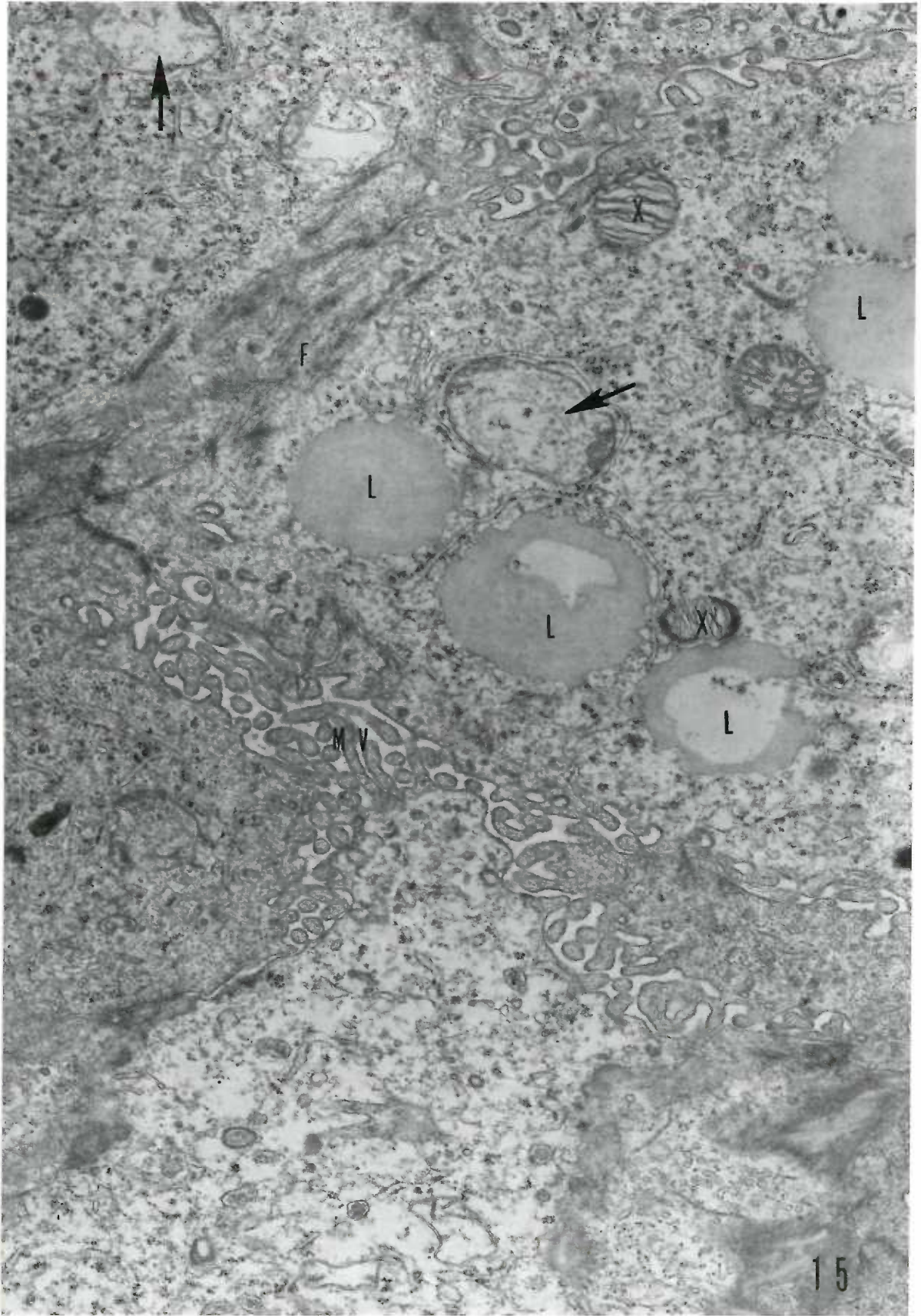


Figure 16. Tumor cells of a fifteen month old urethane treated, Group V mouse -- effect of fixation. This relatively low magnification picture reveals the effect on tumor cells of the use of a glutaraldehyde-osmium combined fixative solution. The appearance of the tissue is clearly denser than when other fixatives are used. Intracytoplasmic membrane systems are not uniformly preserved. Mitochondria often show vacuolization (arrows). Many of the cytosomes (X) are solid, rather than lamellar. Centrioles (Cn) are well preserved. Fixed in glutaraldehyde-OsO<sub>4</sub> (1:1) combination, buffered with cacodylate. X 13,100.

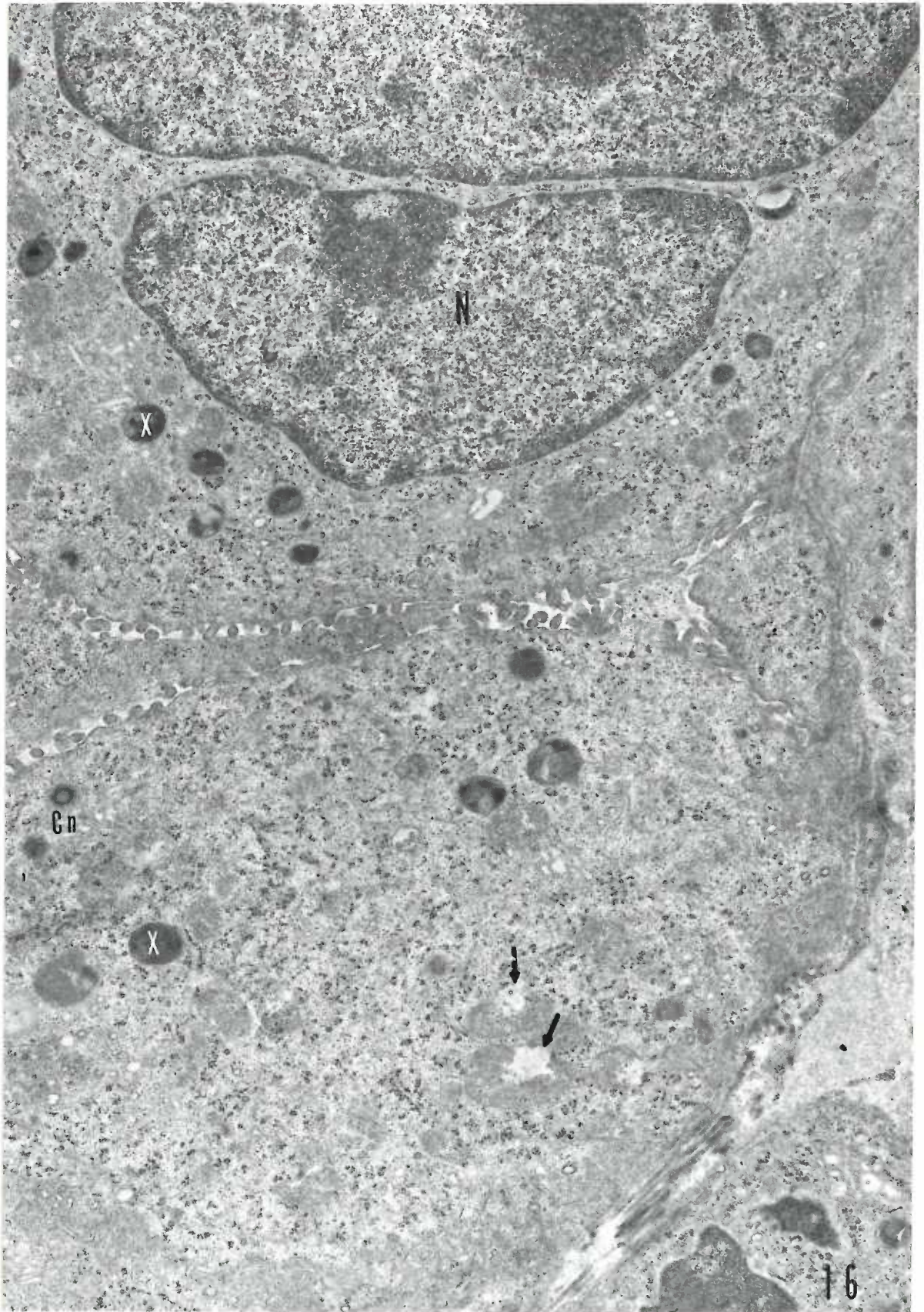




Figure 17. Tumor cells of a fifteen month old, urethane treated, Group V mouse -- effect of fixation. These tumor cells, shown at moderate magnification, further indicate the effect of the combined glutaraldehyde-osmium fixative. Membranes of mitochondria (Mit), endoplasmic reticulum (E), and Golgi apparatus (G) are visualized with difficulty. Ribosomes are preserved as are the cytosomes (X) which appear dense and almost structureless in this micrograph. Multivesicular bodies (M) are irregular in shape. Fine fibrils (F) throughout the cytoplasm are preserved, but, except for those located at the apical portion of the cell (terminal web), are difficult to distinguish in the dense cytoplasm. Fixed in glutaraldehyde-OsO<sub>4</sub> (1:1) combination, buffered with cacodylate. X 35,700.

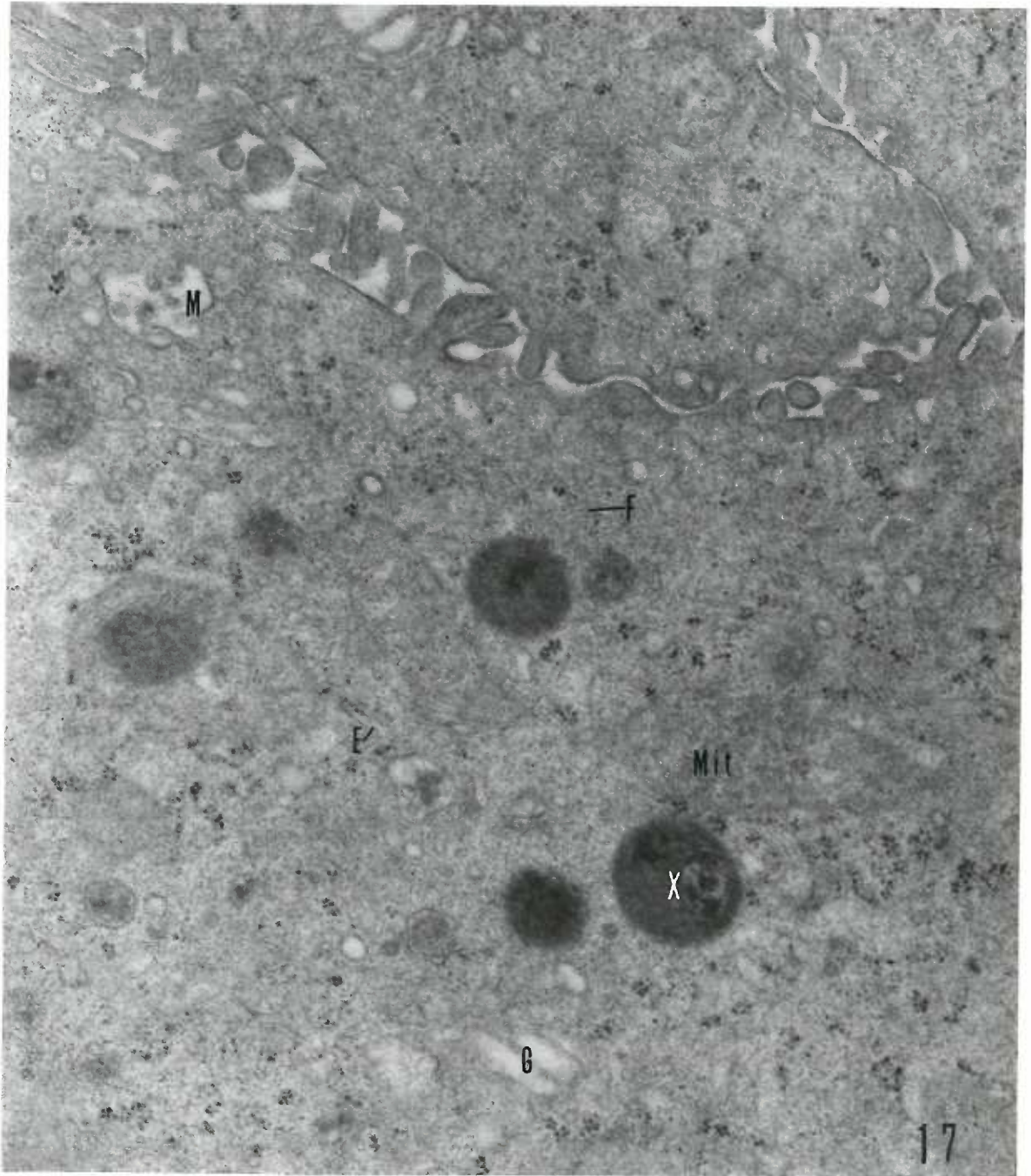


Figure 18. Tumor cells of a fifteen month old, urethane

treated, Group V mouse -- effect of fixation.

Preservation of cytoplasmic elements with the combined fixative used in this and the previous two illustrations is not uniform. The tumor cells (T) contain cytosomes having the lamellar form. An empty cleft (arrow) appears in one cell. Granules of the eosinophil (Eos) in the adjacent capillary show both typical crystalloids and atypical dense appearances. Fixed in glutaraldehyde- $\text{OsO}_4$  (1:1) combination, buffered with cacodylate.  
X 13,800.



Figure 19. Type B cell of an eleven week old, Group III mouse -- effect of urethane. This mouse received drinking water containing urethane for two days. The type B cell shown is similar to that seen in Fig. 5, in that the cell appears to have been caught moving through a narrow opening (straight arrows) in the alveolar wall. The cytosomes (X) have the lamellar form in this cell. Multivesicular bodies (M) are present. An unusual structural configuration is noted (S) and appears to consist of a dilated, U-shaped loop of granular endoplasmic reticulum. A basement membrane (EM) separates the type B cell from the capillary endothelial cells (En). A characteristic long junction (curved arrows) of type A and type B cell cytoplasm occurs where these two cell types meet. In three dimensions, this junction would look like a "cuff" around the sides of the type B cell. Epon embedded. RCA. X 21,000.

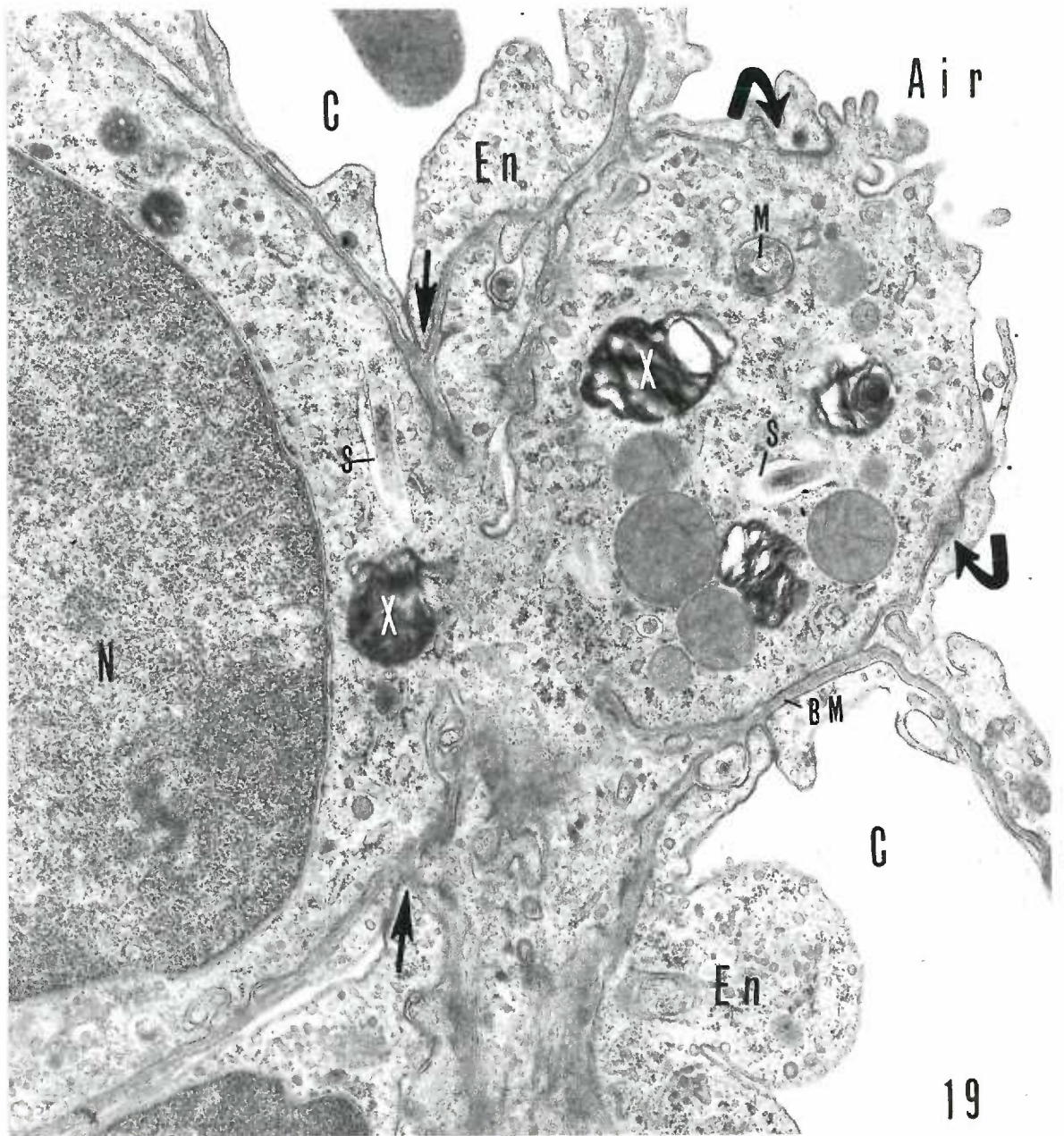


Figure 20. Type B cell of an eleven week old, Group III mouse -- effect of urethane. This mouse received drinking water containing urethane for two days. The type B cell shown appears to be bridging the alveolar septum between two adjacent alveolar air spaces. Dark, lamellar, and vacuolated forms of cytosomes (X) occur in this cell. Epon embedded. X 13,800.

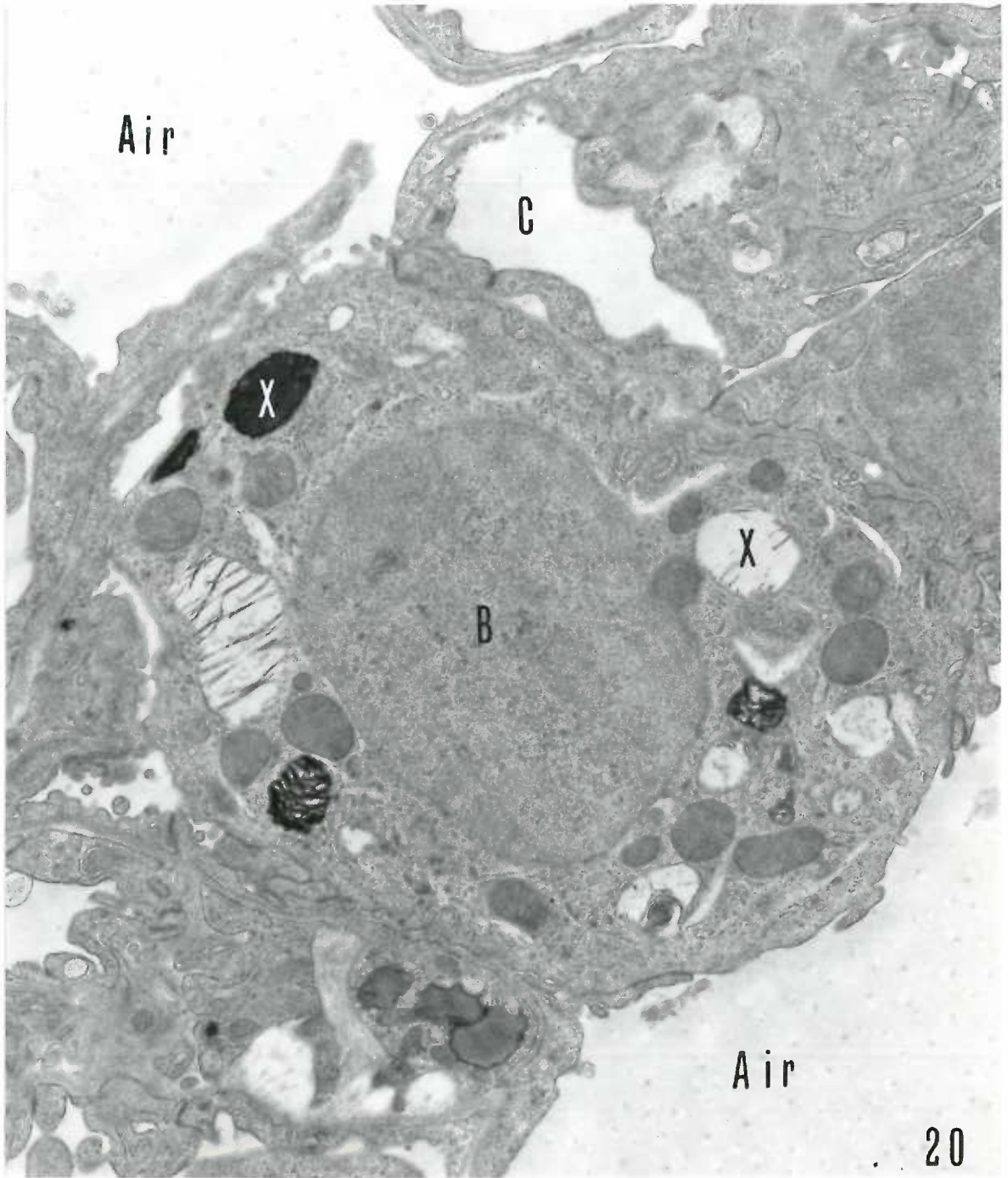




Figure 21. Type A cell of an eleven week old, Group III mouse -- effect of urethane. This mouse received drinking water containing urethane for four days. A type A alveolar epithelial cell is illustrated. The perinuclear cytoplasm consists of a small amount of rough endoplasmic reticulum (E), a small Golgi apparatus (G), and numerous vesicles adjacent principally to the air space and basement membrane, which are probably pinocytotic. Away from the perinuclear region, the cytoplasm attenuates very rapidly (arrows) to line the greater portion of the alveolar surface. Generally, capillaries do not occur in the alveolar wall immediately adjacent to the nucleus of the type A cell. Collagen (CF) and elastic (EF) fibers are noted in the connective tissue of the alveolar septum. Epon embedded. X 13,800.

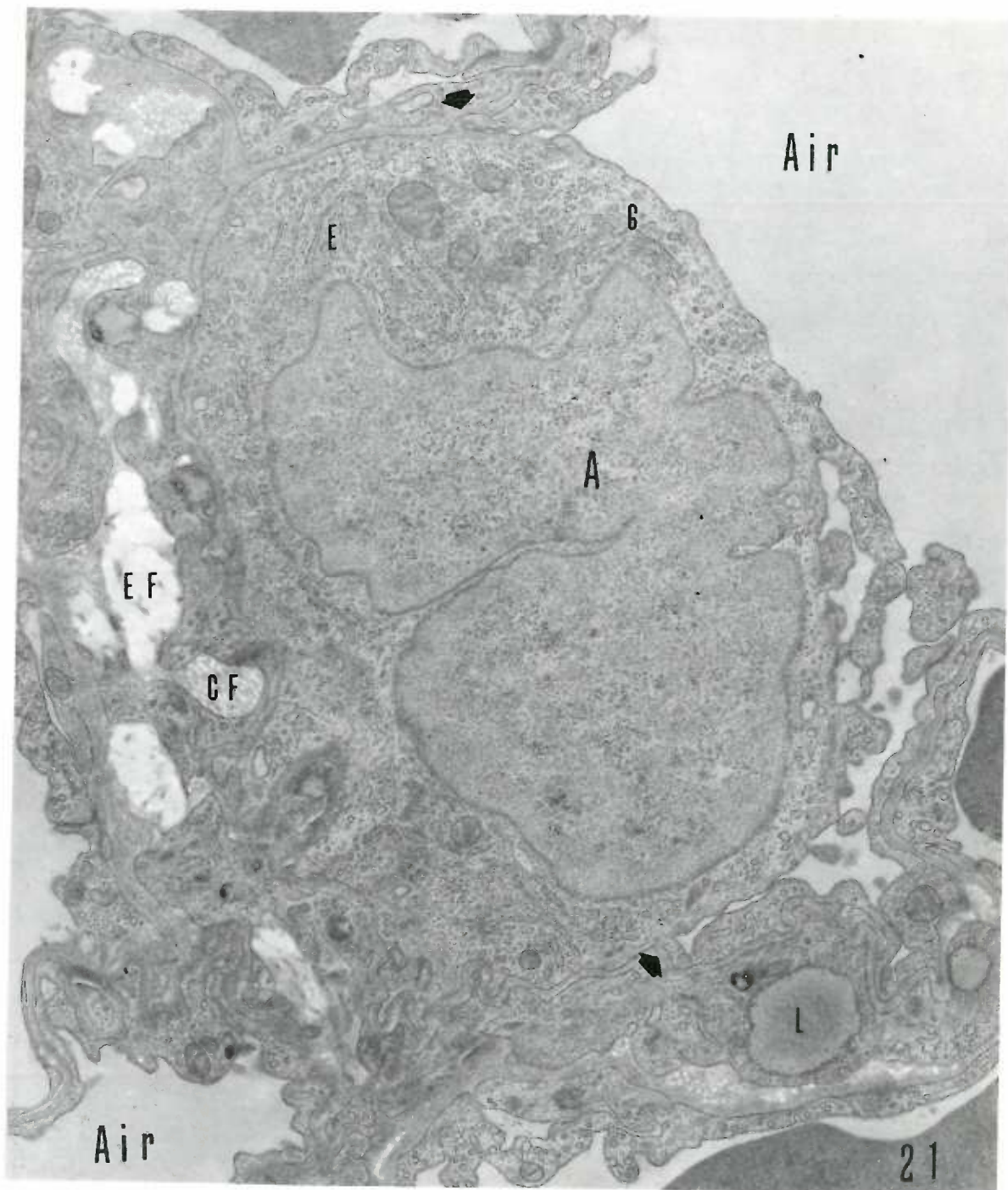


Figure 22. Type B cell of an eleven week old, Group III mouse -- effect of urethane. This mouse received a drinking water containing urethane for four days. The type B cell appears to be very active as judged by the presence of numerous mitochondria, multivesicular bodies, cytosomes, and free ribosomes. Epon embedded. RCA.  
X 15,500.

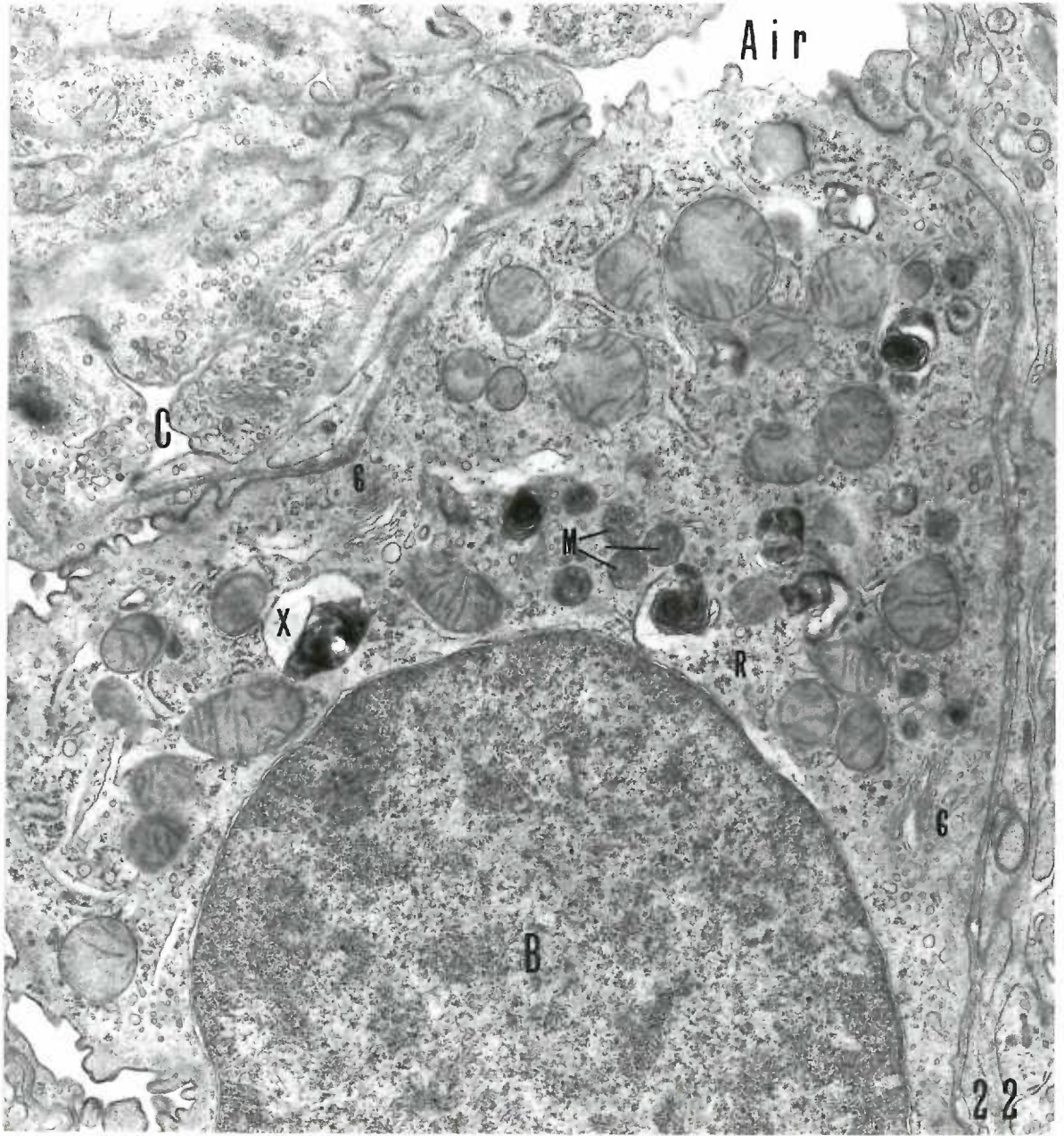


Figure 23. Type B cell of a twelve week old, Group III mouse -- effect of urethane. This mouse received drinking water containing urethane for six days. A vacuolated form of cytosome in this type B cell appears to be in the process of opening into the alveolar air space (arrow). This cell does not show obvious differences when compared to the previous pictures in this series. Epon embedded. X 13,800.

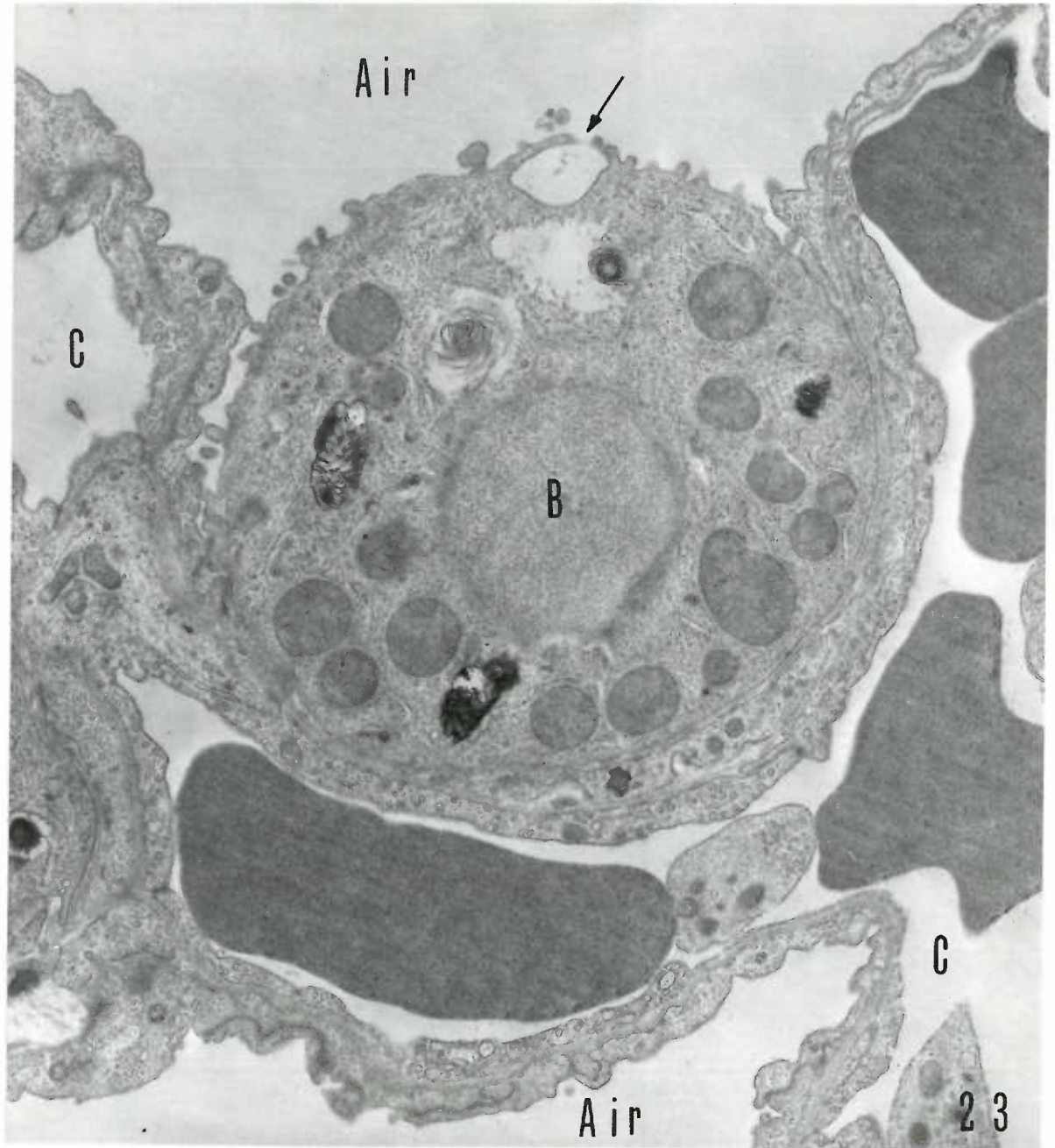


Figure 24. Tumor cells of an eighteen week old, Group III mouse -- effect of urethane. This mouse received drinking water containing urethane for 55 days. This micrograph illustrates a group of tumor cells (T) encroaching on normal alveolar tissue. The tumor cells are seen to be morphologically similar to the type B cells previously shown. The junction (J) between type A cell and tumor cell appears to be identical to that found between type A and type B cell in normal lung. X 13,800.

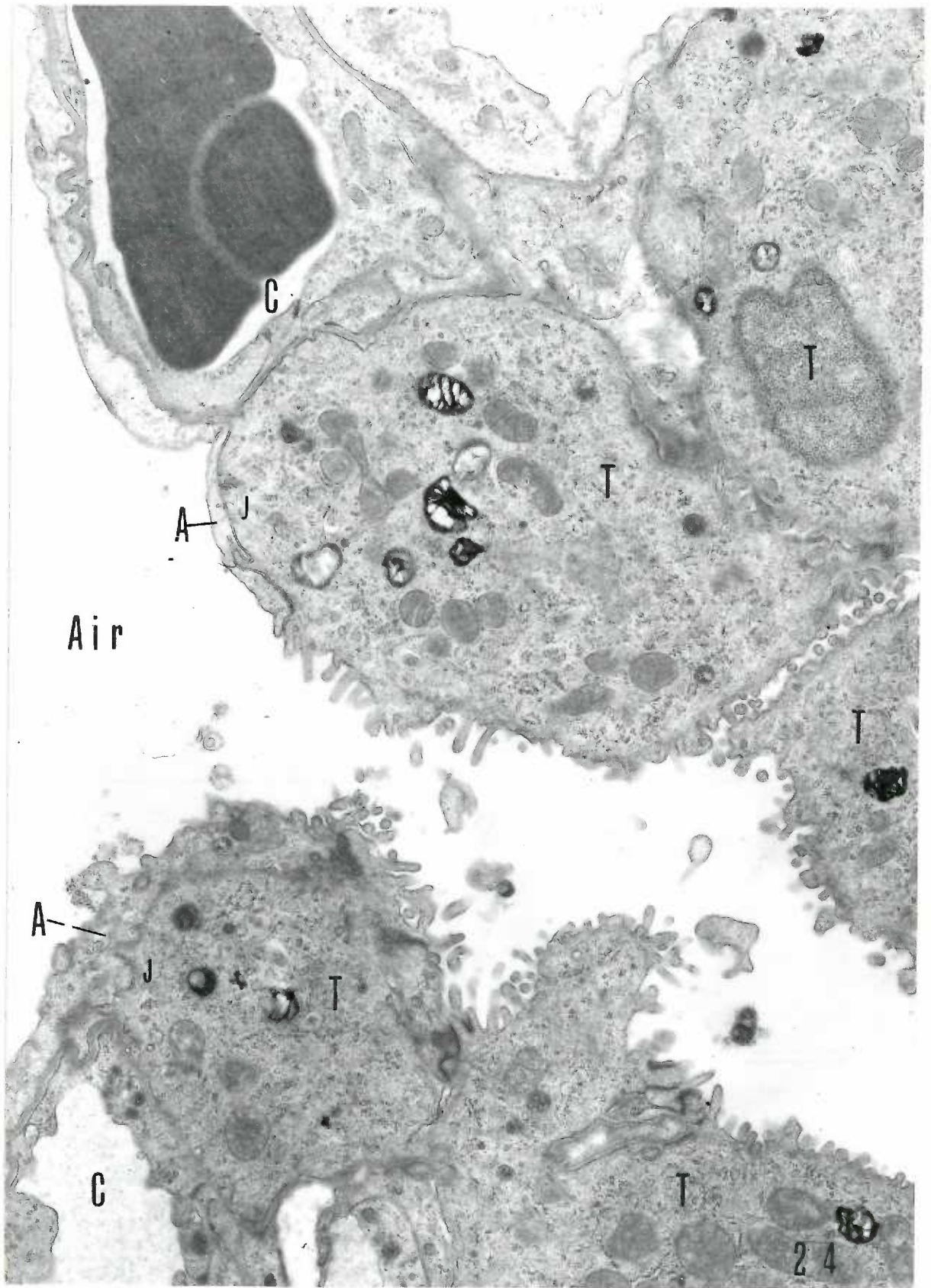




Figure 25. Tumor cells of a twelve month old, Group V mouse.

The tumor cells illustrated reveal several features common to many, but not all such cells. With this fixative, cytosomes (X) have a lamellar form, with the exception of one shown (thick arrow). This cytosome appears as if it is enclosed within another membrane-bound body, the latter containing loosely dispersed, finely granular material. A large, membrane-enclosed, vacuolated dense mass (thin arrow) occurs in one cell. This structure has also been observed in other tumor cells from time to time. Small inclusions are present in the tumor cell nuclei. Nuclear inclusions are frequently found in tumor cells. X 13,800.

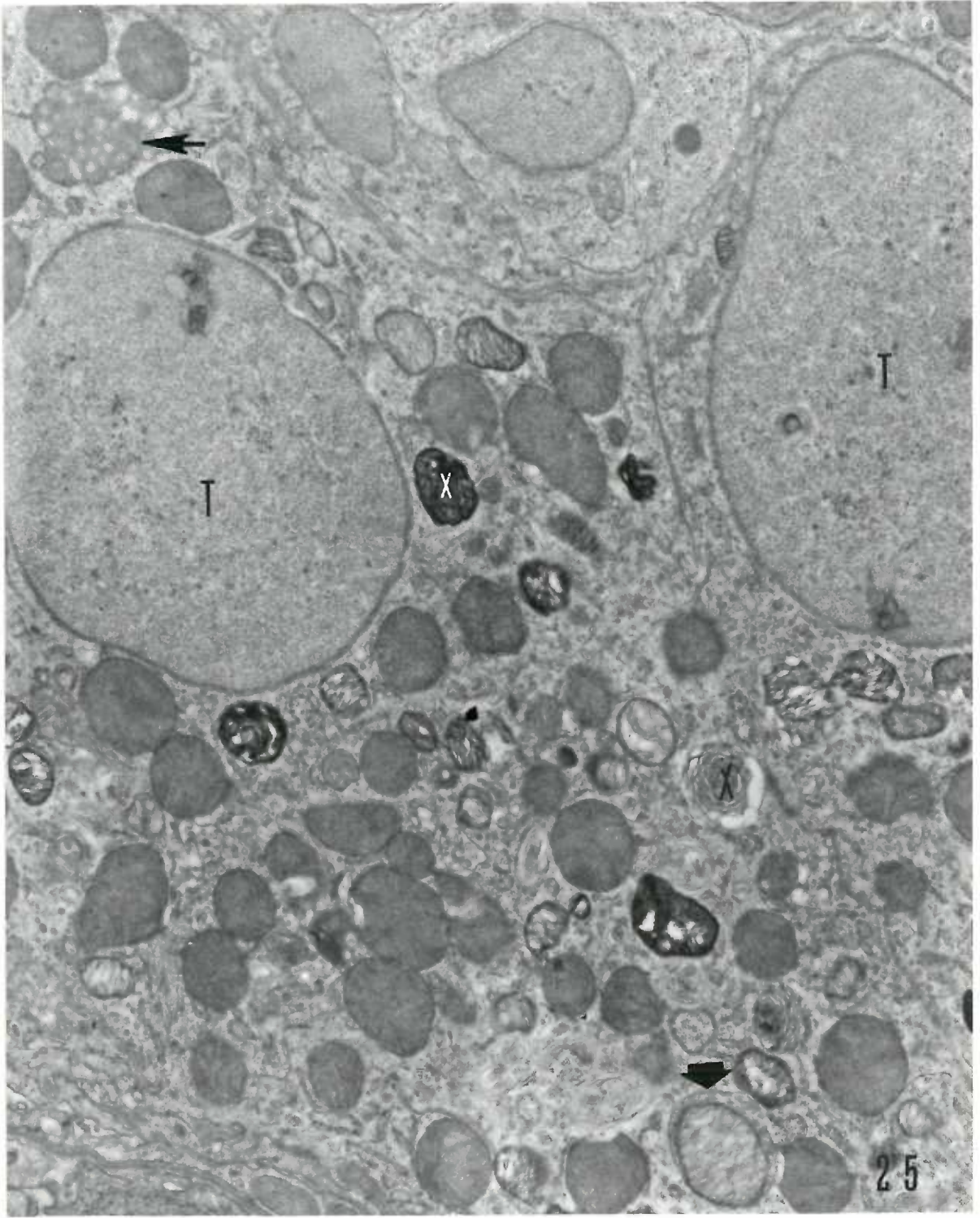


Figure 26. Tumor cells of a sixteen month old Group V mouse.

Portions of two tumor cells are illustrated. The loose joining together of these cells, mainly by interdigitating cytoplasmic processes is typical of most, but not all lung tumor cells. Short, relatively straight stretches of closely apposed cell membranes of adjacent cells may represent an attachment device referred to as adhering zonules. Membranes of the Golgi apparatus (G) are prominent throughout the cytoplasm. Endoplasmic reticulum (E), although moderately abundant, runs loosely through the cell and is rarely organized into regular aggregates or patterns. Vesicles (V) are very numerous in tumor cells, and are generally located in the Golgi regions. Nuclear pores (Np), cut tangentially, are noted in one cell. Cytosomes (X) are pleomorphic in many tumor cells. Some are dense. One cytosome (arrow head) has three components: a dense crystalloid part, a less dense granular part, and a vesicular part. Another (arrow) contains a dense part tending towards the lamellar form. Fixed in glutaraldehyde-osmium (3:2) combination, buffered with cacodylate, rinsed with buffer, and postfixed in  $\text{OsO}_4$ . X 22,900.

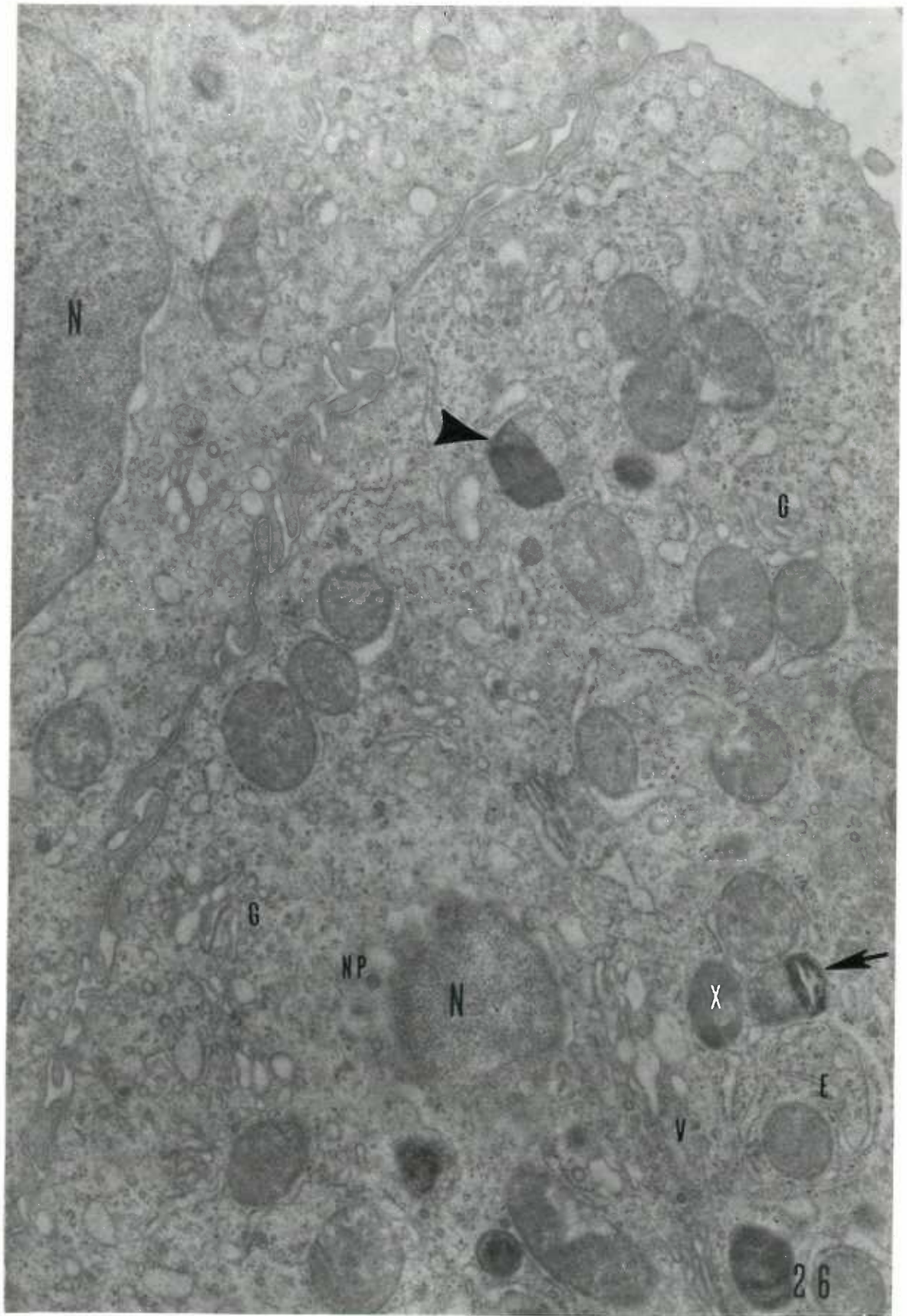


Figure 27. Alveoli of a seven day old, Group IV mouse ---  
effect of urethane. The mother of this mouse had  
received drinking water containing urethane from the  
13th through the 19th day of gestation. This moderately  
low magnification picture shows portions of three type B  
cells as well as other cell types. The alveolar septum  
is somewhat thickened, and the connective tissue cells  
(CT) are very active in appearance. One example of  
apparent release of a cytosome from a type B cell is  
noted (arrow). X 13,800.

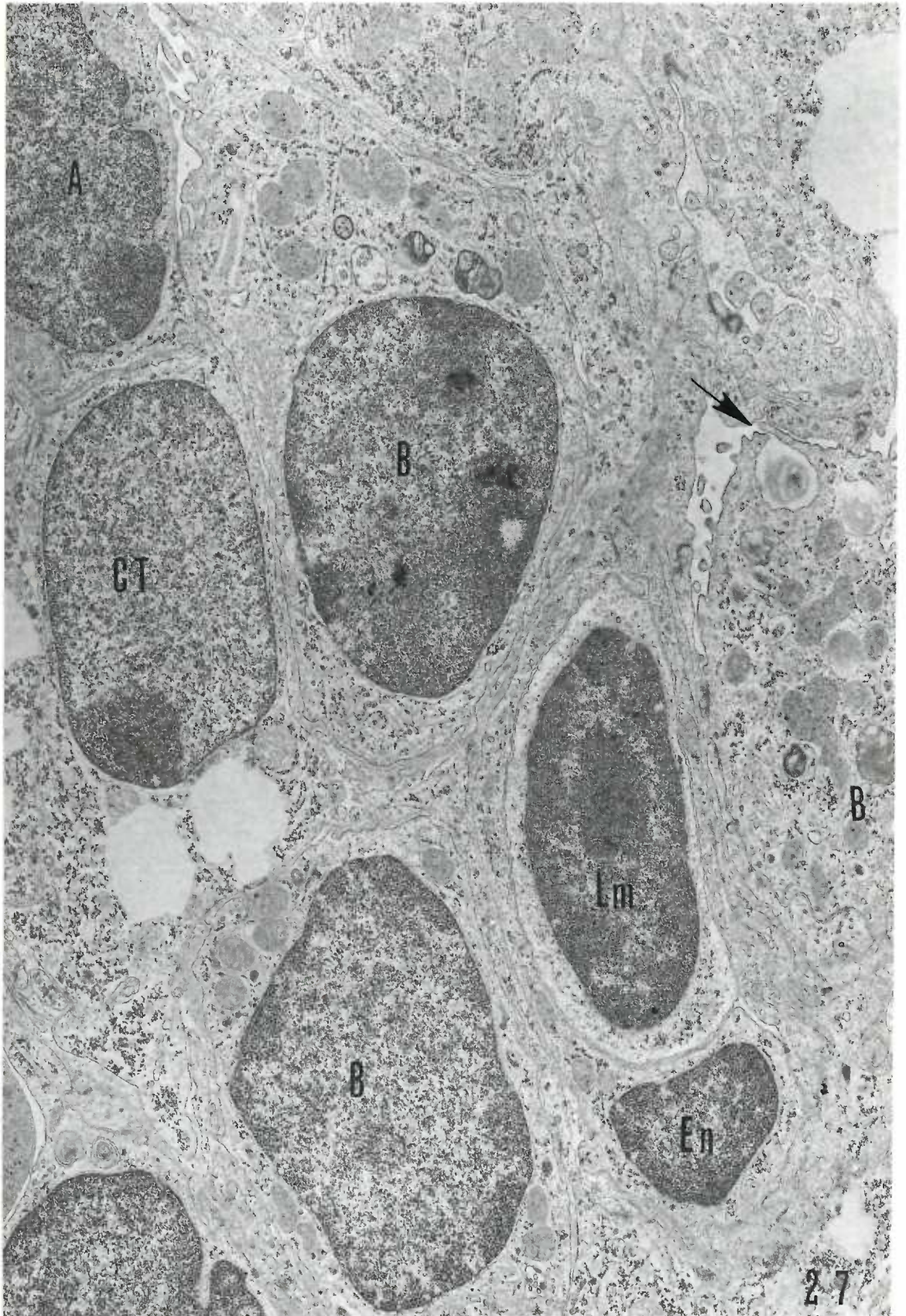


Figure 28. Type B cell of a seven day old, Group IV mouse -- effect of urethane. The mother of this mouse received drinking water containing urethane from the 13th through the 19th day of gestation. The type B cell shown reveals features already noted in this cell type. Multivesicular bodies (M), cytosomes (X), and a peculiar configuration of the endoplasmic reticulum (S) are present. X 18,300.

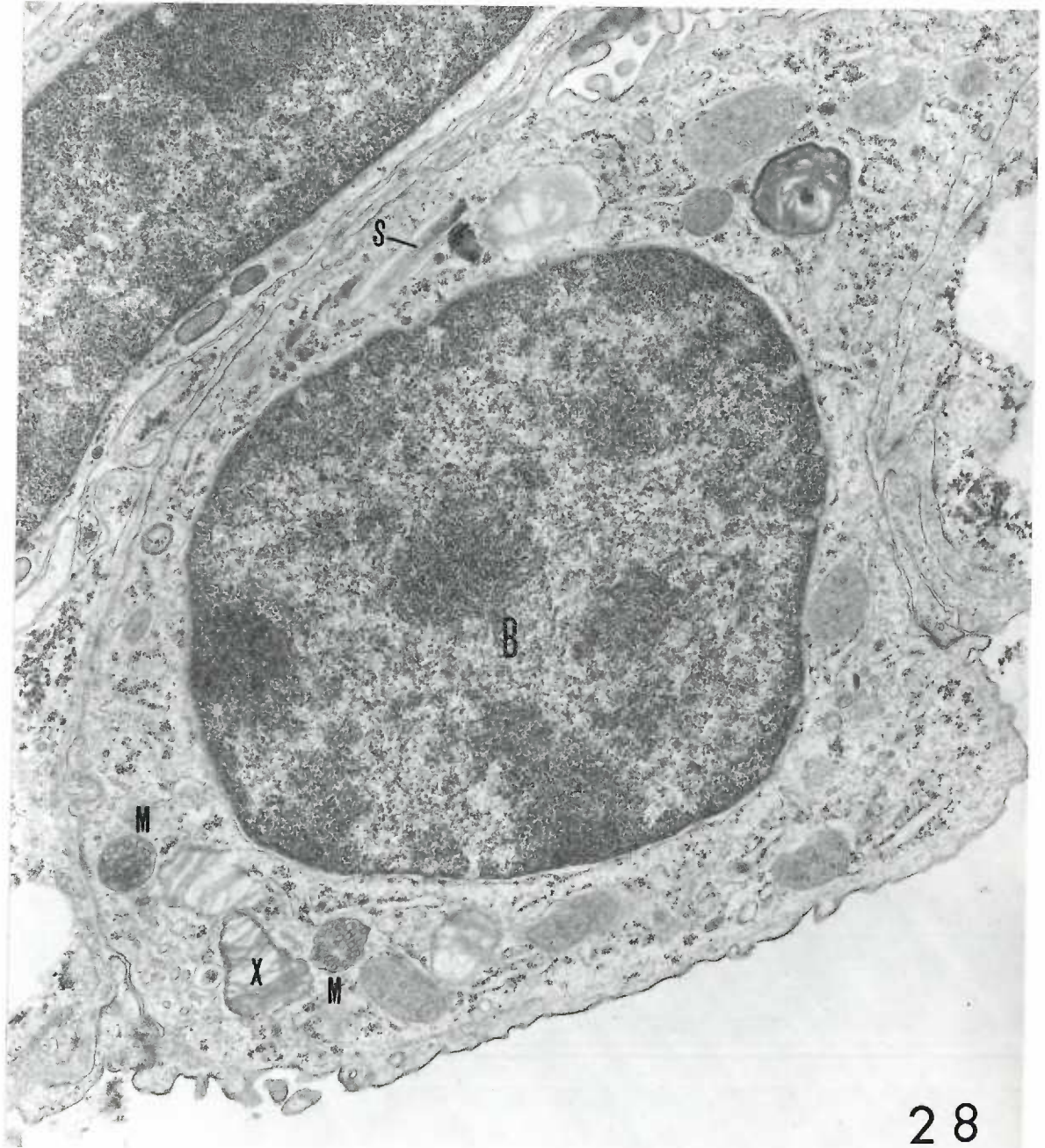




Figure 29. Type B cell of a nine day old, Group IV mouse -- effect of urethane. The mother of this mouse received drinking water containing urethane during the last three days of gestation and for the first three days after delivery. The type B cell illustrated has prominent Golgi regions (G), several cytosomes (X), and two forms of multivesicular body (M). The multivesicular body closer to the nucleus is filled with vesicles and that closer to the cell periphery has only a few vesicles and is irregular in shape. The relatively empty, irregular outermost multivesicular body may be in the process of formation, whereas the innermost body may be fully formed. X 22,900.



Figure 30. Type B cell of a seven day old, Group IV mouse --

effect of urethane. This higher magnification picture of the central type B cell shown in Fig. 27 reveals several important features. The two cytosomes seen are clearly multicomponent in construction, having lamellar, granular, and vesicular components. The body noted by the arrow may represent a section through the vesicular portion of another cytosome. The endoplasmic reticulum (E) is characterized by the scarcity of ribosomes attached to the membranes and the tendency to form either in short straight or in crescentic segments. Where the endoplasmic reticulum takes the unusual configuration seen at the bottom of the micrograph (S), very few ribosomes are found attached to the membranes. The close topographical relation between the Golgi vesicles (V) and multivesicular bodies is frequently encountered. A thickening at the edges of some multivesicular bodies (arrow head) can be seen in many multivesicular bodies, generally the ones thought to be forming, as noted in the previous figure.

X 38,800.



Figure 31. Alveolar macrophage of a nine day old, Group IV mouse -- effect of urethane. The mother of this mouse had received drinking water containing urethane during the last three days of gestation and the first three days following delivery. For purposes of comparison, a macrophage (Mac) adjacent to the plasma membrane of a type A alveolar cell is shown. A broad pseudopod (Ps) extends from one portion of the cell. Vacuolar remnants of ingested materials, as well as various pleomorphic dense bodies appear in the cytoplasm. Some of the smaller of these dense bodies may represent elementary bodies of mycoplasma. X 13,800.

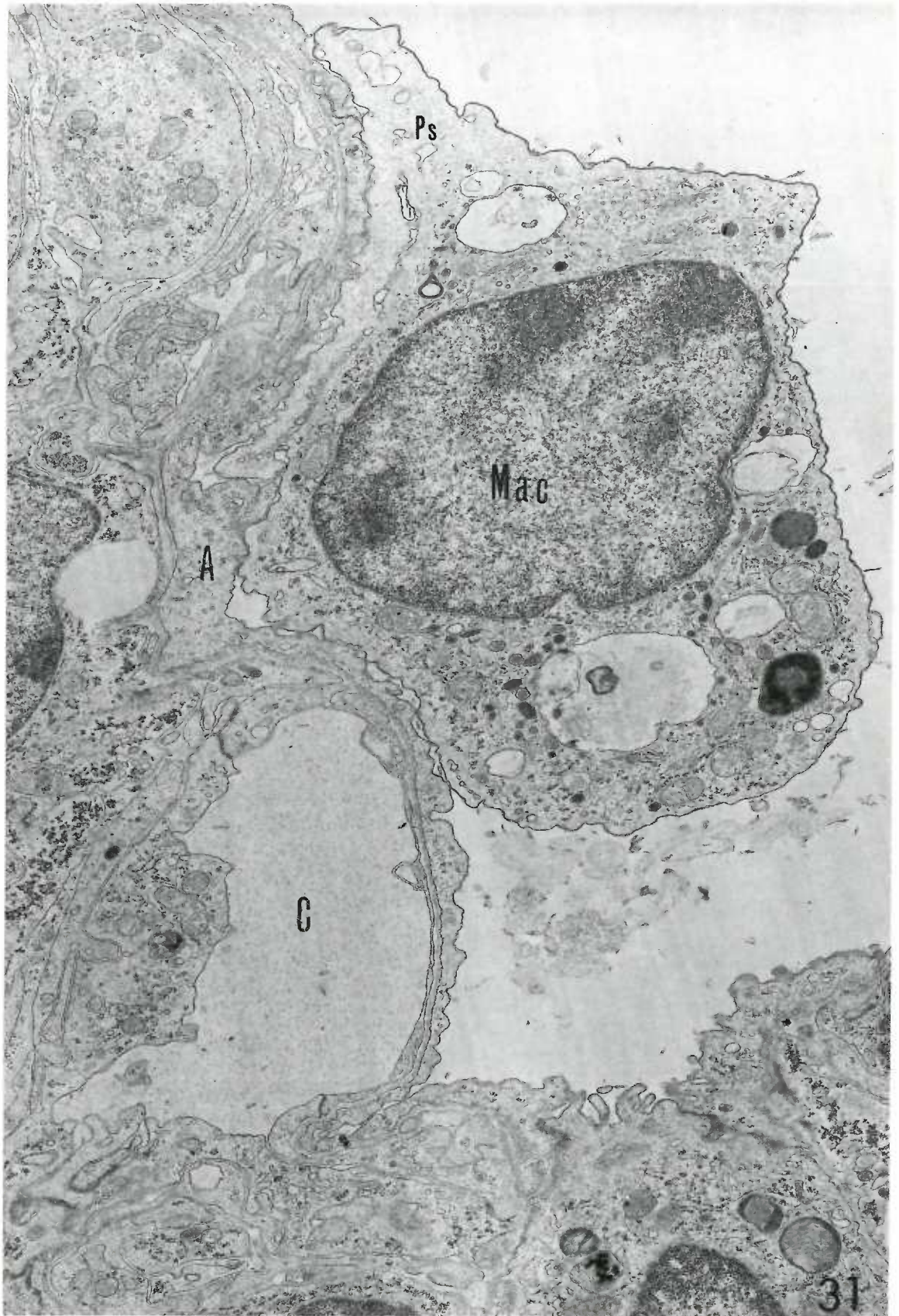


Figure 32. Tumor cells of a forty-three day old, Group IV mouse -- effect of urethane. The mother of this mouse received drinking water containing urethane from the 12th through the 17th day of gestation. A group of tumor cells borders an air space in this micrograph. The cytosomes in these cells are, for the most part, in a non-lamellar form. The underlying stromal elements are indicated.

X 8,400.

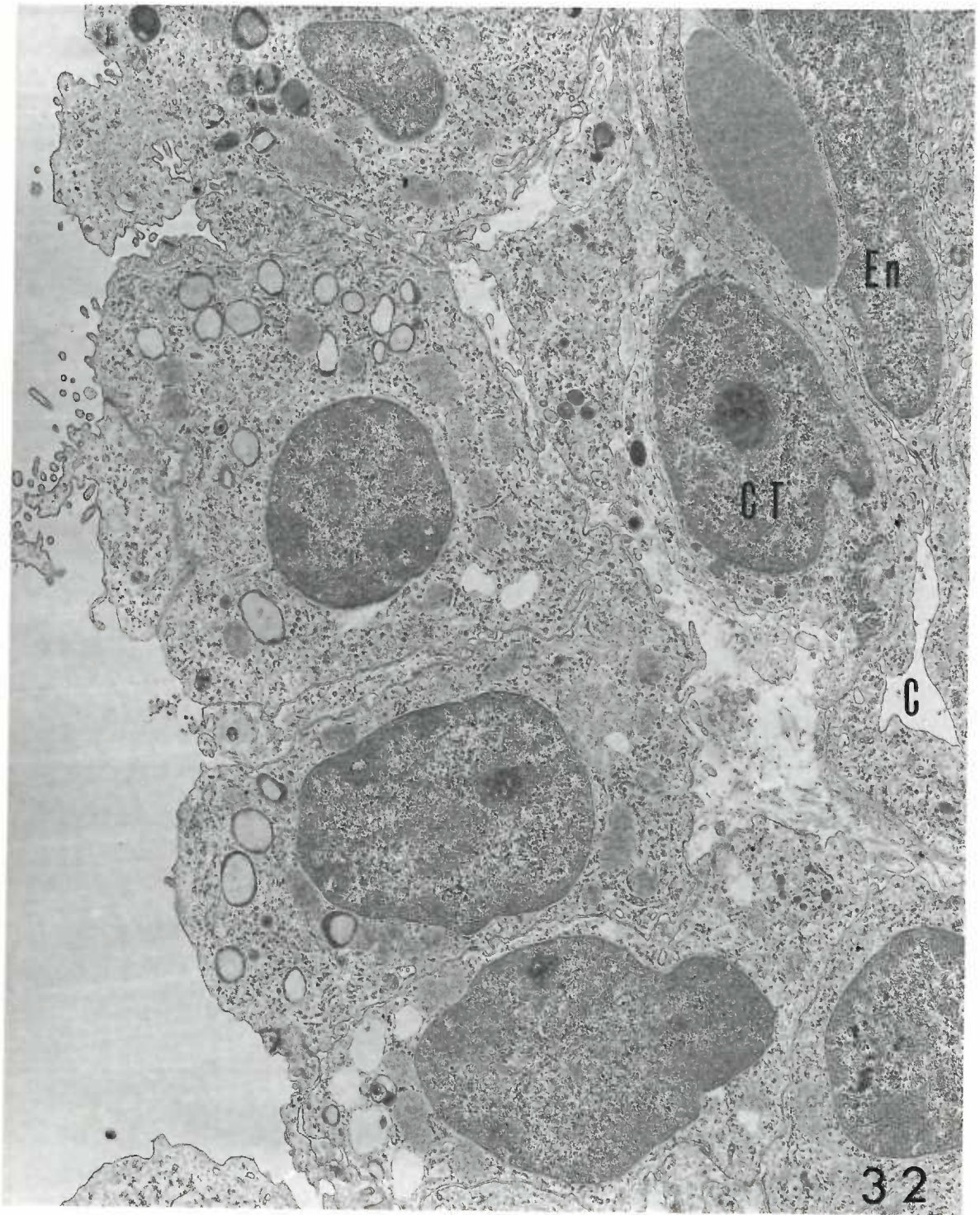




Figure 33. Tumor cells of a fifty-six day old, Group IV mouse -- effect of urethane. The mother of this mouse had received drinking water containing urethane from the 16th day of gestation through the 21st day following delivery. At this low magnification, the tumor cells appear to grow as a sheet joined together by tight junctions, interdigitating processes, and adhering zonules. In these cells, cytosomes are almost all uniformly dense. The red blood cells at the bottom of the micrograph have probably leaked from cut surfaces of the tissue into the air spaces. X 8,400.

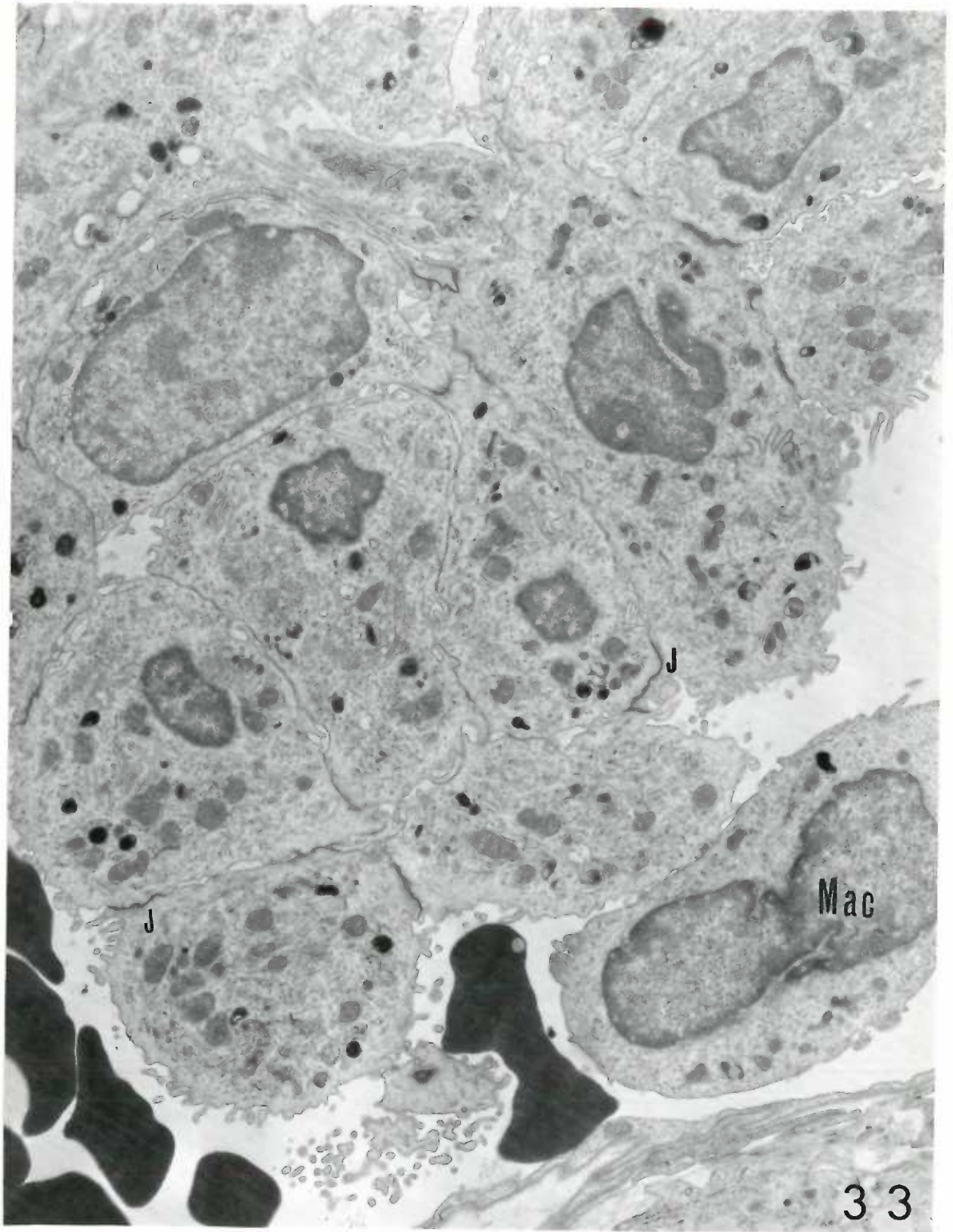
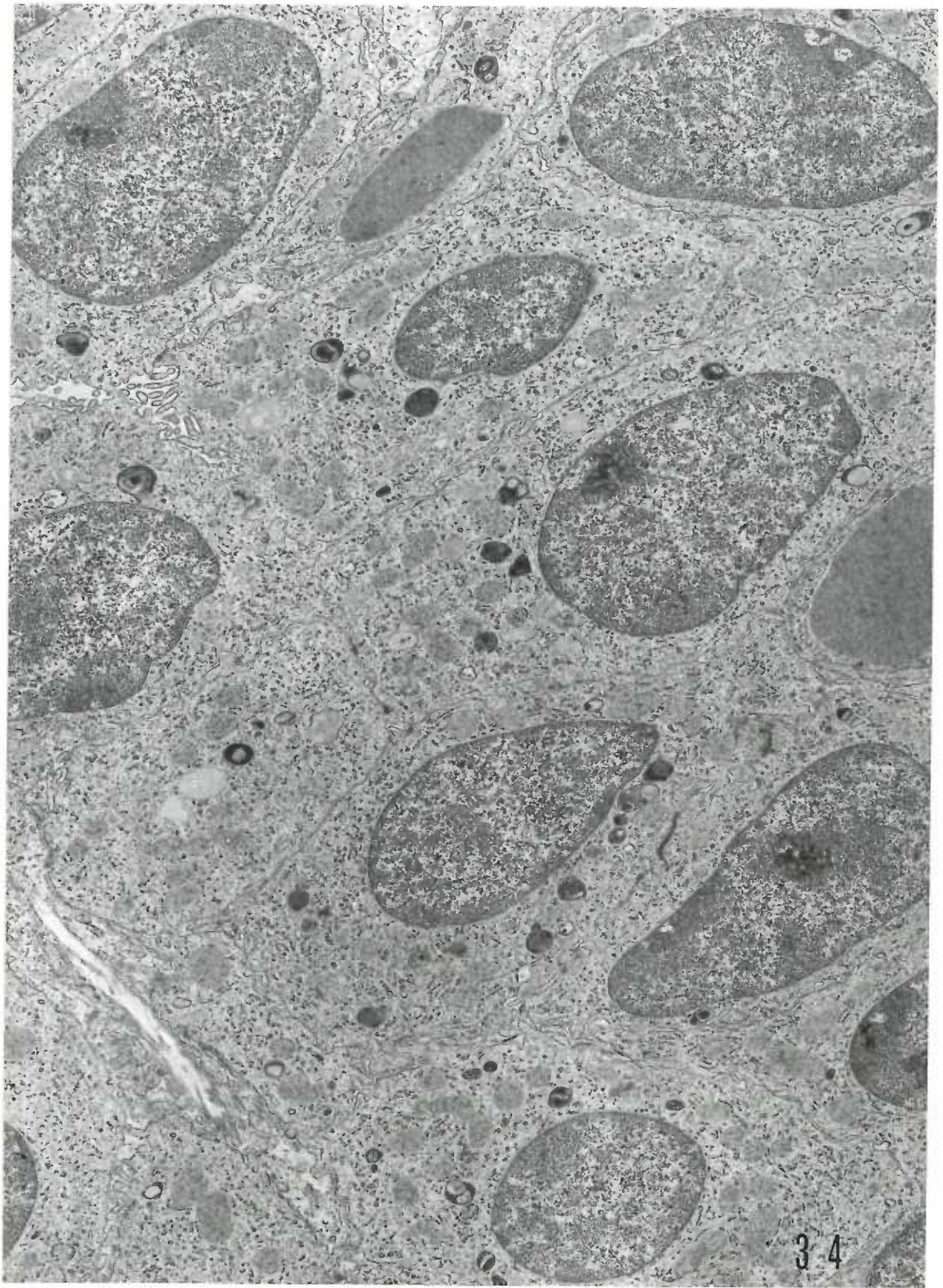


Figure 34. Tumor cells of a forty-three day old, Group IV mouse -- effect of urethane. The mother of this mouse received drinking water containing urethane from the 12th through the 17th day of gestation. In this low magnification picture, the almost solid appearance of the tumor is evident. Cytosomes are not numerous, but when they are present both solid and mixed-component forms are seen. X 8,400.



34

Figure 35. Tumor cells of a fifty-six day old, Group IV mouse -- effect of urethane. The mother of this mouse received drinking water containing urethane from the 16th day of gestation until the 21st day following delivery. The tumor cells shown at this moderate magnification have all the characteristics of type B cells. The cytosomes in these tumor cells appear in all the forms previously described. X 13,800.

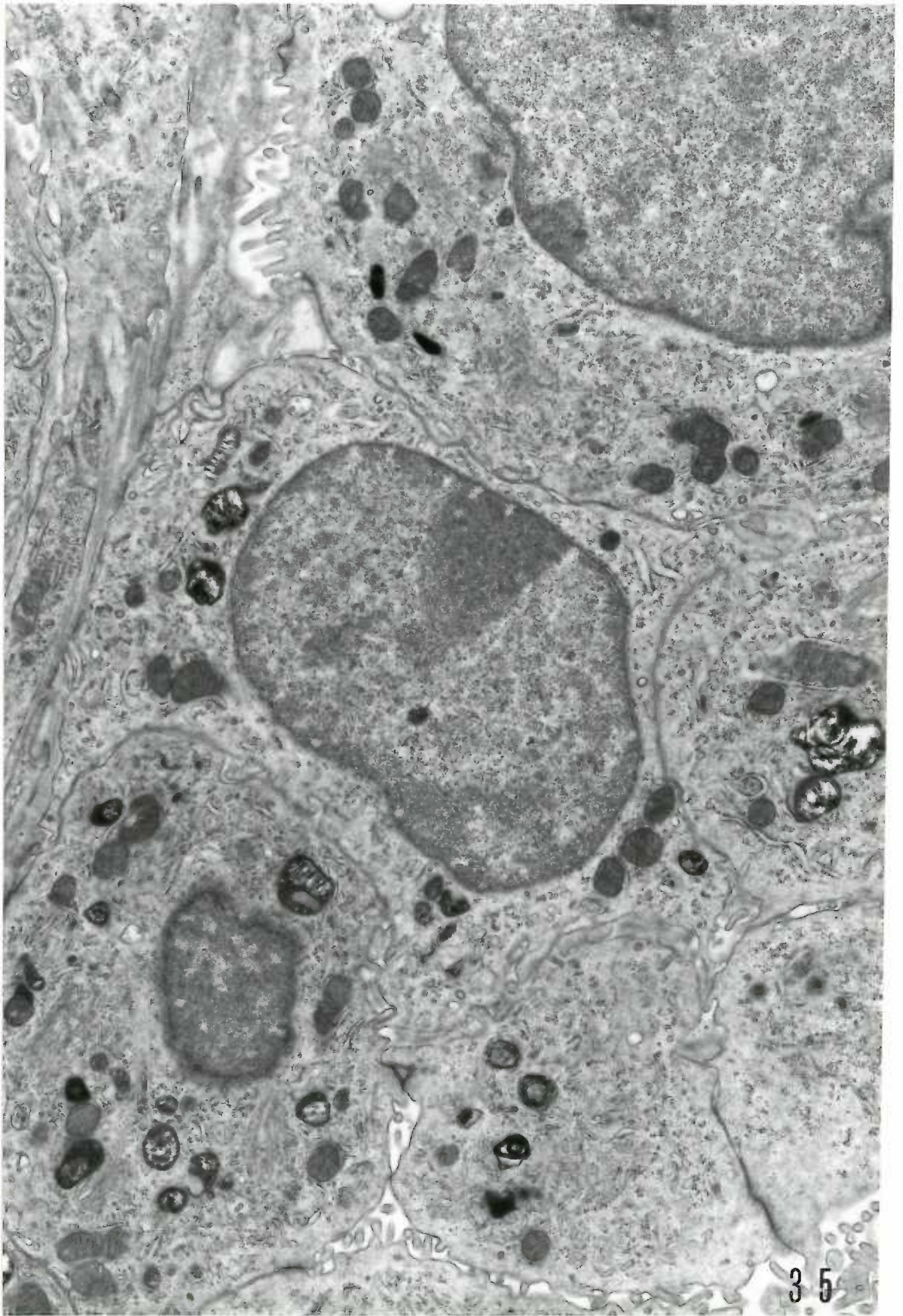


Figure 36. Tumor cells of a fifty-six day old, Group IV mouse -- effect of urethane. The mother of this mouse received drinking water containing urethane from the day of delivery through the 21st day following delivery. The tumor cells illustrated appear to be very active and give every indication of being secretory in nature.  
X 13,800.

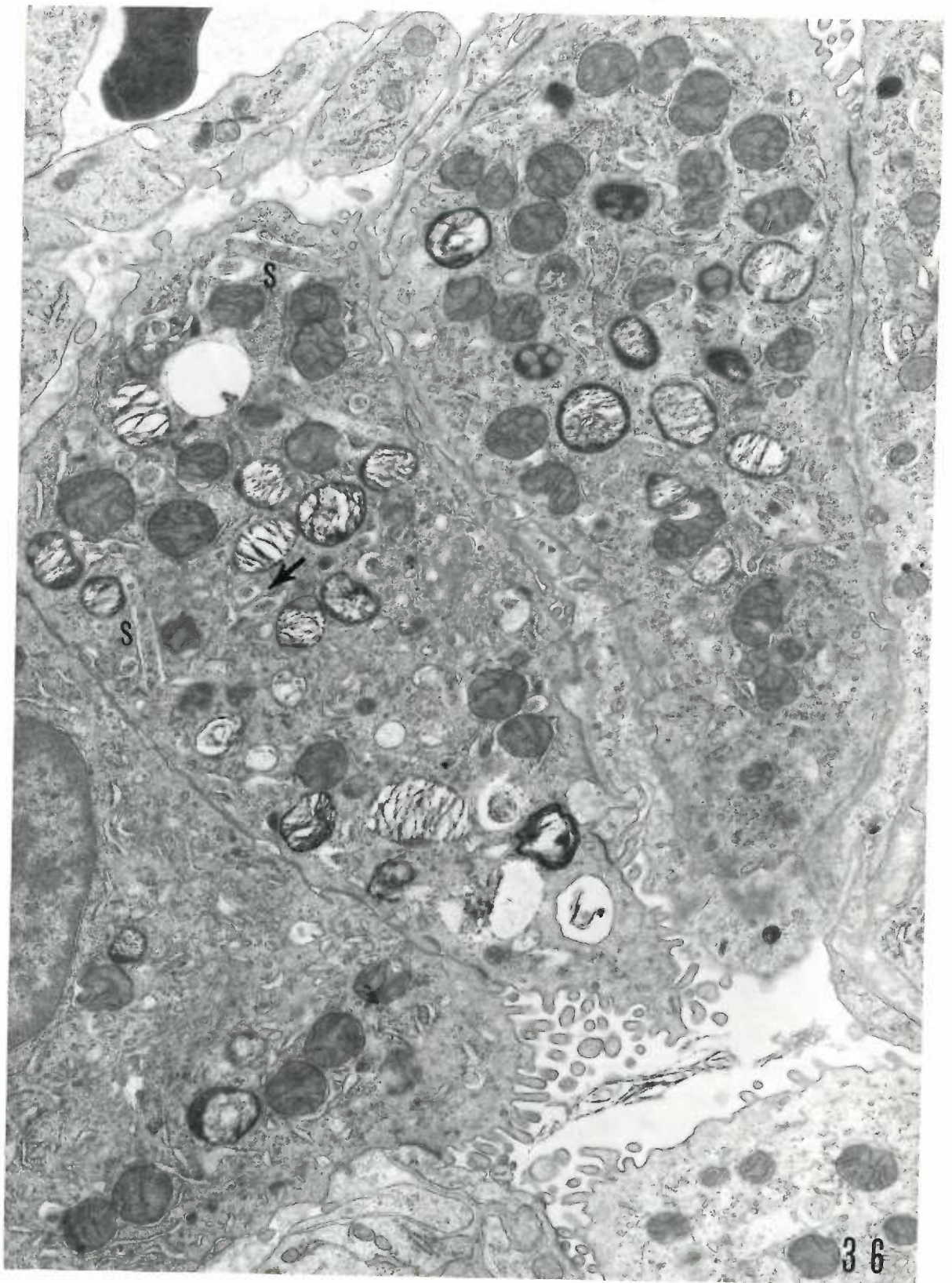




Figure 37. Tumor cells of a forty-three day old, Group IV mouse. The mother of this mouse had received drinking water containing urethane from the 12th through the 17th day of gestation. Commencing with this picture, and extending through the next four figures, tumor cells will be depicted wherein the cytosomes are not of the lamellar form. At the moderate magnification of this picture, many of these bodies are seen to have a very dense, and in some cases angular, internal structure (arrows). X 13,800.

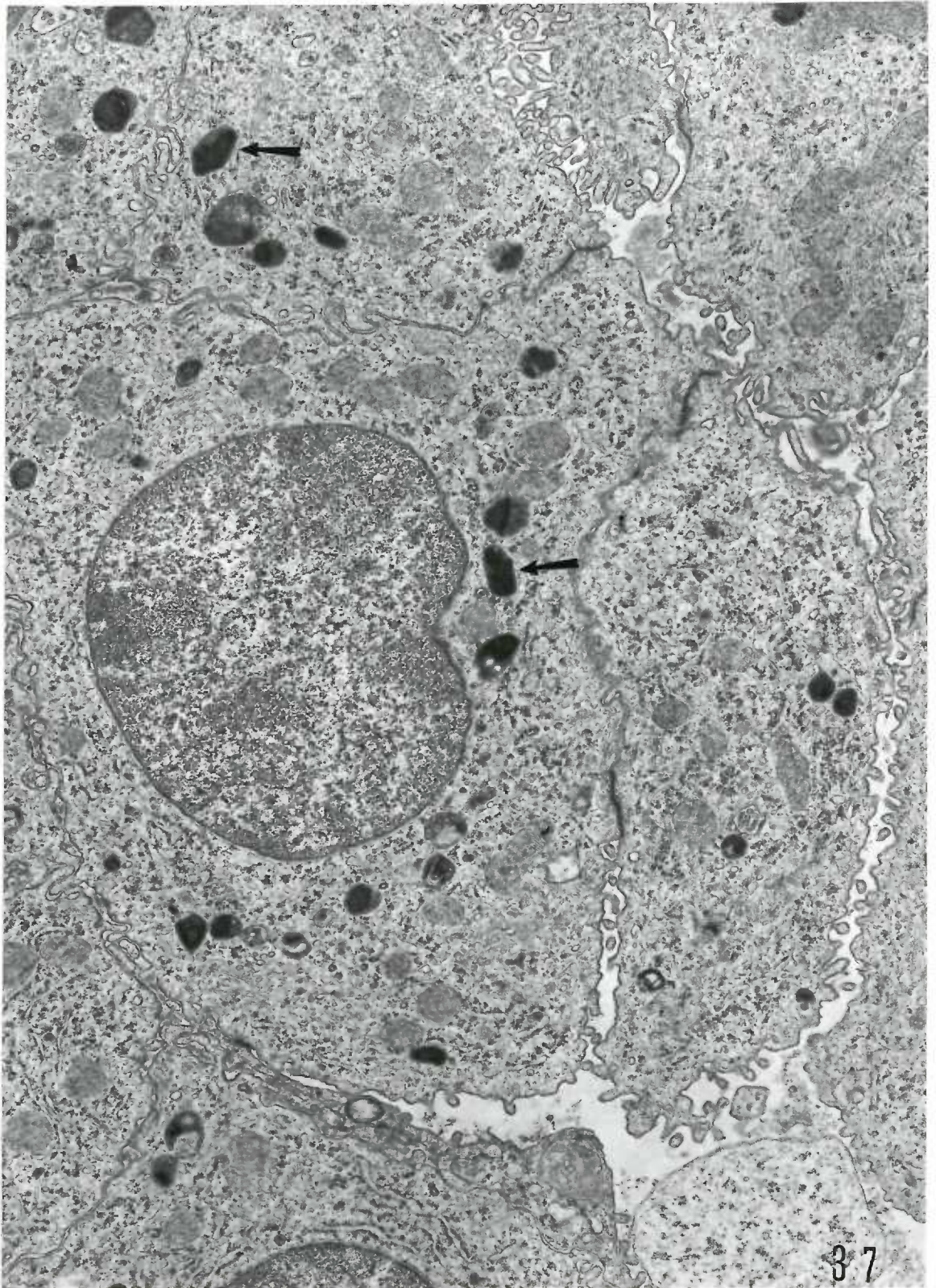


Figure 38. Tumor cells of a forty-three day old, Group IV mouse -- effect of urethane. The mother of this mouse had received drinking water containing urethane from the 12th through the 17th day of gestation. The tumor cell illustrated contains several cytosomes with included crystalloids. One such body (triangle) contains vesicles of the same size as those found in the multivesicular bodies elsewhere in the cell. X 22,900.

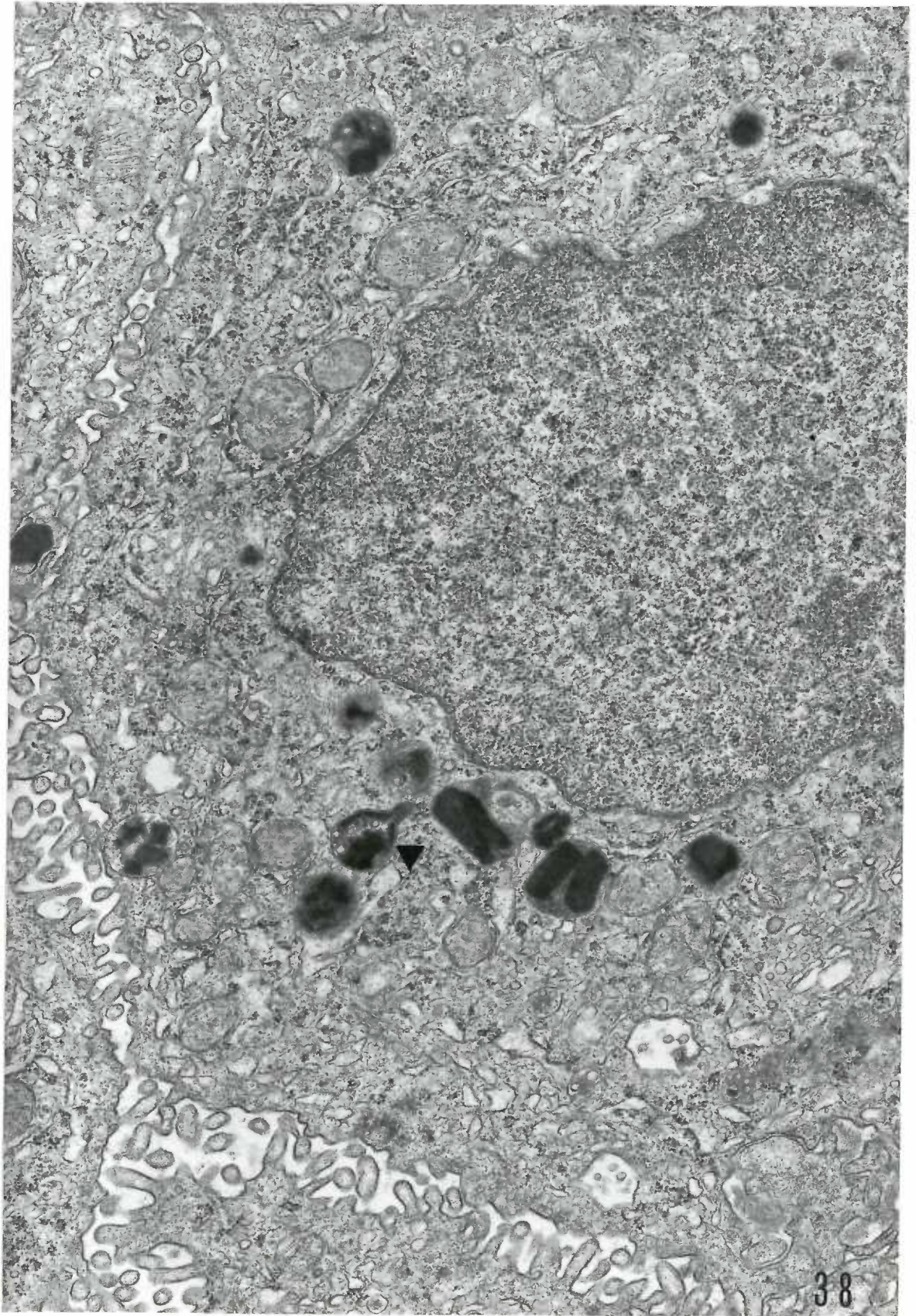
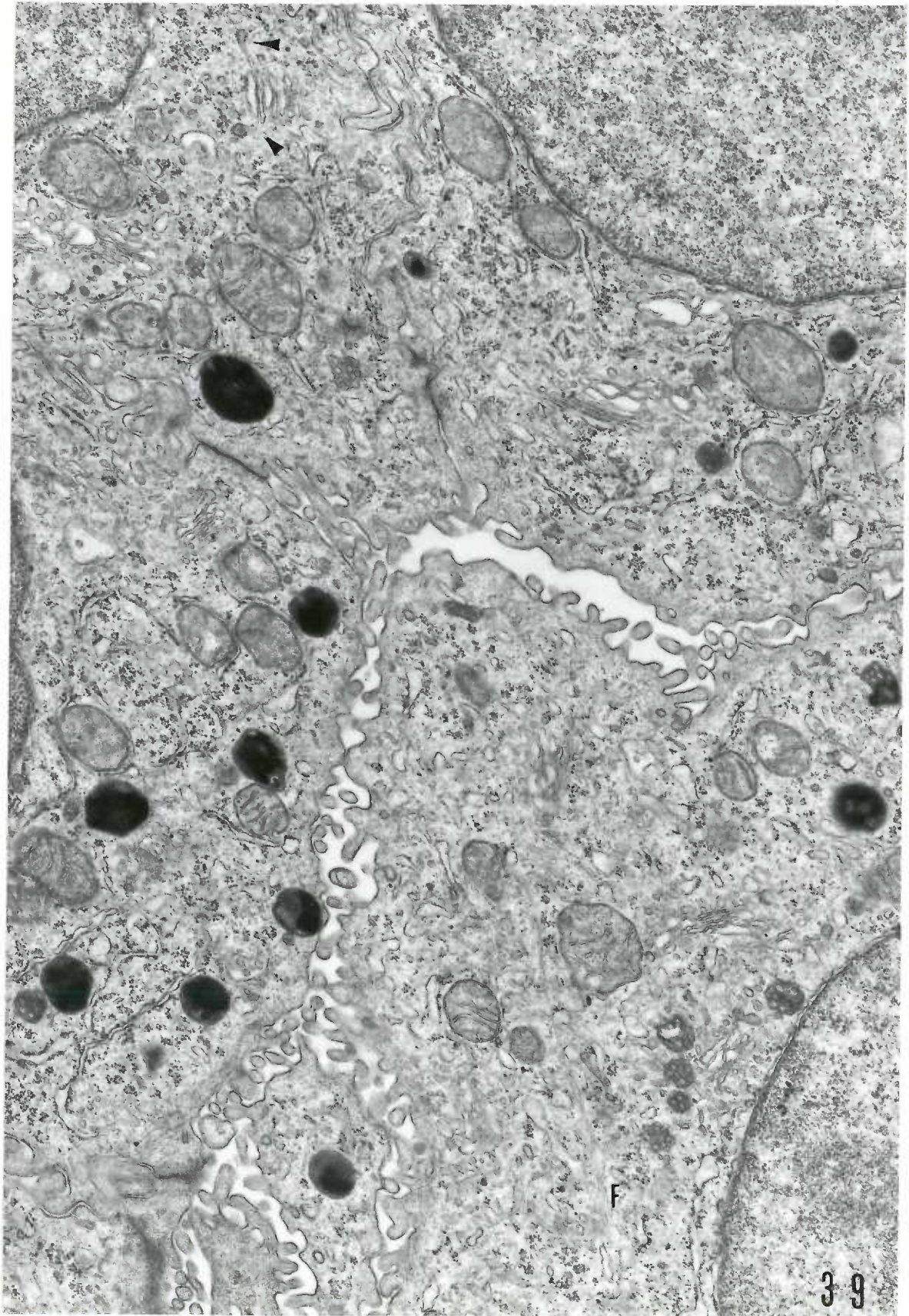


Figure 39. Tumor cells of a fifty-six day old, Group IV mouse -- effect of urethane. The mother of this mouse had received drinking water containing urethane from the 16th day of gestation through the 21st day following delivery. As in the previous figure, the cytoplasmic bodies are dense, and in some cases angular, presenting a crystalline appearance. Fine fibrils (F) appear in different areas of the cytoplasm. An apparent relation of Golgi membranes to coated vesicles is noted at the top of the micrograph (arrow heads). X 22,900.



F

Figure 40. Tumor cells of a fifty-six day old, Group IV mouse -- effect of urethane. The mother of this mouse received drinking water containing urethane from the 16th day of gestation through the 21st day following delivery. The two tumor cells illustrated are located at the edge of normal lung tissue. An extensive Golgi apparatus (G) is evident in both tumor cells. A large, perhaps forming, multivesicular body (M), and the U-shaped endoplasmic reticulum configuration (S) are noted. X 22,900.

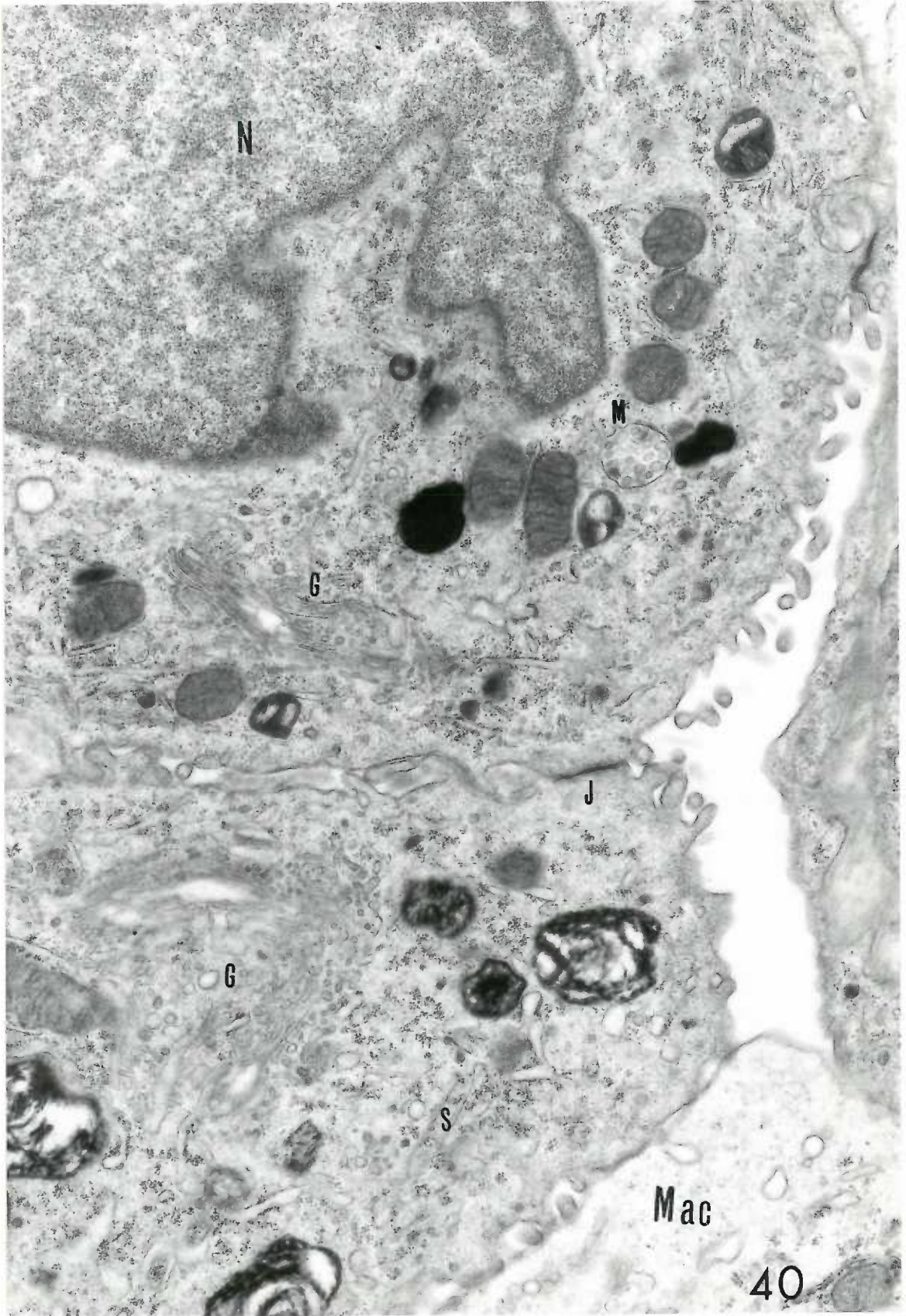




Figure 41. Tumor cell and macrophage of a fifty-six day old, Group IV mouse. The mother of this mouse had received drinking water containing urethane from the 16th day of gestation through the 21st day following delivery. A comparison of portions of macrophage and tumor cell cytoplasm is offered in this illustration. At this magnification, the cell types are differentiated by noting the junctional complex between tumor cells, the microvilli along the apical borders of the tumor cells, and the macrophage pseudopod. A confusing feature is the similarity between dense bodies in the macrophage and in the tumor cells. X 22,900.

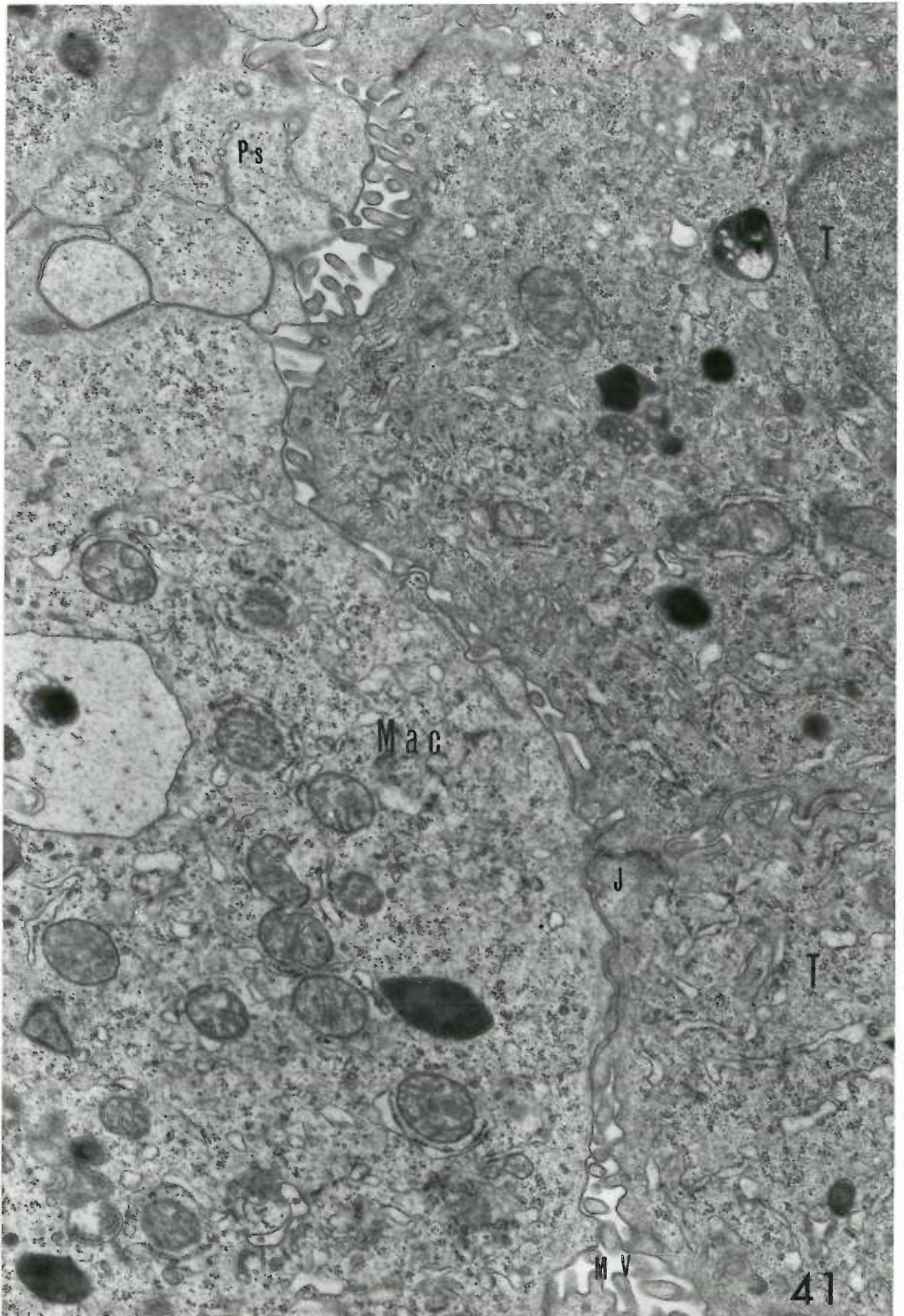


Figure 42. Tumor cells of a fifty-six day old, Group IV mouse -- effect of urethane. Tissue is from the same animal as shown in the previous two figures. This illustration reveals, in addition to the extremely widespread Golgi region in the tumor cells, many dense, irregular bodies (small arrows) within tumor cells which could be confused with similar bodies in macrophages. In the tumor cells such structures are probably peculiar sections through cytosomes formed as the one shown in the lower left corner (large arrow). X 22,900.

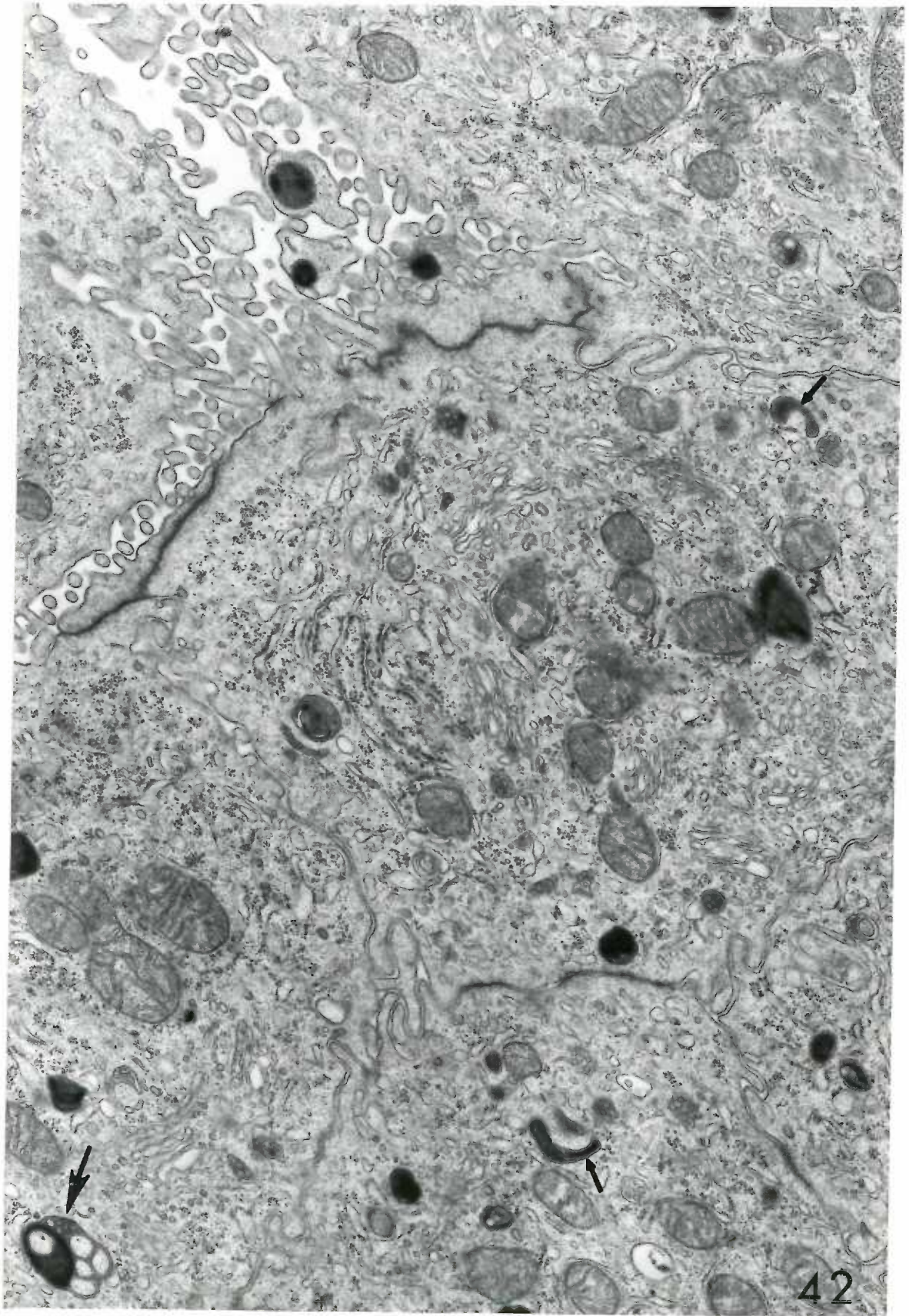


Figure 43. Tumor cells of a twelve month old, untreated, Group I mouse. This micrograph illustrates tumor cells and stroma from a typical "spontaneous" tumor. The endothelial-lined capillary is surrounded by a basement membrane, which in this animal tends to be abnormal in that there is a proliferation of fine fibrils that merge with the basement membrane often obscuring it. Adjacent to the endothelium, and partly surrounding the capillary, are thin cytoplasmic processes from some unknown cell (Y), a pericyte, or possibly a fibroblast. A basement membrane separates these cellular processes from the tumor cells. The bases of the tumor cells are both smooth and irregular giving an impression, in the latter case, of lack of contact with the connective tissue elements. The tumor cells are similar to others shown previously. The cytosomes in these cells appear, for the most part, in the dense, lamellar form. Epon embedded. X 13,800.

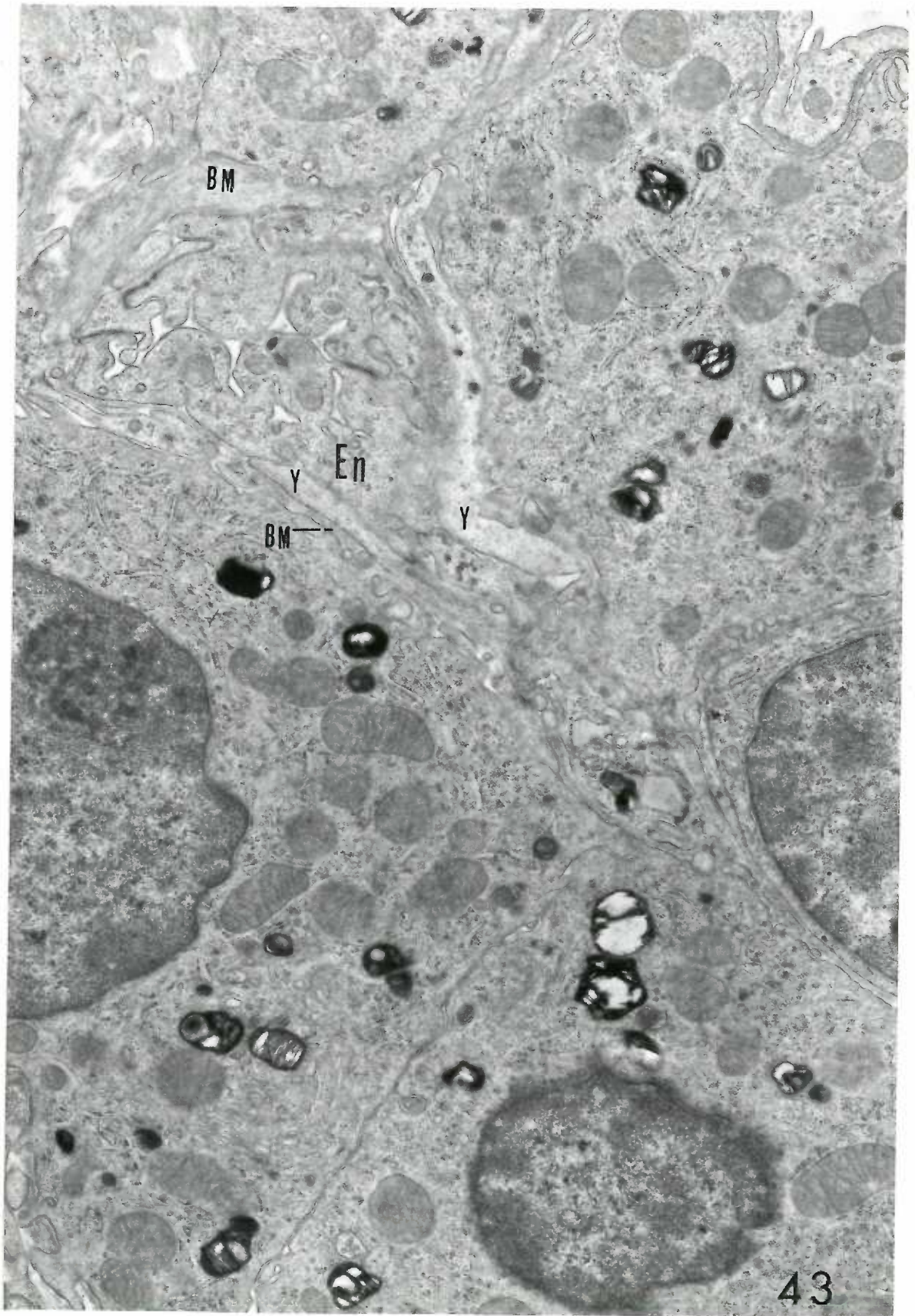


Figure 44. Tumor cell of a sixteen month old, untreated, Group I mouse. The tumor cell illustrated is in juxtaposition to an area of non-neoplastic lung tissue, the air spaces of which are noted to contain debris from degenerated cells. Fibrin is not seen, indicating that the blood vessels in this area have not broken. The attenuated cytoplasm of the type A cells (A) still remains. In the nucleus of the active appearing tumor cells, there are, in addition to the nucleolus (No), and chromatin masses (CM), two small bodies (arrows) morphologically similar to discrete structures, called nuclear bodies, found in other cell types.

X 13,800.

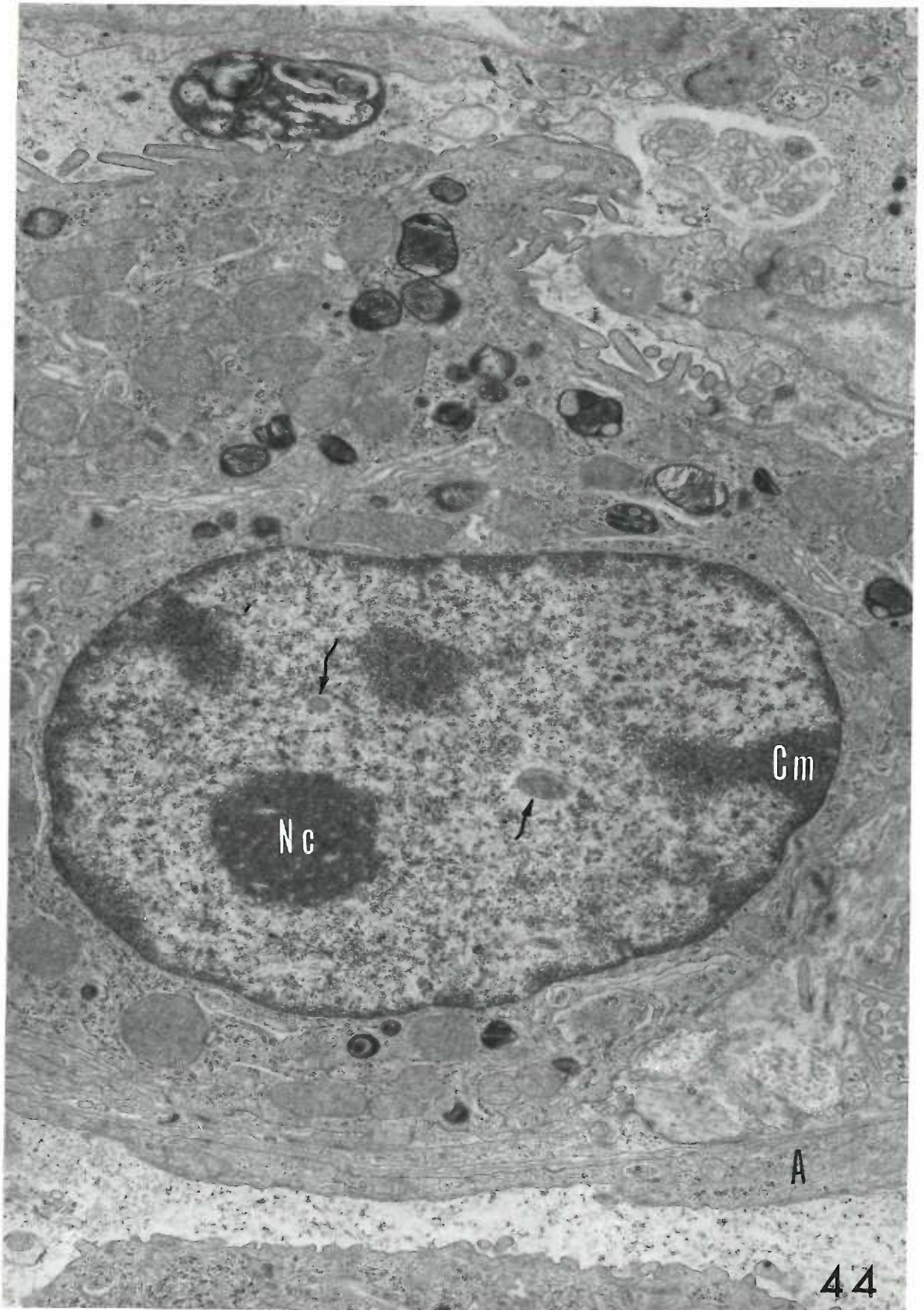




Figure 45. Tumor cell of a twenty-one month old, untreated, Group I mouse. This cell from a "spontaneously" occurring pulmonary adenoma illustrates the very active appearance of tumor cells in animals of this age. Particularly abundant in the cell shown are small vesicles (V) characterized by a fuzzy exterior, the so-called coated vesicles. In the nucleus, in addition to the nucleolus, there is noted a small dense, granular body (arrow), and a small zone containing fine fibrils (arrow head). X 22,900.

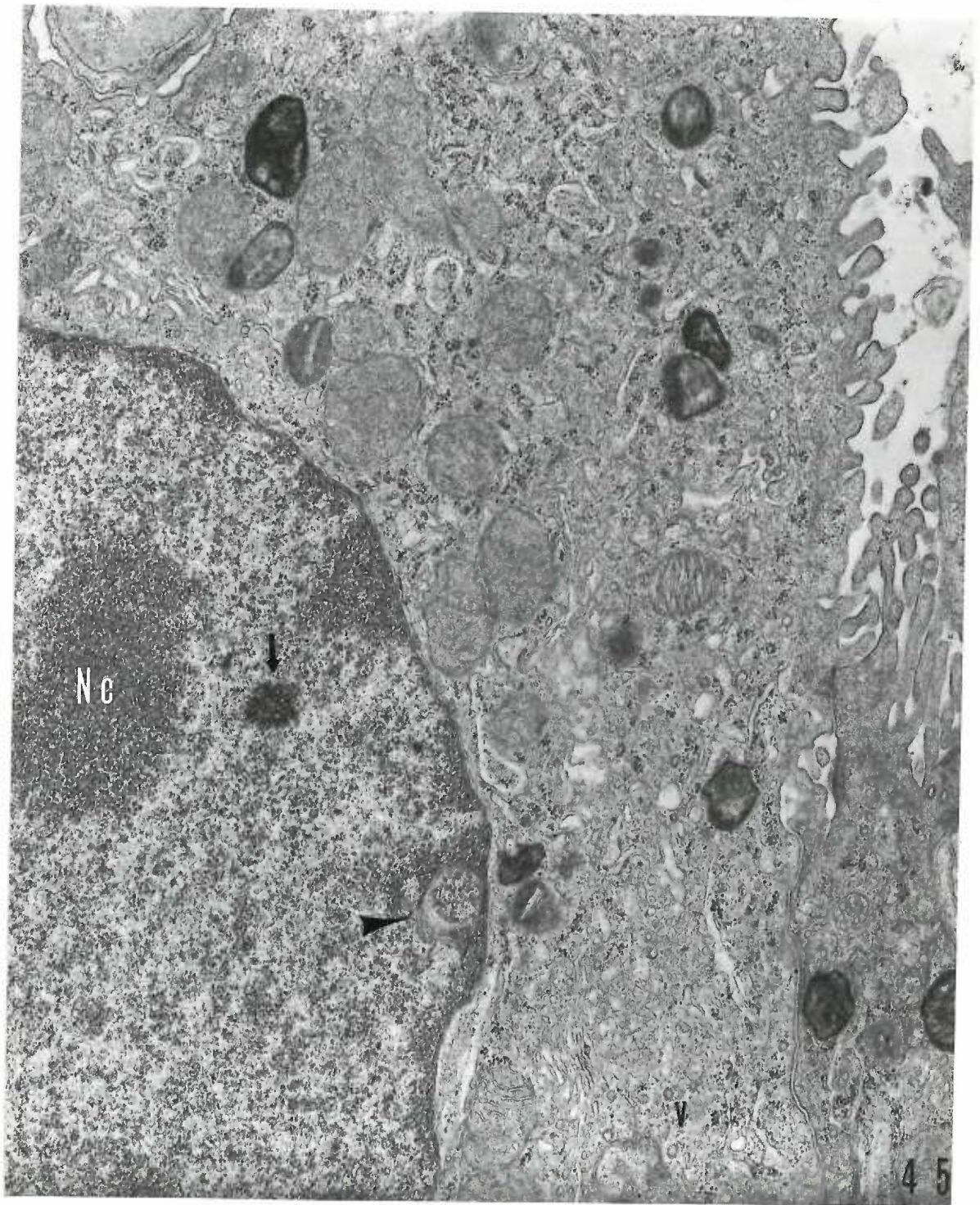


Figure 46. Tumor cell of a twelve month old, untreated, Group I mouse. Pleomorphism of cytosomes is illustrated in this micrograph. Most of these bodies consist of the three components previously noted. Coated vesicles (V) are numerous near the Golgi region. One vesicle (arrow) appears to be budding off from a Golgi membrane. Epon embedded. X 22,900.

Figure 47. Type B cell of a seven day old, Group IV mouse. The mother of this mouse had received drinking water containing urethane from the 13th through the 19th day of gestation. In this cell, there is close structural similarity between a plasma membrane infolding at the side of the cell (curved arrow) and coated vesicles. A Golgi apparatus is also immediately adjacent to this area, as are multivesicular bodies. One of the cytosomes (straight arrow) may represent a transitional form between multivesicular body and cytosome. The granular endoplasmic reticulum shows the irregular shapes characteristic of the type B and tumor cells. X 34,900.

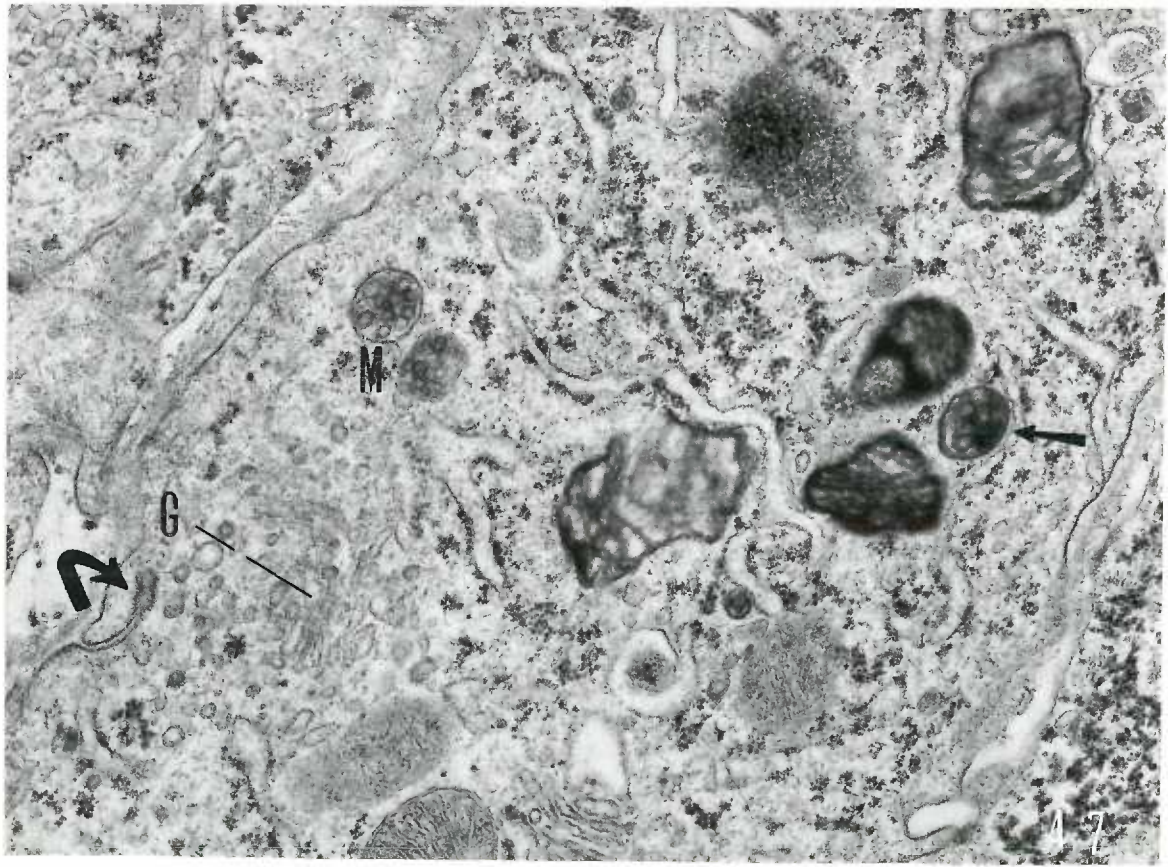
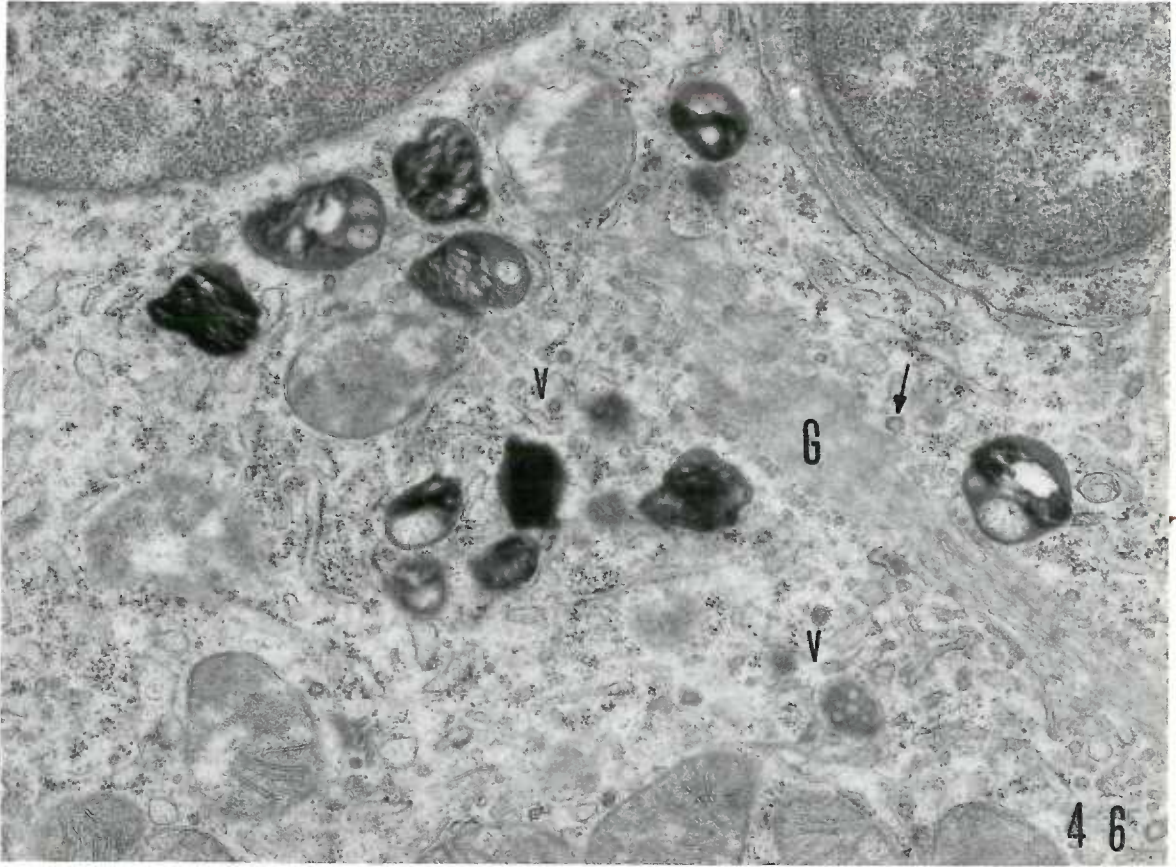


Figure 48. Tumor cell of a sixteen month old, untreated, Group I mouse. Portions of two adjacent tumor cells are illustrated. The body indicated by the arrow appears to be similar, in part, to a multivesicular body, and in part to a lamellar form of cytosome. X 22,900.

Figure 49. Type B cell of a nine day old, Group IV mouse. The mother of this mouse had received drinking water containing urethane from the last three days of gestation through the third day following delivery. One of the cytosomes in this micrograph (arrow) is similar to the one noted in the figure above. Both indicate that the cytosome may arise from the multivesicular body. X 22,900.

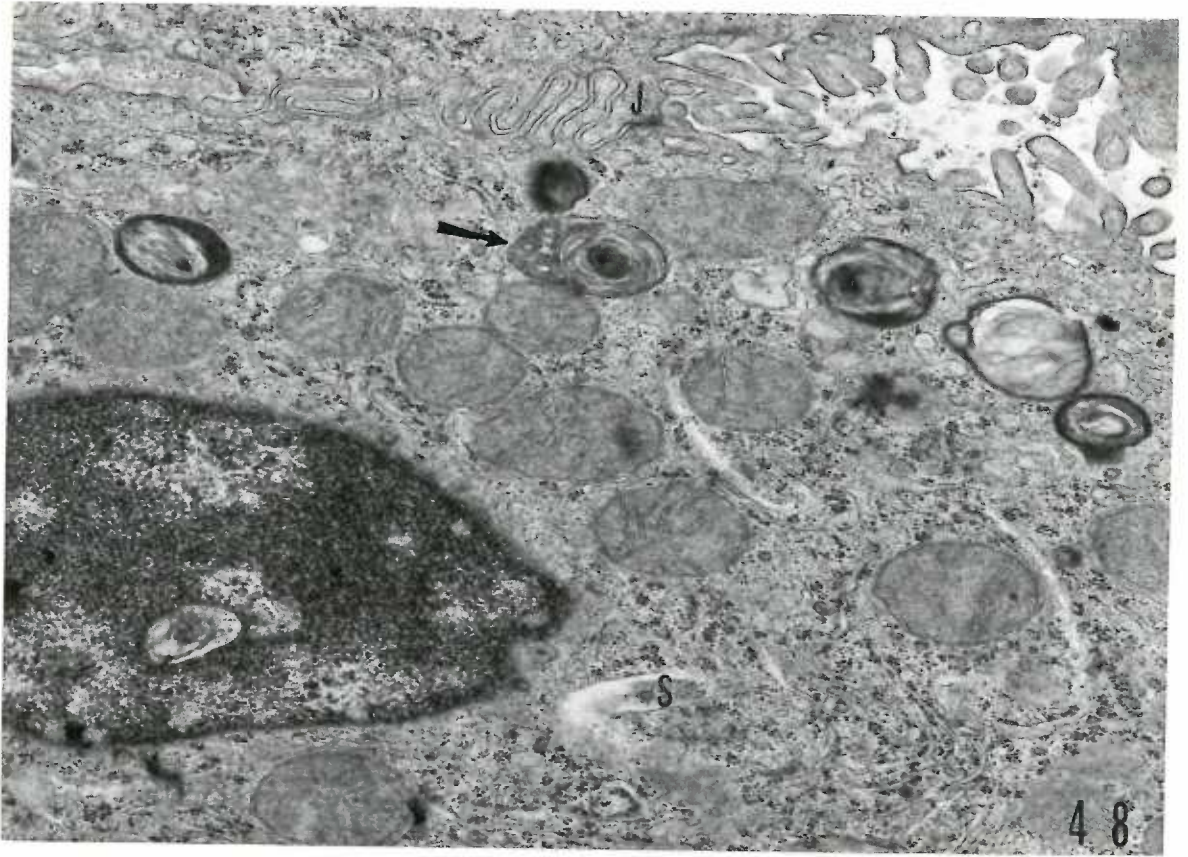


Figure 50. Tumor cell of a fifty-six day old, Group IV mouse.

The mother of this mouse had received drinking water containing urethane from the 16th day of gestation through the 21st day following delivery. The multivesicular bodies shown have different densities, different degrees of regularity of outline, and one seems to be open to the cytoplasm at one side (arrow). X 38,000.

Figure 51. Tumor cell of a fifty-six day old, Group IV mouse.

The tissue was from the same mouse as in the figure above. The diverse forms taken by the cytosomes are shown in this micrograph. It would appear that the dark, lamellar portion of the bodies is cup-like, being U-shaped in longitudinal section (single arrow) and circular in cross section (double arrow). The two bodies noted by the solid arrows present aspects of both multivesicular bodies and cytosomes and may represent intermediate forms. A possible assembly of a multivesicular body from Golgi vesicles is noted (hollow arrow). X 38,800.

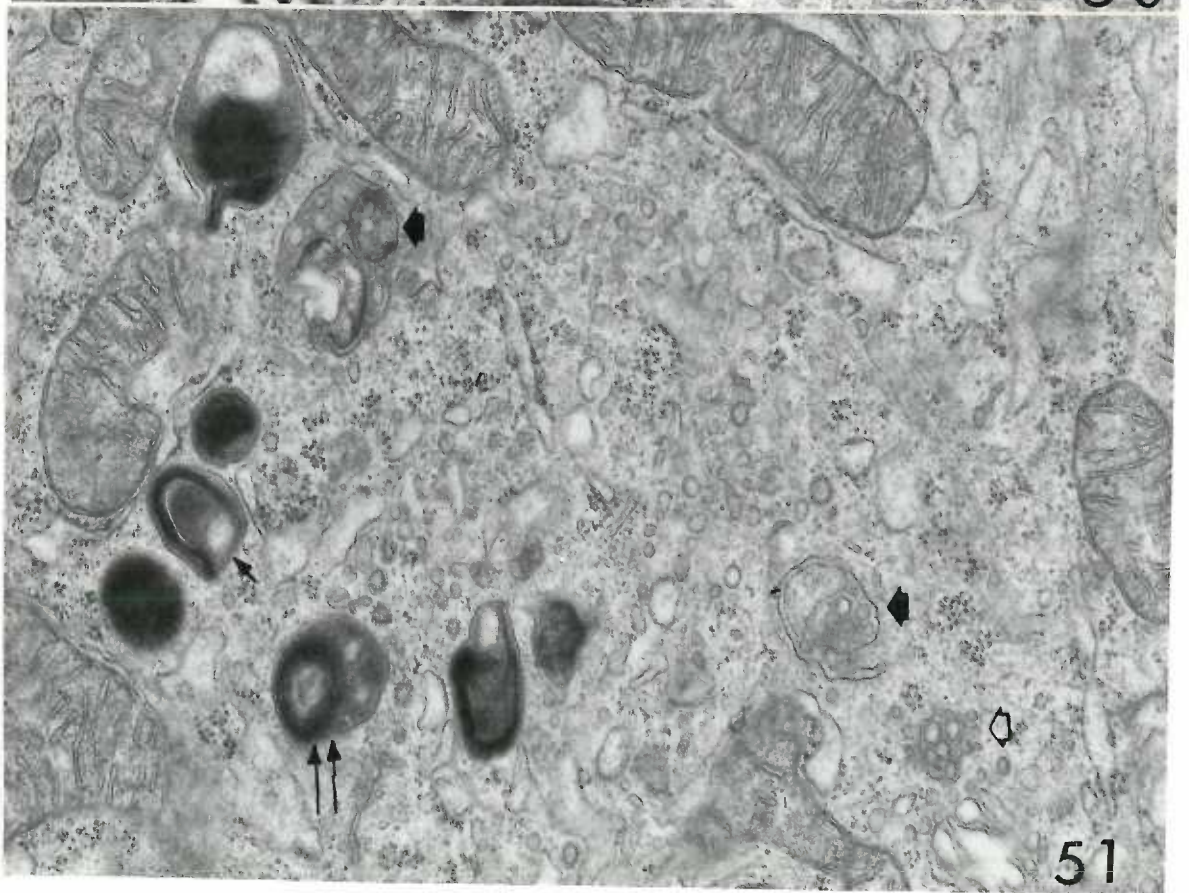
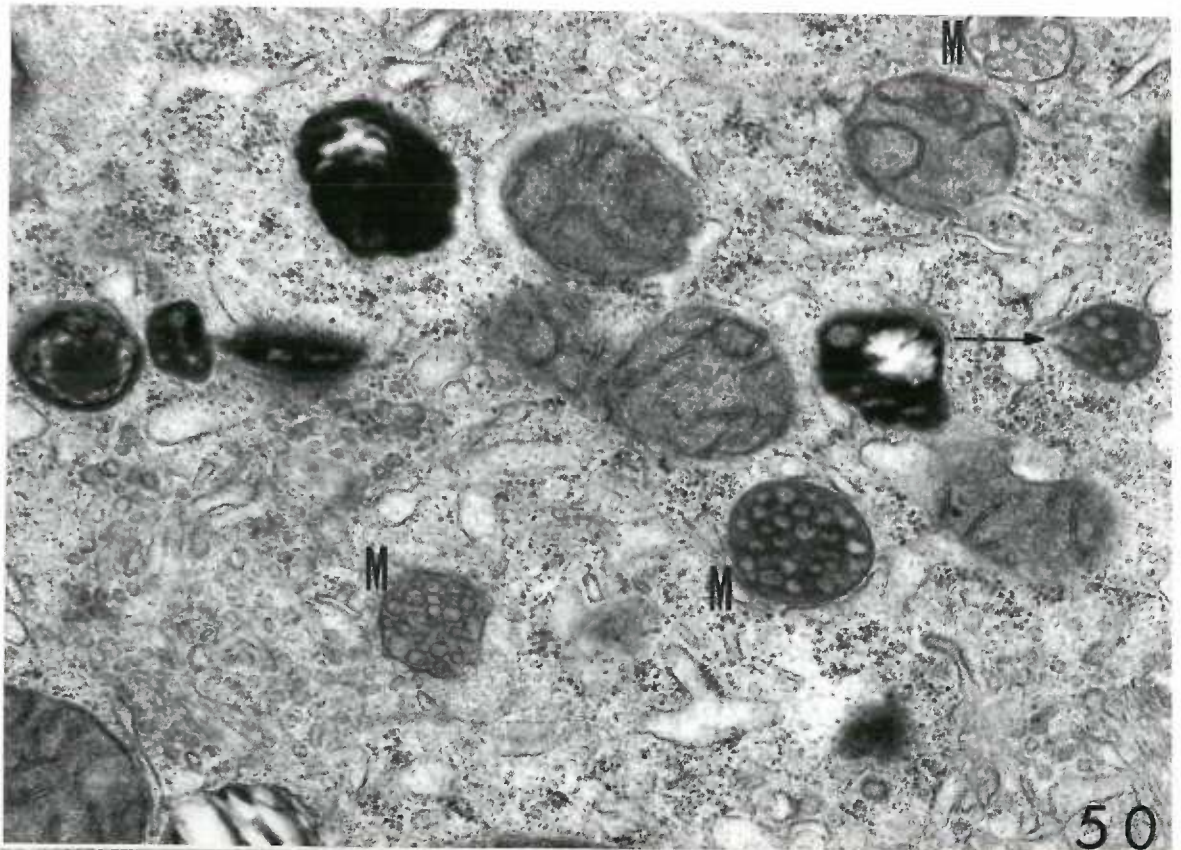




Figure 52. Tumor cell of a fifteen month old, Group V mouse.

The appearance of the various cell components varies according to the fixative used, as indicated in the initial series of illustrations. Following glutaraldehyde-osmium combination fixation, the cytosomes of the tumor cell are relatively dense and contain very dark, membrane enclosed vesicles.

Tissue fixed in glutaraldehyde- $\text{OsO}_4$  (1:1) combination.

X 67,300.

Figure 53. Tumor cell of a fifteen month old, Group V mouse.

A multivesicular body of a cell, fixed as in the figure above, contains well preserved coated vesicles.

The contour of this body is irregular. X 34,000.

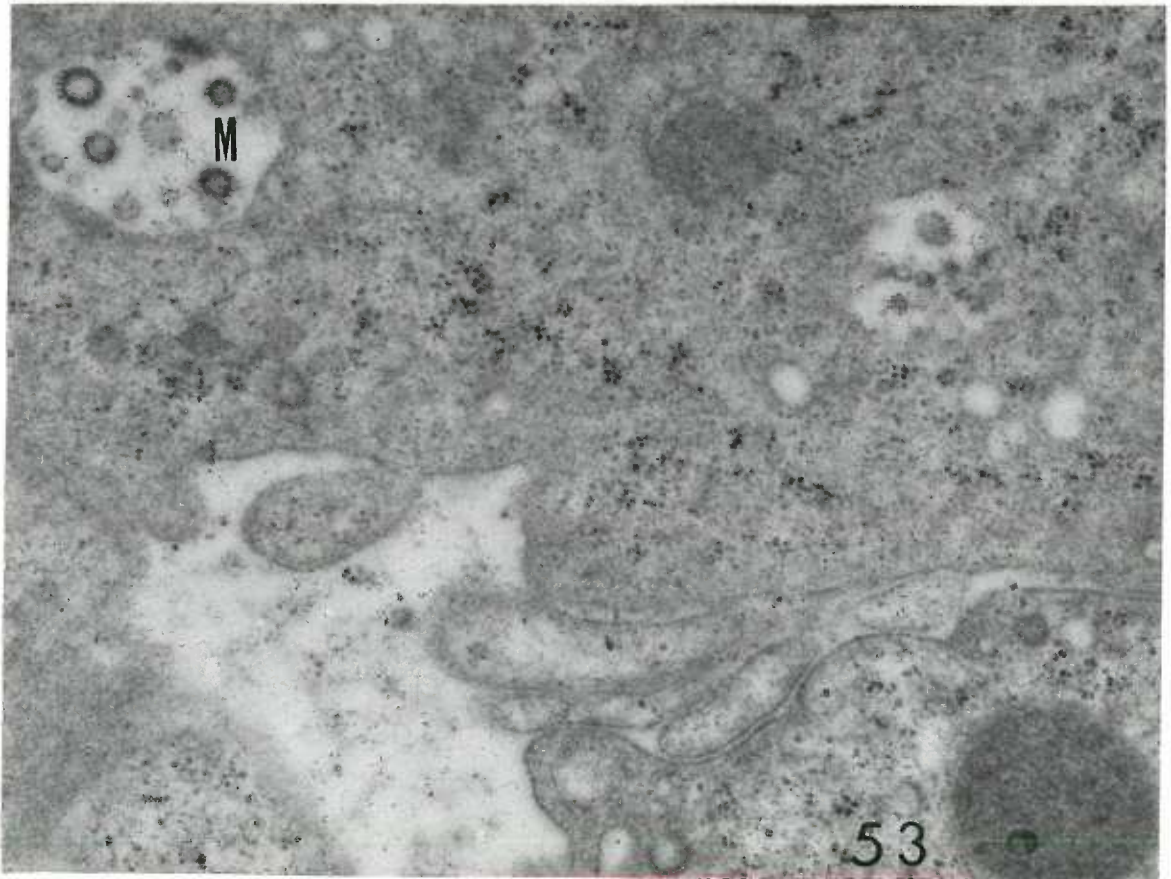
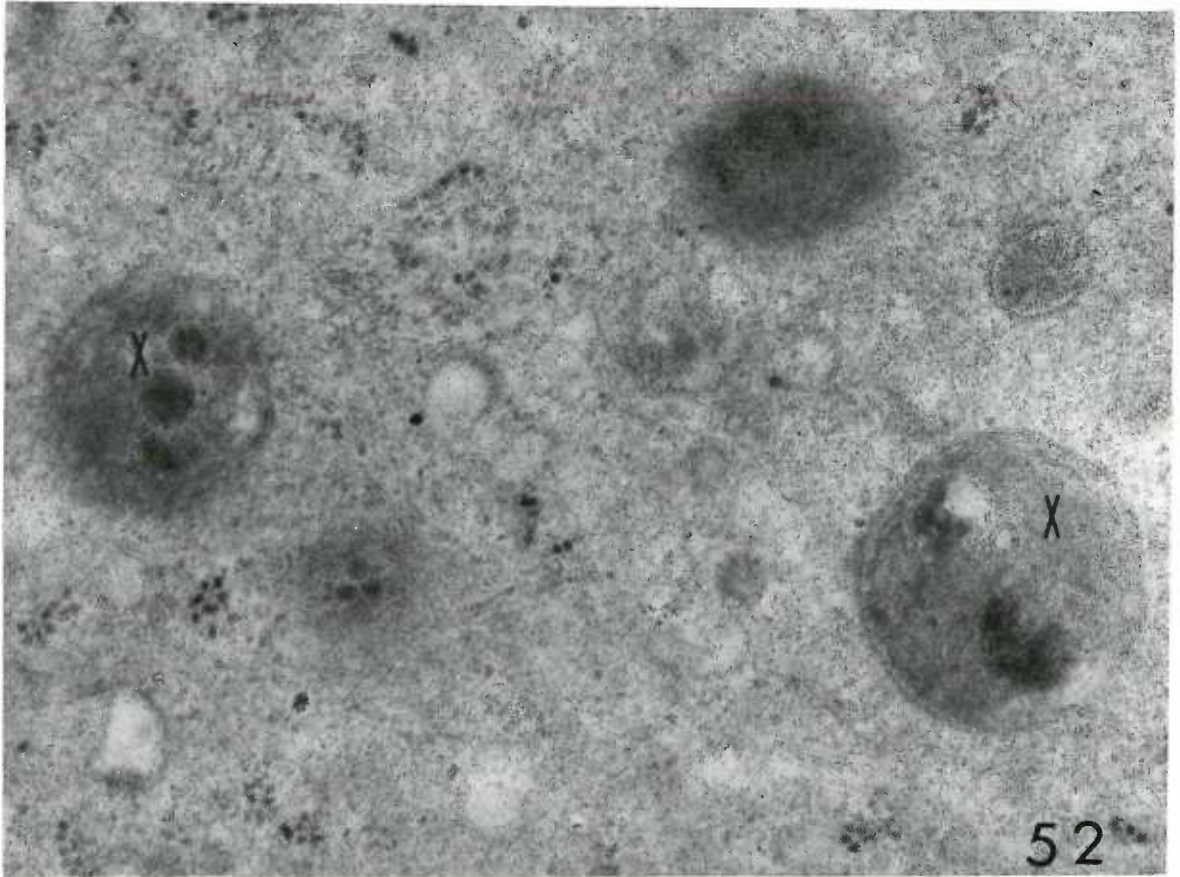


Figure 54. Tumor cells of a fifty-six day old, Group IV mouse. The mother of this mouse had received drinking water containing urethane from the day of delivery through the 21st day following delivery. This micrograph, again, shows the marked effect of fixation on organelle structure. The cytosomes reveal the typical three components preserved by osmium fixation. There is a suggestion of crystalloid structure in one of these bodies (arrow). X 67,300.

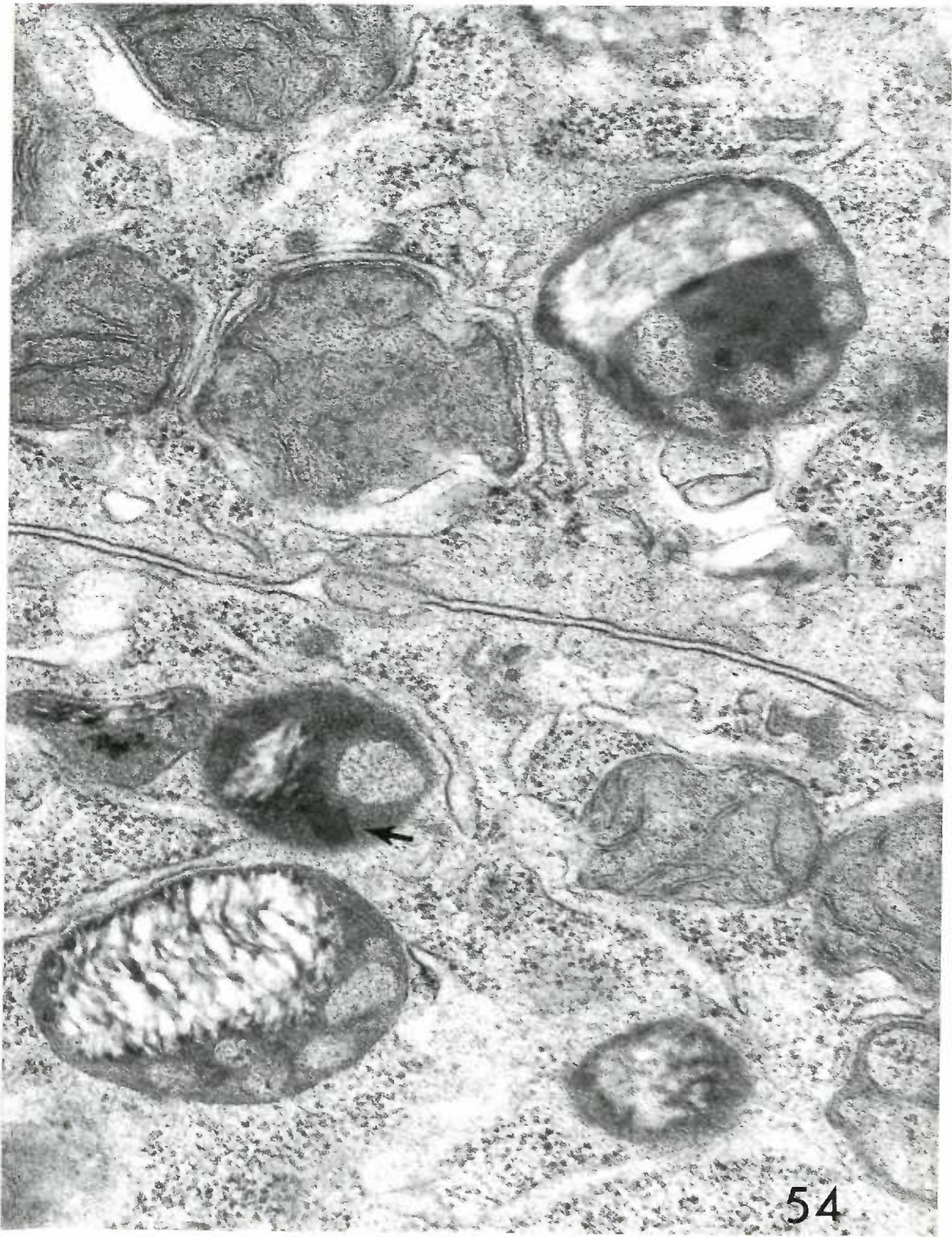


Figure 55. Tumor cell of a forty-three day old, Group IV mouse. The mother of this mouse had received drinking water containing urethane from the 12th through the 17th day of gestation. As seen in previous figures, many of the cytosomes contain dense components having crystalloid shape. The crystalloids in the cytosomes of this cell do not reveal a crystalline substructure at this magnification and with this fixative. X 22,900.

Figure 56. Tumor cell of a fifteen month old, Group V mouse. The use of a combined glutaraldehyde-osmium fixative produces several differences in tissue ultrastructure. In this micrograph, the cytosomes are seen to lack the loose lamellar component, instead, a definitely crystalline inclusion is present (arrow). An enlargement of this cytosome is shown in Fig. 58. Following fixation with the combined fixative, the cytosomes present a relatively uniform, ovoid shape, about 6000 Å by 8000 Å. The membrane-bound cytosomes contain, in addition to the crystalline material, non-crystalline dense substances, and membrane-enclosed vesicles of various sizes. Fixed in glutaraldehyde-OsO<sub>4</sub> (1:1) combination. X 22,900.

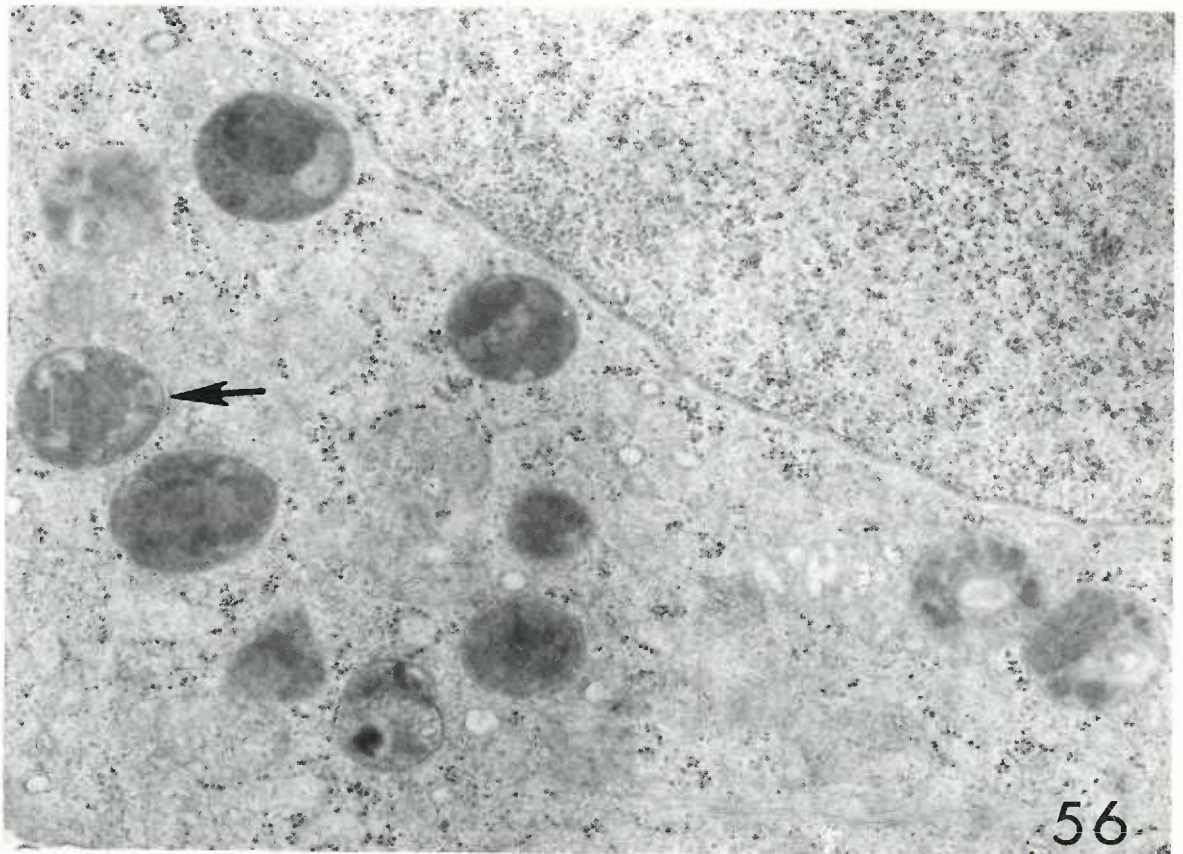
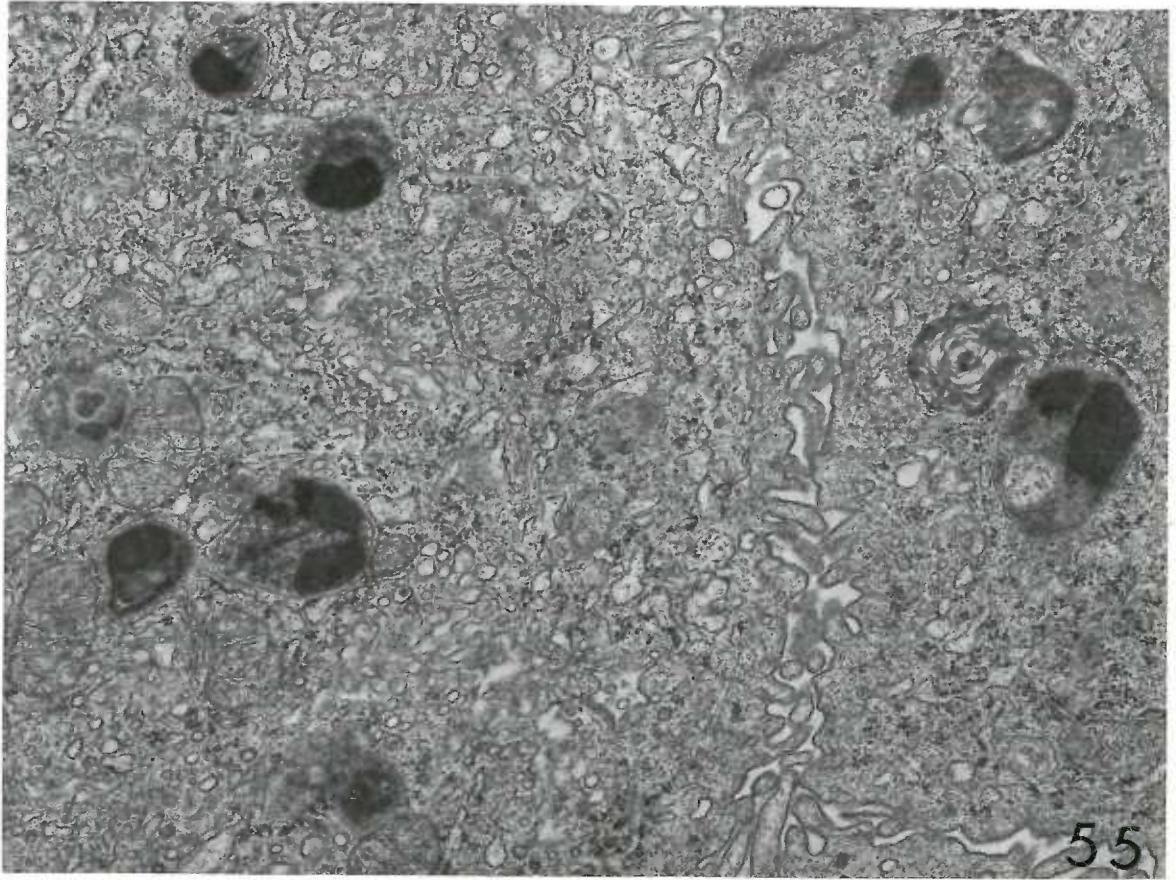


Figure 57. Tumor cell of a fifteen month old, Group V mouse.

At a higher magnification than in the previous figure, the crystalline nature of the cytosomal component is better visualized. In section, the crystal appears as thin rods in parallel array. This appearance could be obtained if the crystal were made up of parallel plates. When sectioned at approximately right angles to the plates, these would appear as thin rods. Planes of section approximately parallel to the plates would produce a relatively dense mass. The multicomponent nature of the cytosomes are clearly seen with this fixation and may be compared to that seen with osmium fixation, Fig. 54. Fixed in glutaraldehyde- $\text{OsO}_4$  (1:1) combination. X 67,300.

Figure 58. An enlargement of a part of Fig. 56. The regular array of the crystal is apparent. X 48,000.

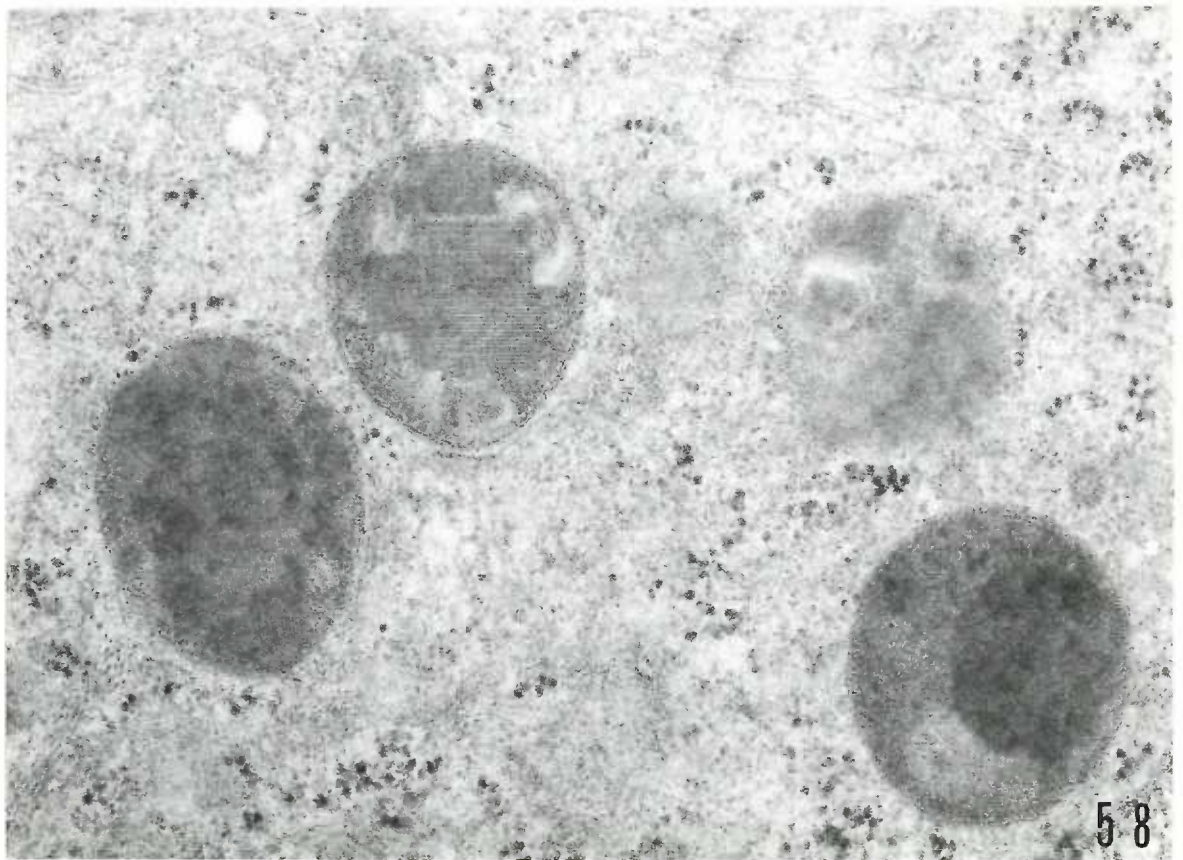
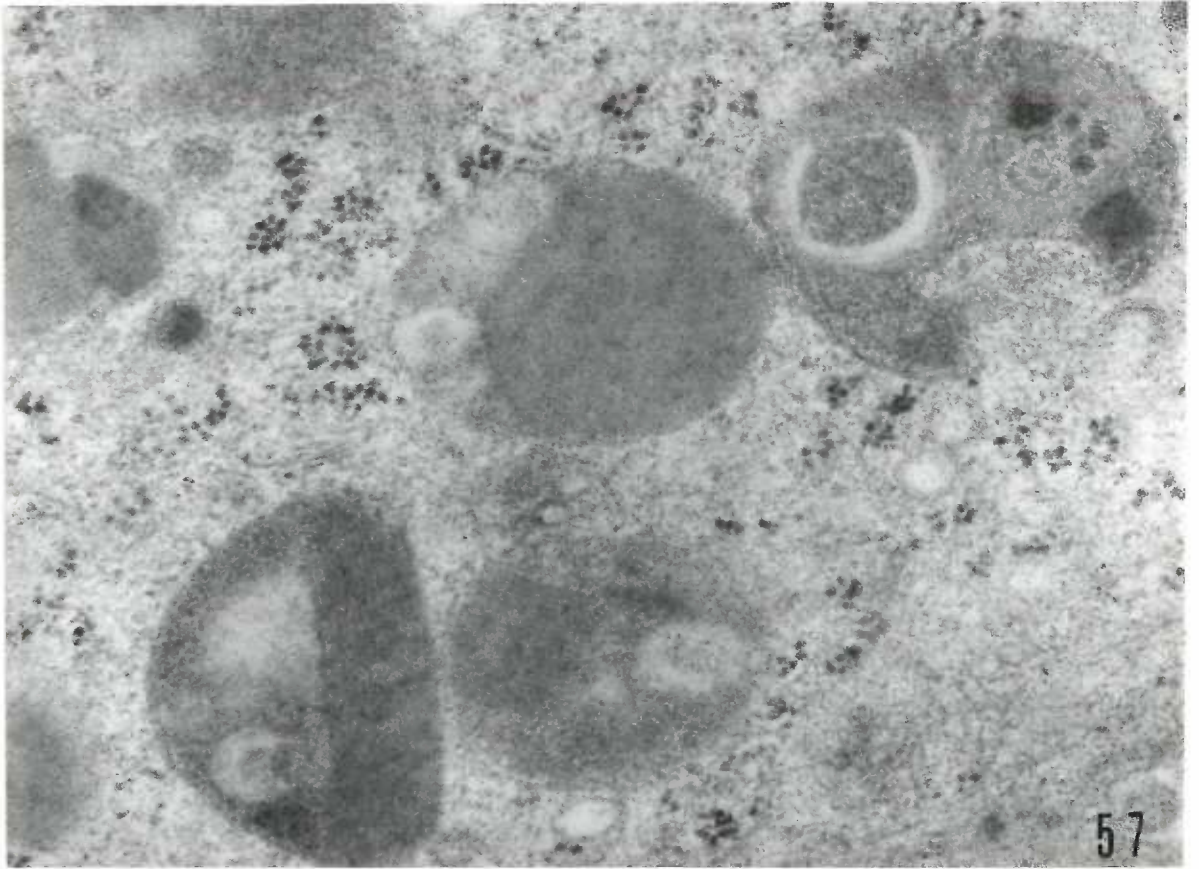




Figure 59. Tumor cell of a fifteen month old, Group V mouse. The cytosome shown is enclosed by a single membrane having unit membrane structure. The crystal within the cytosome consists of dark and light bands, each approximately  $33 \text{ \AA}$  wide. There is a suggestion that the dark bands fray off at the sides of the crystal to give irregular bands somewhat similar to the lamelli observed with other fixatives. X 272,800.

Figure 60. Tumor cell of a fifty-six day old, Group IV mouse. The mother of this mouse had received drinking water containing urethane from the 16th day of gestation through the 21st day following delivery. Accumulations of glycogen (arrow) in tumor cells is common in some tumors but absent in others. The angular empty spaces in the glycogen region are probably artifacts of fixation, however there is a close resemblance between these spaces and the U-shaped endoplasmic reticulum configuration previously noted. X 22,900.

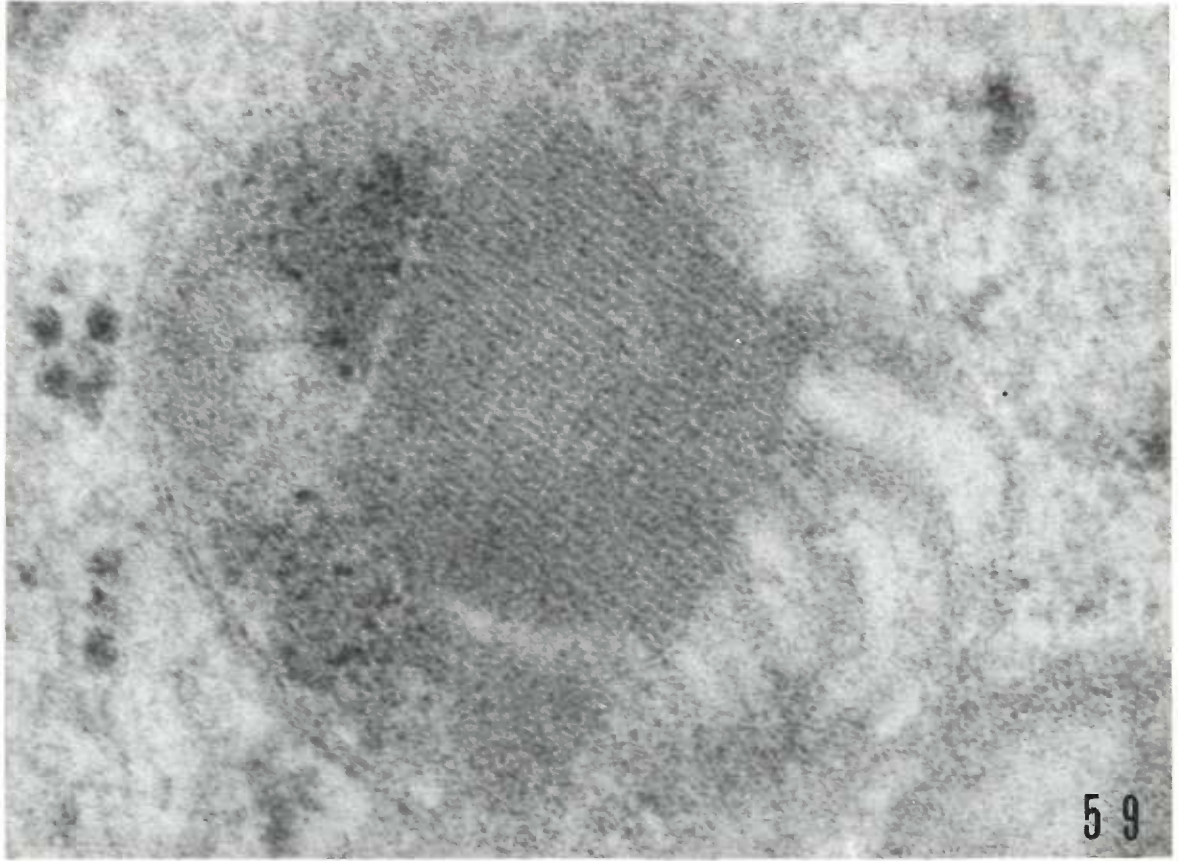
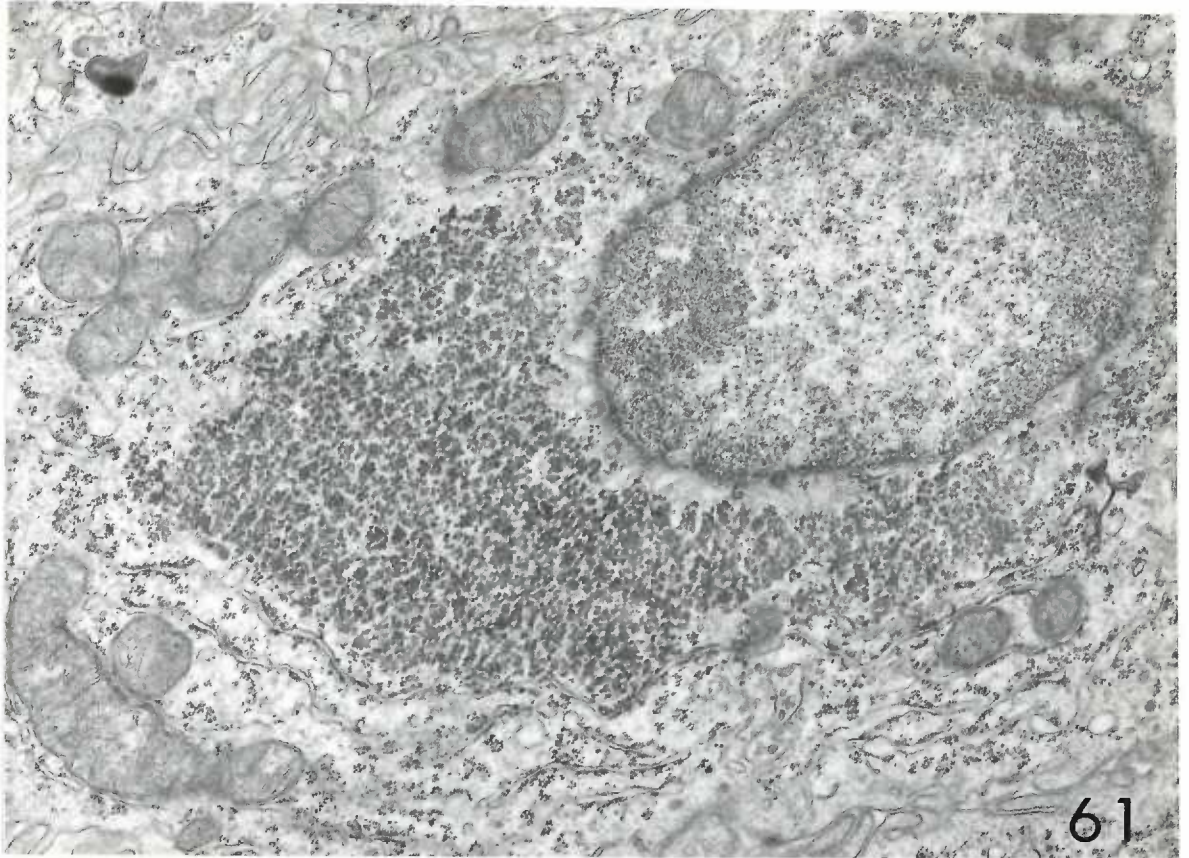
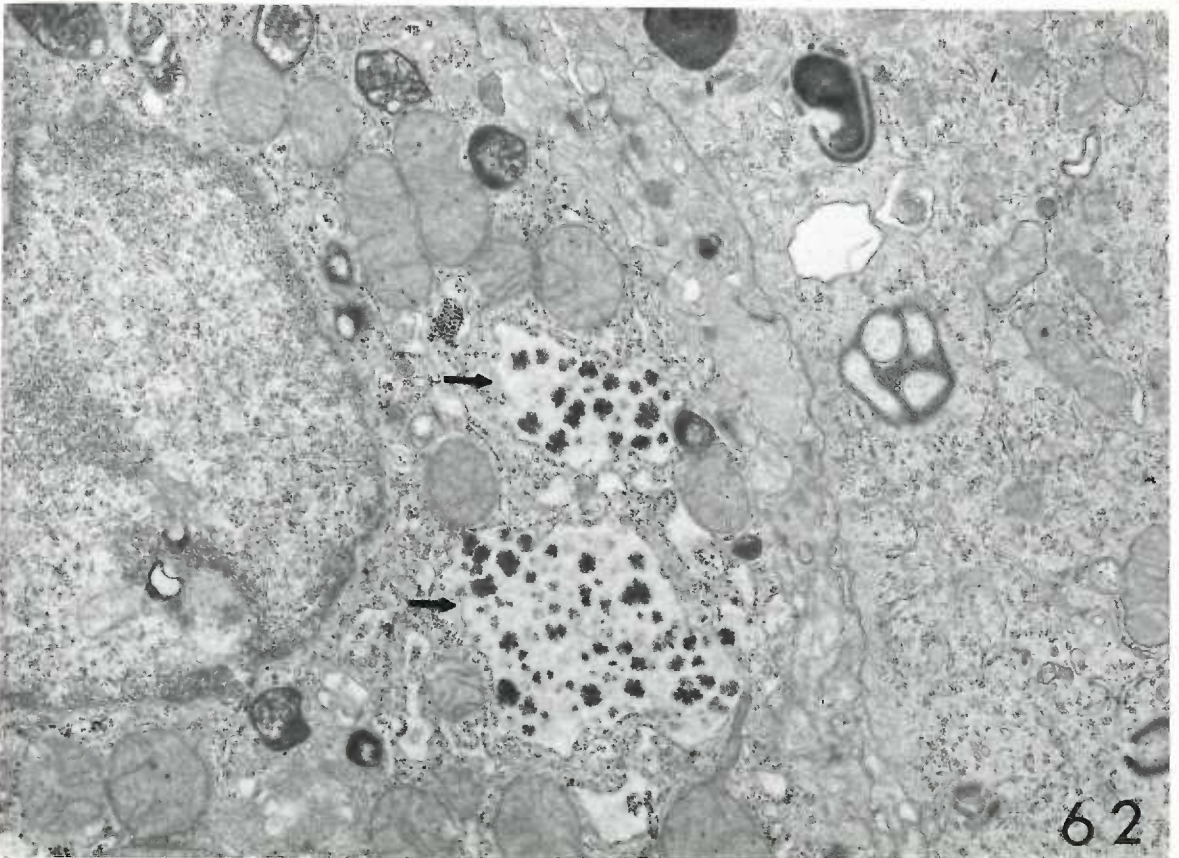


Fig. 61. Tumor cell of a fifty-six day old, Group IV mouse. This is tissue from the same mouse as shown in Fig. 60. The glycogen mass in this tumor cell is not associated with the membranes and empty spaces seen in the previous figure. It is to be noted that tumor cells containing an accumulation of glycogen tend not to have a well developed Golgi apparatus, and contain relatively fewer cytosomes. X 22,900.

Fig. 62. Tumor cells of a sixteen month old, Group V mouse. Rarely, membrane-enclosed regions (arrows) containing irregular, granular material surrounded by slightly dense matrix substance are found in tumor cells. These irregular granules are considered to be made up of glycogen particles. X 22,900.



61



62

Figure 63. Tumor cell of a twenty-one month old, Group I mouse. A portion of a tumor cell, bordering what is probably a non-functional air space, reveals possible excretion of cytosomal material from the cell.

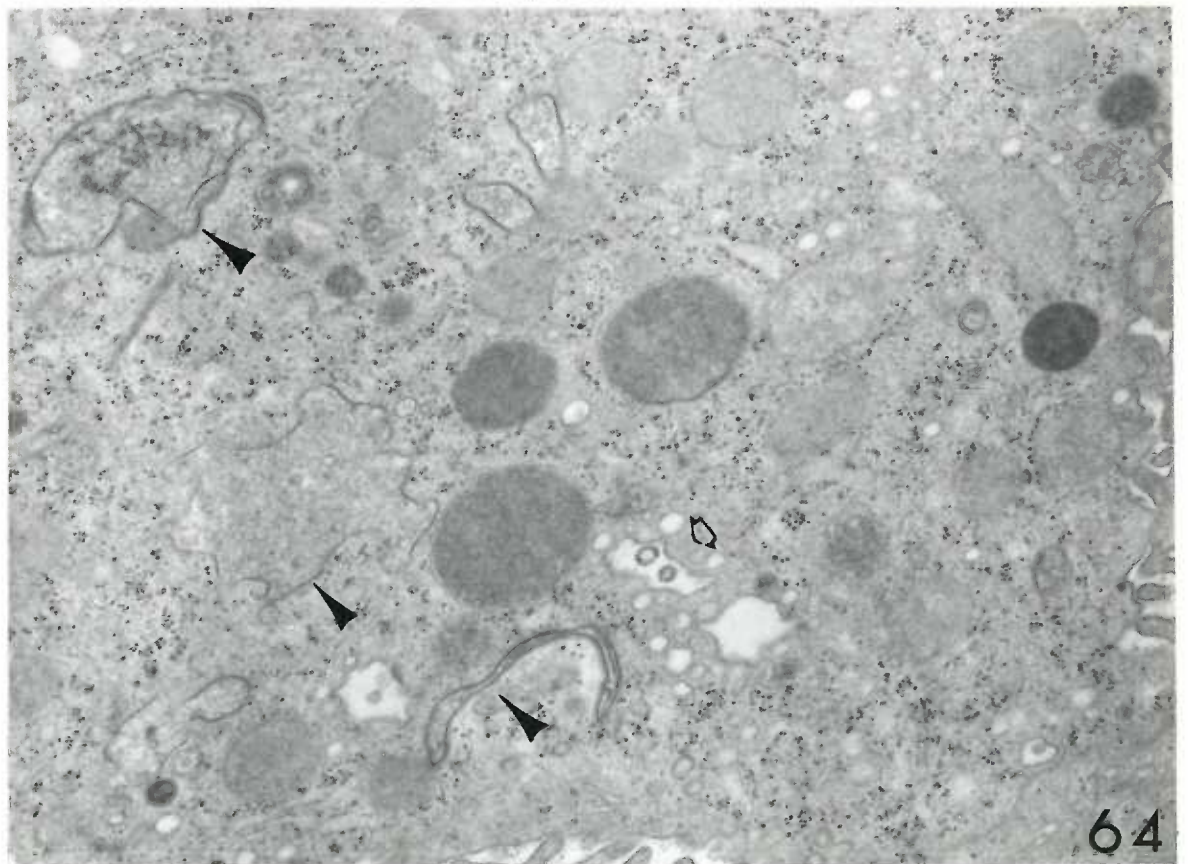
X 22,900.

Figure 64. Tumor cell of a fifteen month old, Group V mouse.

With glutaraldehyde-osmium combination fixative, some atypical, membrane-bound bodies (arrowheads) occur. These irregularly shaped bodies contain small vesicles (in one body shown) and a homogeneous matrix substance. The enclosing membrane appears to be thicker than mitochondrial and cytosomal membranes. The outer membrane of one multivesicular body (hollow arrow) appears to be contacting, and possibly fusing with, the membrane of small vesicles. X 22,900.



63



64

Figure 65. Tumor cell of a twenty-one month old, Group I mouse. This tumor cell appears to be bi-nucleated. Both nuclei contain various inclusions. Some "inclusions" are probably more properly interpreted as fortuitous sections through portions of an irregularly contoured segment of nucleus that includes bits of cytoplasm. Other inclusions (I) are probably true inclusions, of unknown nature. X 22,900.

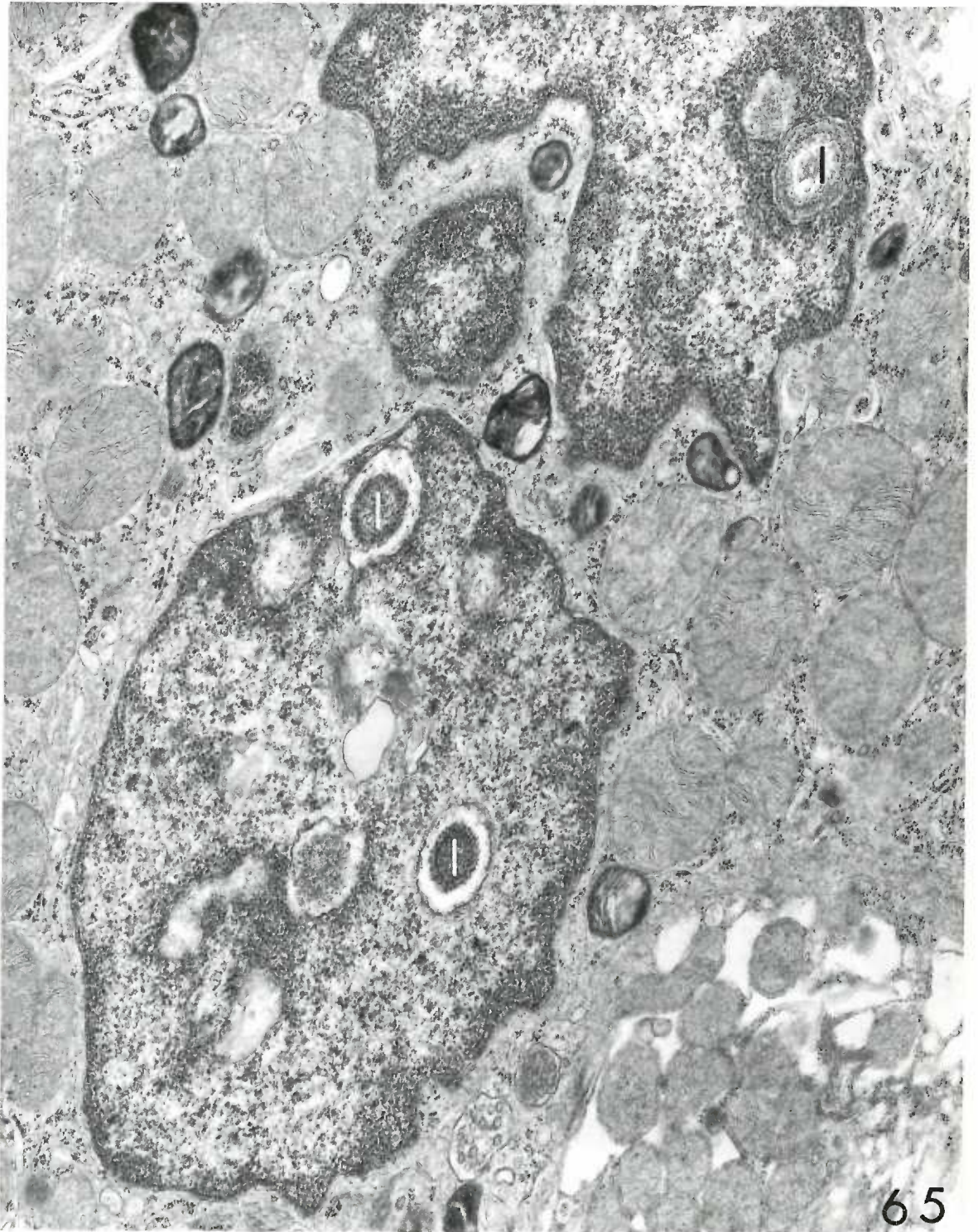




Figure 66. Type B cell of a twelve month old, Group I tumor-bearing mouse. The type B cell illustrated occurred in a normal portion of lung near an adenoma. The cell is very active in appearance and contains numerous cytosomes. Epon embedded. X 8,400.



Figure 67. Type B cell of a twelve month old, Group V, tumor-bearing mouse. Portions of two cells are shown. The cell above is thought to be a normal type B alveolar cell. The cell below is considered to be a tumor cell. If this interpretation is correct, there would be some difference in structure between the two cell types, at least in this example. The difference lies primarily in the greater density of the cytoplasm of the cell identified as a tumor cell. X 13,800.

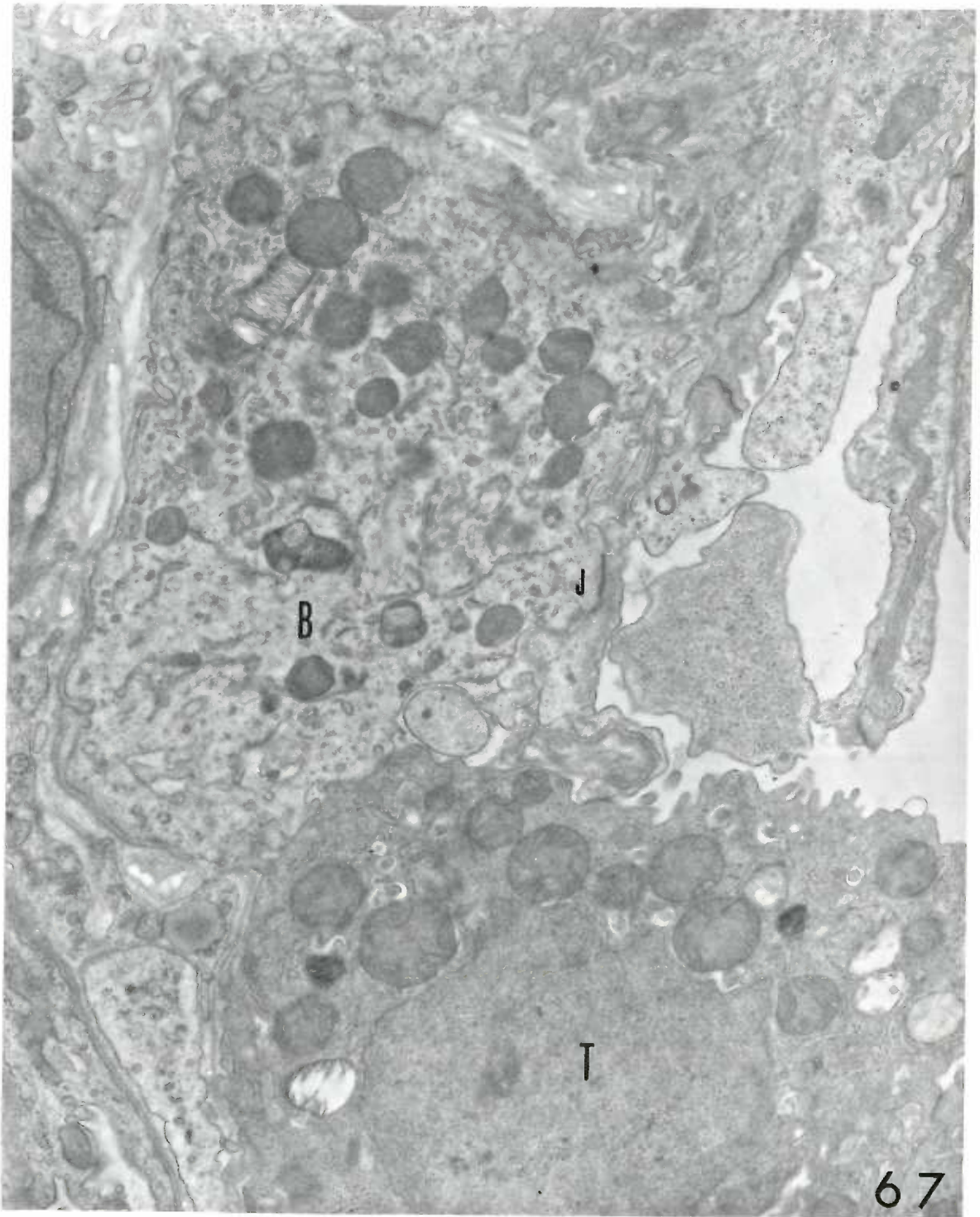


Figure 68. Tumor cells of a twenty-one month old, Group I mouse. A rare finding is the capacity of pericapillary tumor cells for partial attenuation of cytoplasm in a fashion which mimics that of type A alveolar cells.  
X 8,400.

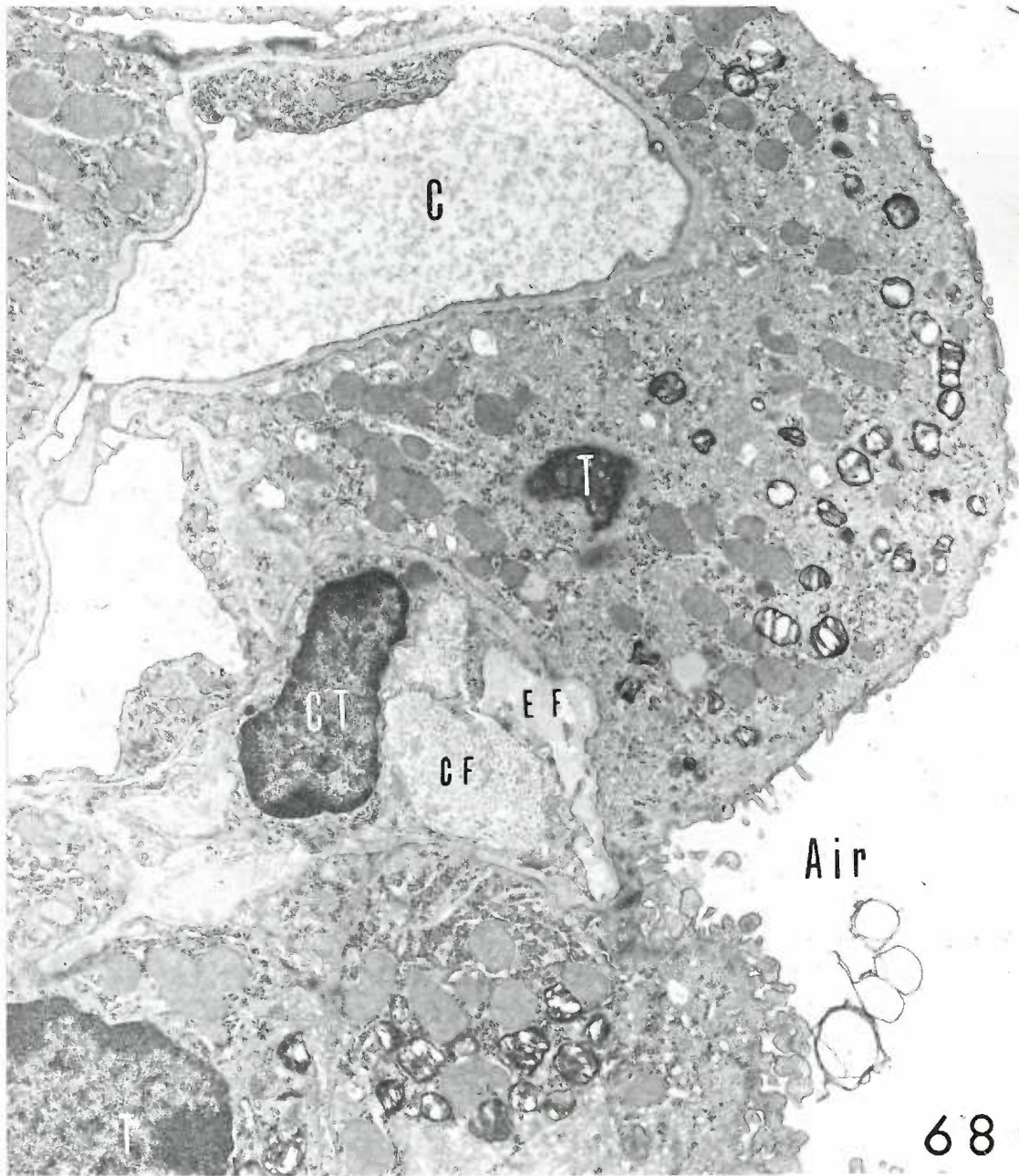


Figure 69. Macrophage of a forty-three day old, Group IV mouse. The mother of this mouse had received drinking water containing urethane from the 12th through the 17th day of gestation. A part of a macrophage within a tumor is depicted. The similarity between macrophage and tumor cell can be very great. Identifying features are: 1) lack of junctional complex between macrophage and tumor cells, 2) relative absence of short, narrow microvilli at the macrophage border, and 3) presence of pleomorphic materials in the macrophage cytoplasm.

X 22,900.

Figure 70. Macrophage of a forty-three day old, Group IV mouse. The tissue was taken from the same animal as in the above figure. This micrograph affords an additional comparison of macrophage to tumor cell.

X 22,900.

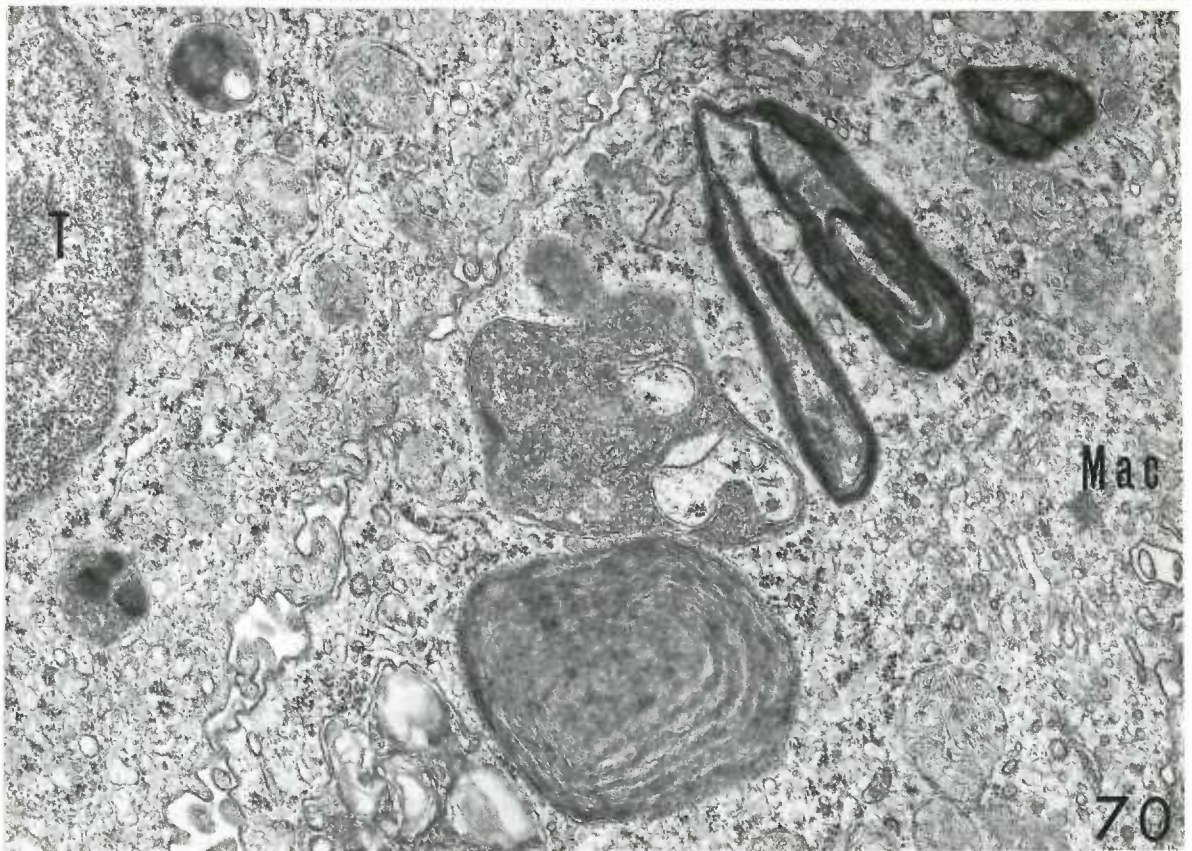
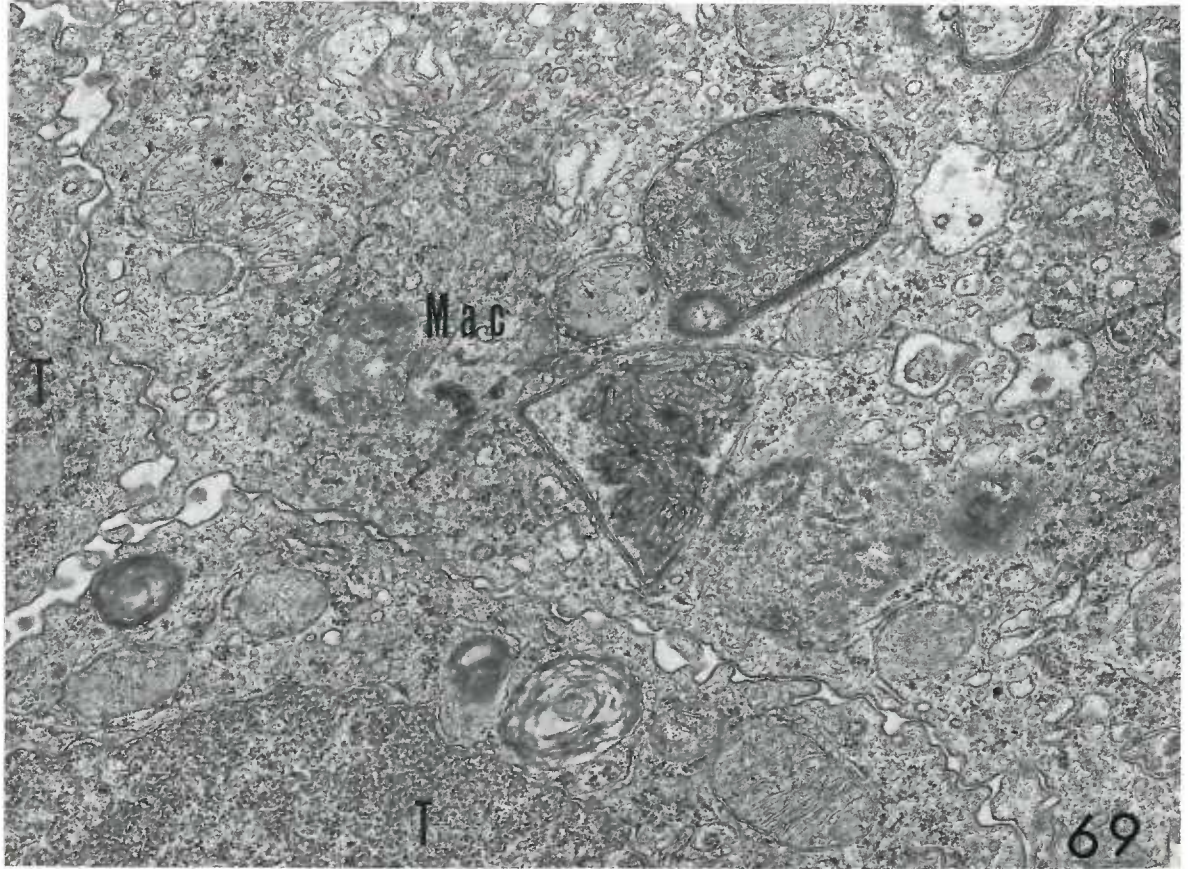




Figure 71. Macrophage and tumor cells of a fifteen month old, Group V mouse. The pleomorphic bodies seen in macrophages do not always serve to distinguish these cells from tumor cells. In this micrograph, an area of normal lung is being invaded by tumor cells. The large, phagocytized body in the macrophage in the center of the picture is not altogether unlike a body occurring in what is thought to be a tumor cell in the figure below. X 8,400.

Figure 72. Tumor cells of a fifteen month old, Group V mouse. Although the magnification of the micrograph and the fixation of the tissue is different from that in the figure above, similarity exists between the large bodies seen in both cells. Identification of the cell in this figure as a tumor cell is based on the presence of cytosomes not included in this picture. However, this cell shows other features of a typical macrophage, and it is possible that the identification is incorrect. X 22,900.

Fixed in glutaraldehyde- $\text{OsO}_4$  (1:1) combination.

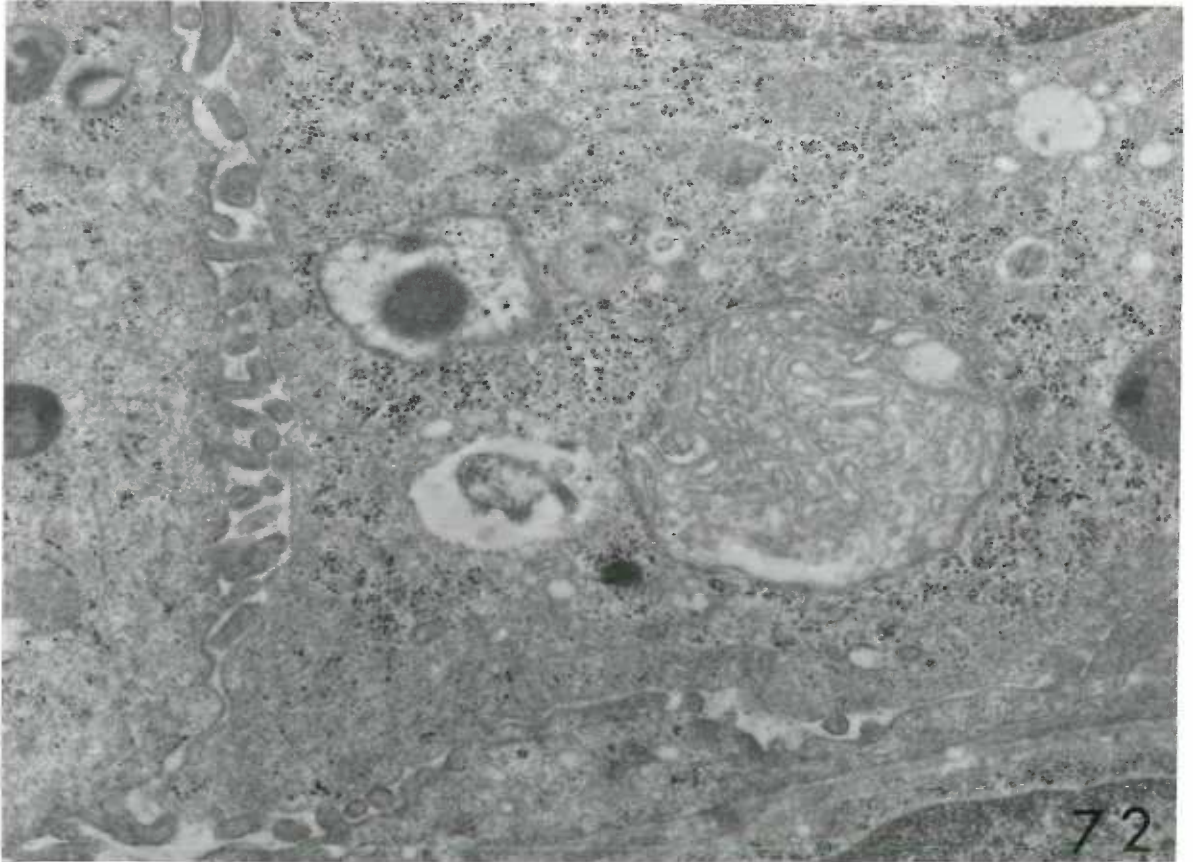
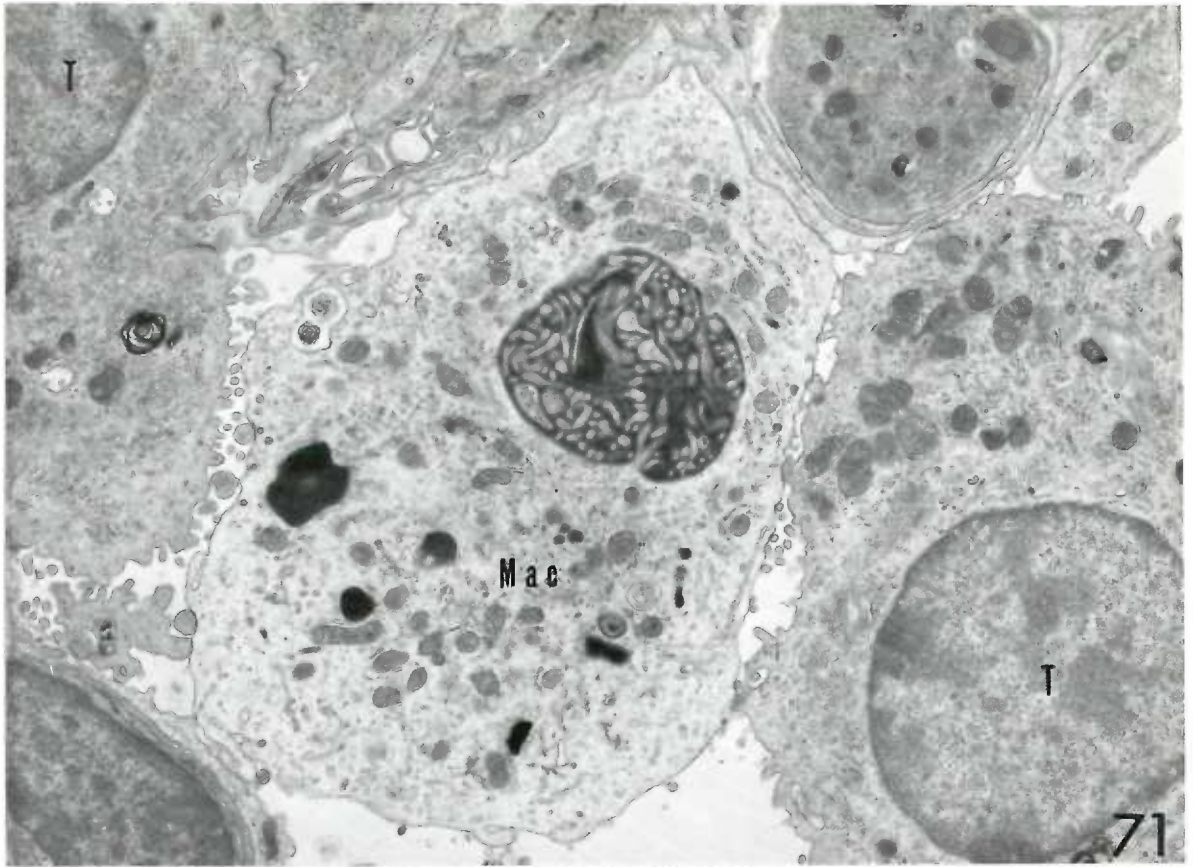
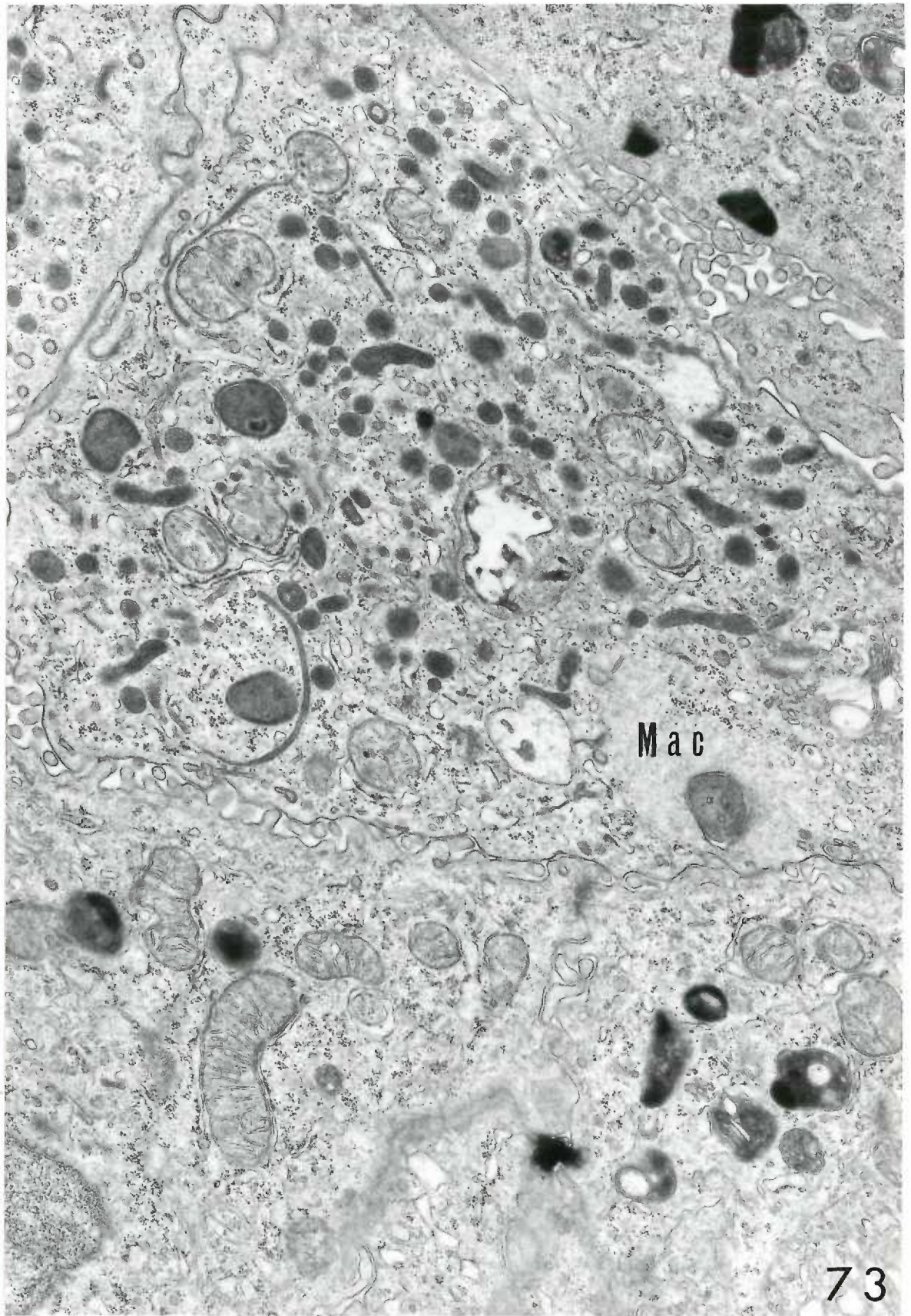


Figure 73. Macrophage and tumor cells of a fifty-six day old, Group IV mouse. The mother of this mouse had received drinking water containing urethane from the 16th day of gestation through the 21st day following delivery. The portion of cytoplasm shown is filled with what are considered to be the several forms of mycoplasma. The forms vary from a curved, thin, dense, membrane-bounded structure with an internal dense lamina, to round or irregularly shaped bodies ranging in size from about 1000 Å in diameter to about 1500 Å by 10,000 Å. Larger, membrane-bounded bodies, about one-half to one micron in diameter have the same density as the smaller forms. The smaller bodies may represent elementary bodies of mycoplasma and the larger ones may be more mature forms of the organism.

X 22,900.



Mac

Figure 74. Macrophage of a fifty-six day old, Group IV

mouse. Tissue was from the same animal as in the previous figure. The structure of elementary bodies of mycoplasma (thin arrows), and what is believed to be more mature forms (thick arrows), can be compared. Note, however, that the body at the bottom of the micrograph, and those near it, have a thick enclosing membrane, whereas that at the left-center of the picture has a thin enclosing membrane. It may be that the latter body is, in reality, a cytosegrosome, and is not related to the mycoplasma. X 48,000.

